THROUGHFLOW IN AXIAL TURBOMACHINES WITH VARIABLE WALL GEOMETRY

Thesis by

Gordon Cedric Oates

In Partial Fulfillment of the Requirements

For the Degree of

Doctor of Philosophy

California Institute of Technology

Pasadena, California

1959

ACKNOWLEDGEMENTS

The research work described herein was carried out with the greatly appreciated and invaluable assistance of Professor Frank E. Marble, to whom I extend my most sincere thanks. My thanks are also due to Mrs. Ingrid Stenberg for her most competent assistance with the necessary extensive calculations.

I also wish to thank the Air Force Office of Scientific Research for the support given this work under Contract Number AF 49(638)-497.

ABSTRACT

The theory of three-dimensional flow in axial turbomachines was extended to include the effects of variable hub and tip radii such as occur in the entrance stages of conventional axial flow compressors and, to a larger extent, in mixed flow compressors. The problem is simplified by assuming an infinite number of infinitely thin blades in each blade row, so that axially symmetric fluid motion results.

The effect of variable hub and tip radii of the annulus walls is investigated when the tangential velocities are small but arbitrary, and when they are large but of special form. The combined effect of heavily loaded inlet guide vanes and variable hub radius is also investigated for the case in which the inlet guide vanes impart a motion very nearly of the solid-body type. The boundary conditions for the variable hub radius require linearization, thus restricting the magnitude of perturbation to be induced by the wall. Finally, the effect of a loaded blade row placed behind the inlet guide vane is determined.

The local axial and tangential velocities induced by the variable wall radius were found to be of the same general magnitude as the velocities induced by a normal rotor or stator blade row. Although the forms of the solutions are somewhat complex for routine application in turbomachine design, a sufficiently simple approximate result is obtained for one case and it is indicated how the method of approximation may be extended.

TABLE OF CONTENTS

LIST OF SYMBOLS

r, θ, z	Cylindrical coordinates
u	Velocity in direction r
v	Velocity in direction θ
w	Velocity in direction z
ξ	Vorticity in direction r
η	Vorticity in direction θ
ζ	Vorticity in direction z
F_r	Blade force imparted in direction r
F_θ	Blade force imparted in direction θ
F_z	Blade force imparted in direction z
J_0	Bessel function of first kind and order zero
Y_0	Bessel function of second kind and order zero
J_1	Bessel function of first kind and order one
Y_1	Bessel function of second kind and order one
$U_0(\delta r)$	Linear combination of Bessel functions of order zero
	$J_0(\delta r) Y_1(\delta r_t) - J_1(\delta r_t) Y_0(\delta r)$ $\quad$ δ is dummy variable here.
$U_1(\delta r)$	Linear combination of Bessel functions of order one
	$J_1(\delta r) Y_1(\delta r_t) - J_1(\delta r_t) Y_1(\delta r)$
$W_0(\delta r)$	Linear combination of Bessel functions of order zero
	$J_1(\delta r_h) Y_0(\delta r) - Y_1(\delta r_h) J_0(\delta r)$
$W_1(\delta r)$	Linear combination of Bessel functions of order one
	$J_1(\delta r_h) Y_1(\delta r) - Y_1(\delta r_h) J_1(\delta r)$
ξ_n	Characteristic number for Bessel function
$V_0(\xi_n r)$	Linear combination of Bessel functions of order zero
	$\frac{U_0(\xi_n r)}{r_h U_0(\xi_n r_h) + q W_0(\xi_n r_t)}$

$V_1(\xi_n r)$ Linear combination of Bessel functions of order one

$$\frac{U_1(\xi_n r)}{r_h U_0(\xi_n r_h) + r_t W_0(\xi_n r_t)}$$

p Fluid static pressure

P Fluid total pressure

ρ Fluid density

P Fluid total head

ψ Stream function in cylindrical coordinates

v_s Velocity in meridional plane

ω Angular velocity of blade row

$\overline{\overline{W}}$ Axial velocity perturbation about mean flow

$\overline{V}$ Dimensionless tangential velocity $\frac{V}{W_{(0)}}$

$\hat{U}_{(r,\kappa)}$ Fourier transform of radial velocity

$$\frac{1}{\sqrt{2\pi}} \int_{-\infty}^{\infty} U_{(r,z)} e^{-i\kappa z} dz$$

k_c Rotational parameter to describe tangential velocity

C Parameter to describe tangential velocity imparted by rotor row

$$\Delta V r = C$$

ν Axial position of rotor row

L One half axial length of wall contraction

A Maximum slope of wall contraction

r_t Tip radius

r_h Hub radius

ΔH One half of radial contraction of wall shape

α Contraction ratio $\frac{\Delta H}{r_t - r_h}$

Δ Transform of boundary condition

$$\Delta = \frac{1}{\sqrt{2\pi}} \int_{-\infty}^{\infty} \hat{U}_{(r_h,\kappa)} \frac{U_1(\sqrt{\kappa^2 - \bar{\omega}^2} r)}{U_1(\sqrt{\kappa^2 - \bar{\omega}^2} r_h)} e^{i\kappa z} d\kappa$$

Δ_0 Value of Δ at $z = 0$

$\left(\frac{\partial \Delta}{\partial z}\right)_0$ Value of $\frac{\partial \Delta}{\partial z}$ at $z = 0$

Δ_n N^{th} coefficient of series $\Delta = \sum_{n=1}^{\infty} \Delta_n V_1(\xi_n r)$

$\left.\frac{\partial \Delta_0}{\partial z}\right|_n$ N^{th} coefficient of series $\frac{\partial \Delta}{\partial z} = \sum_{n=1}^{\infty} \left.\frac{\partial \Delta_0}{\partial z}\right|_n V_1(\xi_n r)$

R Radially dependent portion of solution for axial velocity perturbations

$$R = \left[\frac{i(J_0(i\frac{\pi r}{2L})}{J_1(i\frac{\pi r_n}{2L})} + \frac{4Lr_n}{\pi(r_t^2 - r_n^2)} \right]$$

I. INTRODUCTION

It has become usual in the theory of turbomachine flow to divide the process of describing the flow field into two nearly independent parts. One is the calculation of the effective mean flow field in which the individual blade rows may be considered located; the second is the calculation of the detailed flow about the individual blades. This subdivision is, of course, not strictly accurate, since it does not permit the treatment of important problems of secondary flow and other strictly three-dimensional phenomena.

The flow field calculated in the first step is designated the throughflow, and is almost invariably calculated as axially symmetric. Physically, this implies an infinite number of infinitely thin, lightly loaded bladees in each blade row. Some general, qualitative considerations of the throughflow were given by Ruden (1) and, although he did not develop any method for calculating the flow field in detail, he did note many of the simplifying features that have since gone into the development of the theory. The first actual calculation was a rather highly simplified treatment where only the flow field far downstream of a single blade row was determined when the flow far upstream was given. This calculation, which has become known as the radial equilibrium theory, was apparently conceived by several people almost simultaneously. W. Traupel (2) published an early account employing this approximation while Rannie (3) had been employing similar results in this country several years earlier. It appears now, too, that somewhat similar work had been done in England during the same general time period.

The only shortcomings of the radial equilibrium theory were that it applied only to compressor or turbine stages where the inner and outer radii were constant for a considerable distance upstream and downstream of the blade row, and that it gave no indication as to how this change in flow field developed between the stations far upstream and downstream of the blade row or through the blade row.

This latter difficulty was overcome to a large extent by Marble (4), who developed solutions for detailed flow field in the neighborhood and through a blade row of arbitrary loading. The blade row was, of course, considered to produce an axially symmetric flow field and consequently, the approximation within the blade row was likely to be poorer than that a short distance outside it. These calculations probably give more detail than the approximations of infinite blade number merit. Consequently, Marble (5), and later Marble and Michelson(6), developed a rather elementary approximation which, although less accurate than the original linearized treatment, is much simpler and convenient to apply in practice. This technique, which has become known as the exponential approximation, has since been exploited to a considerable extent by Railly (7) and by Horlock(8, 9).

The problem of calculating turbomachine throughflow in the presence of variations in hub and tip shroud radii has, to the present, been treated only by numerical means. The numerical calculations of Wu (10, 11) are more or less typical of the techniques employed. It is not particularly difficult, it turns out, to extend Marble's original linearized analysis to include hub and tip radii that vary by a small fraction of the total blade length. This analysis, carried out

in Chapter III of the following work, permits rather simple calculation of wall shapes of a rather general type in the presence of a lightly loaded blade row. Furthermore, it proves possible to extend the principle of the exponential approximation to include some of the wall shapes and hence the computations become extremely elementary.

Unfortunately, the most important problems are associated with the hub expansion in the neighborhood of the entrance vane and first rotor of an axial flow compressor. Here, because of the high loading of the entrance vane, the foregoing calculation is subject to some questions. This particular problem is treated in detail, therefore, employing a particular radial blade loading on the entrance guide vane, one that is fairly close to a solid body rotation. The equations of motion then become linear even in the presence of a large loading, in a manner similar to that of Bragg and Hawthorne (12), and it proves possible to obtain explicit solutions for an arbitrary, but small, variation of hub radius in the presence of heavily loaded guide vane and rotor.

II. GENERAL THROUGHFLOW THEORY

The flow is described (fig. 2) in a cylindrical coordinate system r, θ, z, by the velocity components u, v, w respectively. The corresponding radial, tangential, and axial vorticity components are

$$\xi = -\frac{\partial v}{\partial z} \tag{1}$$

$$\eta = \frac{\partial u}{\partial z} - \frac{\partial w}{\partial r} \tag{2}$$

$$\zeta = \frac{1}{r}\frac{\partial vr}{\partial r} \tag{3}$$

Denoting the axially symmetric force components corresponding to a blade row by F_r, F_θ, F_z, and denoting the stagnation pressure of the fluid as P, the equations of motion are

$$w\eta - v\zeta = F_r - \frac{\partial}{\partial r}\left(\frac{P}{\rho}\right) \tag{4}$$

$$u\zeta - w\xi = F_\theta \tag{5}$$

$$v\xi - u\eta = F_z - \frac{\partial}{\partial z}\left(\frac{P}{\rho}\right) \tag{6}$$

Variations in Total Pressure For the particular case of incompressible flow, the Euler turbine equation may be obtained in a simple manner. The first law of thermodynamics for a flow system with no external heat addition, states that the rate of increase of total head of the fluid is equal to the rate of work input to the fluid. It is advantageous, then, to follow fluid mass along the streamlines. If the length S is the distance measured from an arbitrary origin along the axially symmetric stream surface in a fixed meridional plane, then the derivative along the stream surface, moving with the fluid, is

$$V_s \frac{\partial}{\partial s} = u \frac{\partial}{\partial r} + w \frac{\partial}{\partial z} \tag{7}$$

where $V_s = \sqrt{u^2 + w^2}$ is the meridional velocity along the stream surface. Since the rate of work input to the fluid by the blades is simply $\omega r F_\theta$, where ω is the angular velocity of the blade, the first law may be written

$$V_s \frac{\partial}{\partial s}\left(\frac{P}{\rho}\right) = \omega r F_\theta \tag{8}$$

Equation 7, used with equations 1, 3 and 5 leads to

$$V_s \frac{\partial vr}{\partial s} = r F_\theta \tag{9}$$

Equations 8 and 9 may then be combined to give the differential form of the Euler turbine equation as applicable to incompressible flow,

$$V_s \frac{\partial}{\partial s}\left(\frac{p}{\rho}\right) = V_s \frac{\partial}{\partial s}(\omega v r) \tag{10}$$

The Tangential Vorticity The expression for the tangential vorticity, equation 2, shows that the tangential vorticity component includes both the radial and axial velocities, and since these components make up the throughflow, it is appropriate to investigate the propagation of tangential vorticity. In carrying out this analysis it will prove necessary to calculate the variation of quantities normal to the stream surfaces, and hence a length must be introduced to measure distance normal to the stream surface. This may be accomplished using the stream function ψ itself, which is defined by the properties that

$$u = \frac{1}{r}\frac{\partial \psi}{\partial z} \tag{11}$$

$$w = -\frac{1}{r}\frac{\partial \psi}{\partial r} \tag{12}$$

It may be seen from consideration of the flow between two nearby stream-surfaces, that the normal distance between surfaces differing in stream-function by $\delta\psi$ is given by $-\frac{1}{r V_s}\delta\psi$. The differential operator for rates of change normal to a stream surface is just $\frac{w}{V_s}\frac{\partial}{\partial r} - \frac{u}{V_s}\frac{\partial}{\partial z}$ so that we may write

$$-rV_s\frac{\partial}{\partial \psi} = \frac{w}{V_s}\frac{\partial}{\partial r} - \frac{u}{V_s}\frac{\partial}{\partial z} \tag{13}$$

Now, it is a simple matter to calculate the variation of total head $\frac{P}{\rho}$ normal to the streamsurface, by taking $\frac{\partial}{\partial r}\left(\frac{P}{\rho}\right)$ from equation 4, and $\frac{\partial}{\partial z}\left(\frac{P}{\rho}\right)$ from equation 6. Substituting these values into the right side of equation 13 gives

$$-rV_s\frac{\partial}{\partial\psi}\left(\frac{P}{\rho}\right) = \frac{W}{V_s}\left(F_r + V\xi - W\eta\right) - \frac{U}{V_s}\left(F_z + U\eta - V\zeta\right)$$

$$= -V_s\eta + \left(\frac{W}{V_s}F_r - \frac{U}{V_s}F_z\right) + \left(\frac{W}{V_s}V\xi + \frac{U}{V_s}V\zeta\right) \qquad (14)$$

Equation 14 may be interpreted as a relation for the tangential vorticity. The two groups of terms appearing on the right side of the equation, with the tangential vorticity, may be simplified somewhat. Equations 1, 3 and 13 give

$$\frac{W}{V_s}V\xi + \frac{U}{V_s}V\zeta = \frac{V}{r}\left(\frac{W}{V_s}\frac{\partial vr}{\partial r} - \frac{U}{V_s}\frac{\partial vr}{\partial z}\right)$$

$$= -V_s V\frac{\partial vr}{\partial\psi} \qquad (15)$$

The group $\frac{W}{V_s}F_r - \frac{U}{V_s}F_z$ is simply the force component normal to the stream surfaces and consequently it is convenient to define

$$F_\psi \equiv \frac{W}{V_s}F_r - \frac{U}{V_s}F_z \qquad (16)$$

Substitution of equations 15 and 16 into equation 14 leads to

$$\eta = r\frac{\partial}{\partial\psi}\left(\frac{P}{\rho}\right) - V\frac{\partial Vr}{\partial\psi} + \frac{1}{V_s}F_\psi \qquad (17)$$

This result was obtained for the more general case of compressible flow by Marble (13), as well as in more restricted form by Marble and Michelson (6), and Bragg and Hawthorne (12). In this form, the equation is not very useful for determining the tangential vorticity since differentiation occurs with respect to the unknown streamfunction, however, it is a very convenient guide for physical reasoning. The tangential vorticity associated with the force component F_ψ is essentially a "bound vorticity" and is of the same origin as the bound vorticity connected with the lift of a wing. If the angular momentum were invarient with ψ and the tangential vorticity depended on the total head only, then the flow outside of the blade row becomes relatively simple. It is clear from equation 8 that with no blade forces the total pressure remains constant along stream surfaces, and hence η/r is constant along a streamsurface. It is easily shown (4) that this result follows from the fact that the circulation about a physical annular vortex tube remains constant as it moves outside of a force field. On the other hand, if the total head was uniform, and again the space outside a blade row is considered, the tangential vorticity arises only from the angular momentum. But from equation 9, the angular momentum is constant along stream surfaces, and hence the quantity

ηr is constant along a stream surface. This result is related to the fact that the circulation about a given helical stream tube remains constant, but the stream tube itself may have a greater or smaller component in the tangential direction, depending upon how the stream tube is deformed by the flow.

The Mathematical Problem The velocity components U and W are of central interest, and thus the tangential vorticity, equation 17, will be the focus of attention. From equations 2, 11, and 12, it follows that:

$$\eta = \frac{\partial U}{\partial z} - \frac{\partial W}{\partial r} = \frac{\partial}{\partial z}\left(\frac{1}{r}\frac{\partial \psi}{\partial z}\right) + \frac{\partial}{\partial r}\left(\frac{1}{r}\frac{\partial \psi}{\partial r}\right) \tag{18}$$

The partial differential equation for the stream function is thus found to be

$$\frac{\partial}{\partial z}\left(\frac{1}{r}\frac{\partial \psi}{\partial z}\right) + \frac{\partial}{\partial r}\left(\frac{1}{r}\frac{\partial \psi}{\partial r}\right) = r\frac{\partial}{\partial \psi}\left(\frac{P}{\rho}\right) - V\frac{\partial Vr}{\partial \psi} + \frac{1}{V_s}F_\psi \tag{19}$$

The total head and angular momentum are described by equations 8 and 9 respectively.

It is now possible to make some statements regarding the formulation of the inverse problem, that is, where something other than the blade geometry is prescribed. The statements are not really conclusive because the non-linear nature of equation 19 precludes the guarantee of a well behaved solution under boundary conditions of any generality.

The results are of interest, however, because they do delineate the maximum amount of information that must be prescribed.

If one prescribes

1.) $\left(\frac{P}{\rho}\right)_{(r,z)}$ or $rV_{(r,z)}$ or $F_{\theta(r,z)}$ throughout the machine cf. equations 8, 9, 10),

2.) The blade shape or loading at the leading edge (cf. Ref. (6)),

3.) That the flow be tangential to inner and outer walls of given shape,

4.) The values of streamfunction, total head and angular momentum far upstream of any blade row,

5.) That the streamfunction, total head and angular momentum be regular far downstream,

then the details of the throughflow can be determined through solution of equation 19 together with such of equations 8, 9, 10 and 17 as are required for the quantity given under (1) above.

In the past considerable work has been done on the theory that the three dimensional flow field is assumed to be axially symmetrical. (4), (5) and (6) Physically this picture implies that the blade rows must consist of an infinite number of infinitely thin blades. This theory succeeds very well in describing the induced flow field in which the individual blades may be considered to be operating. However, while the description of the flow field induced by the blades is covered adequately by these theories, the effect of a variable hub radius or tip radius has not been considered.

It is nearly always the case in actual turbomachines that hub radius, tip radius or both vary along the direction of flow. In many instances, for example in the early stages of a multistage compressor, the hub and tip radii vary so much that the change of radius through a given blade row must be taken into account in determining the throughflow. While it is true that a significant portion of this change in radius may be to compensate for density changes in the fluid which, in this analysis, are being neglected, the general flow pattern about the mean flow is not so greatly changed by this compressibility effect, so that the incompressible flow pattern gives most of the necessary information. It is the effect of a variable wall radius that is most thoroughly investigated in the following sections.

The results of the following analysis could also be applied to the description of throughflow in axial flow water pumps, in which of course, the compressibility is not a factor. The so-called mixed flow compressor, in which the hub and tip radii are both increased should also be suitable for analysis by the following techniques, though care should be taken that the amplitude of the wall variation should not be such as to invalidate the linearizing assumptions used in the application of the boundary conditions.

III. EFFECT OF VARIABLE HUB AND TIP RADII

The effect of variable hub and tip radii on the flow field is to be determined, and then the results so found may be superimposed on the results previously obtained for the effects of blade loading [4]. The equation to be used for uniform inlet flow with no rotation may be seen from equation 19 to become

$$\frac{\partial}{\partial z}\left(\frac{1}{r}\frac{\partial \psi}{\partial z}\right) + \frac{\partial}{\partial r}\left(\frac{1}{r}\frac{\partial \psi}{\partial r}\right) = 0 \tag{20}$$

In this case, it is convenient to work with the radial velocity itself, and thus taking the derivative by z of equation 20, and making use of equation 11, we find that

$$\frac{\partial^2 u}{\partial r^2} + \frac{\partial}{\partial r}\left(\frac{u}{r}\right) + \frac{\partial^2 u}{\partial z^2} = 0 \tag{21}$$

The problem of throughflow with variable hub and tip radii is then described by equation 21 together with the boundary conditions

$$u(r_1, -\infty) = u(r_1, +\infty) = 0 \tag{22}$$

$$\frac{u}{w} = \frac{dr_t}{dz} \quad , \; r = r_t \tag{23}$$

$$\frac{u}{w} = \frac{dr_h}{dz} \quad , \; r = r_h \tag{24}$$

The quantities r_t and r_h refer to the variable hub and tip radii and will be prescribed for a given geometry. The boundary conditions given by equations 23 and 24 are non linear, and it is thus necessary to linearise them to allow solution of equation 21. This linearization is achieved simply by replacing the axial velocity by the undisturbed entrance velocity at infinity, $W^{(o)}$. This condition, then, restricts the perturbation in wall shape to be of small order. The linearized boundary conditions now become

$$U(r,-\infty) = U(r,+\infty) = 0 \tag{22}$$

$$\frac{U}{W^{(o)}} = \frac{dr_t}{dz} \quad , \quad r = r_t \tag{25}$$

$$\frac{U}{W^{(o)}} = \frac{dr_h}{dz} \quad , \quad r = r_h \tag{26}$$

Throughflow with Variable Hub Radius. - Consider the particular instance where $\frac{dr_t}{dz} = 0$, and $\frac{dr_h}{dz} = f_h(z)$ in equations 25 and 26 above. The most convenient form of solution is the Fourier transform with respect to z , the axial direction.

Denoting the Fourier transform of the radial velocity component by

$$\hat{U}_{(r,\kappa)} = \frac{1}{\sqrt{2\pi}} \int_{-\infty}^{\infty} U_{(r,z)} e^{-i\kappa z} \, dz \tag{27}$$

the homogeneous differential equation 21 becomes

$$\frac{d^2\hat{u}}{dr^2} + \frac{1}{r}\frac{d\hat{u}}{dr} - \left(\kappa^2 + \frac{1}{r^2}\right)\hat{u} = 0 \tag{28}$$

The boundary conditions transform as

$$\hat{u}_{(r_t,\kappa)} = 0 \tag{29}$$

$$\hat{u}_{(r_h,\kappa)} = \frac{W^{(0)}}{\sqrt{2\pi}}\int_{-\infty}^{\infty} f_h(z)\, e^{-i\kappa z}\, dz \equiv W^{(0)} F_h(\kappa) \tag{30}$$

The differential equation 28 has solutions $J_1(i\kappa r)$ and $Y_1(i\kappa r)$, and the constants obtained with substitution of equations 29 and 30 lead to the value for the transform variable of

$$\hat{u}_{(r,\kappa)} = W^{(0)} F_h(\kappa)\, \frac{J_1(i\kappa r)\, Y_1(i\kappa r_t) - J_1(i\kappa r_t)\, Y_1(i\kappa r)}{J_1(i\kappa r_h)\, Y_1(i\kappa r_t) - J_1(i\kappa r_t)\, Y_1(i\kappa r_h)} \tag{31}$$

The Fourier inversion theorem states that the value of the original function $u_{(r,z)}$ is given in terms of the transform variable $\hat{u}_{(r,\kappa)}$ by the relation

$$u_{(r,z)} = \frac{1}{\sqrt{2\pi}}\int_{-\infty}^{\infty} \hat{u}_{(r,\kappa)}\, e^{i\kappa z}\, d\kappa \tag{32}$$

Thus, using equations 31 and 32 the radial velocity induced by the hub variation is given by

$$\frac{(\quad)}{(\quad)} = \frac{1}{\sqrt{2\pi}} \int_{-\infty}^{\infty} F_h(K) \frac{J_1(iKr) Y_1(iKr_t) - J_1(iKr_t) Y_1(iKr)}{J_1(iKr_h) Y_1(iKr_t) - J_1(iKr_t) Y_1(iKr_h)} e^{iKz} dK \qquad (33)$$

Explicit solutions for particular forms of the hub shape are given by evaluation of the integral in equation 33; most generally this involves contour integration.

Simple Sinusoidal Step. - Consider a particular example where the hub slope is given by

$$\frac{\rho}{t_h}(z) = A \cos \frac{\pi z}{2L} \quad ; \quad |z| \leq L \qquad (34)$$

$$\frac{\rho}{t_h}(z) = 0 \quad ; \quad |z| \geq L \qquad (35)$$

as shown in figure 3. Then, the Fourier transform of the boundary shape, equation 30 yields

$$F_h(K) = \frac{A}{L} \sqrt{\frac{\pi}{2}} \frac{\cos(KL)}{\left(\frac{\pi}{2L}\right)^2 - K^2} \qquad (36)$$

In anticipation of employing contour integration to evaluate the integral of equation 33, the integrand may be rewritten in terms of the Hankel functions $H_1^{(1)}(iKr)$ and $H_1^{(2)}(iKr)$ of the first and second kinds to give, together with equation 36,

$$\frac{w(r,z)}{w^{(0)}} = \frac{A}{2L}\int_{-\infty}^{\infty} \frac{\cos(kL)}{\left(\frac{\pi}{2L}\right)^2 - k^2} \frac{H_1^{(1)}(ikr)\,H_1^{(2)}(ikr_t) - H_1^{(1)}(ikr_t)\,H_1^{(2)}(ikr)}{H_1^{(1)}(ikr_m)\,H_1^{(2)}(ikr_t) - H_1^{(1)}(ikr_t)\,H_1^{(2)}(ikr_m)} e^{ikz}\,dk \qquad (37)$$

Now the integral has poles at $k = \pm \frac{\pi}{2L}$ and at the roots of the denominator $H_1^{(1)}(ikr_m)\,H_1^{(2)}(ikr_t) - H_1^{(1)}(ikr_t)\,H_1^{(2)}(ikr_m) = 0$. There are in fact an infinite number of these roots on the positive and negative imaginary k axis. These roots are given by $ik = \pm \xi_n$ where the ξ_n are the roots of the equation

$$J_1(\xi_n r_m)\,Y_1(\xi_n r_t) - J_1(\xi_n r_t)\,Y_1(\xi_n r_m) = 0 \qquad (38)$$

Using the contour shown below, indented about the two singularities on the real axis, the integral along the axis may be evaluated in terms of the residues on the imaginary axis provided the integral along the arc vanishes.

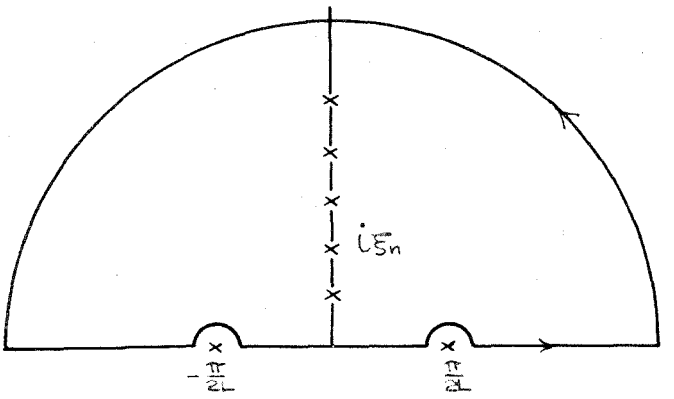

Inspection of the limiting behavior of the Hankel functions (see Copson (16) Pages 335 and 336) shows that this condition is assured when $Z > L$, that is downstream of the wall curvature. The two singularities on the real axis do not contribute in this case, and evaluation of the residues on the imaginary axis gives the value of the definite integral 37 to be

$$\frac{U}{W^{(0)}} = -\frac{A\pi}{L}\sum_{n=1}^{\infty}\frac{\cosh(\xi_n L)}{\xi_n^2 + \left(\frac{\pi}{2L}\right)^2} e^{-\xi_n Z} V_1(\xi_n r) \qquad L \le Z < \infty \tag{39}$$

where $V_1(\xi_n r)$ is the frequently occurring group of Bessel functions

$$V_1(\xi_n r) = \frac{J_1(\xi_n r) Y_1(\xi_n r_t) - J_1(\xi_n r_t) Y_1(\xi_n r)}{r_h\left[J_0(\xi_n r_h) Y_1(\xi_n r_t) - J_1(\xi_n r_t) Y_0(\xi_n r_h)\right] + r_t\left[J_1(\xi_n r_h) Y_0(\xi_n r_t) - J_0(\xi_n r_t) Y_1(\xi_n r_h)\right]} \tag{40}$$

In exactly the same manner, with the exception that the arc of the contour be drawn in the lower half plane, the solution for $Z < -L$ may be written

$$\frac{U}{W^{(0)}} = -\frac{A\pi}{L}\sum_{n=1}^{\infty}\frac{\cosh(\xi_n L)}{\xi_n^2 + \left(\frac{\pi}{2L}\right)^2} e^{\xi_n Z} V_1(\xi_n r) \qquad -\infty < Z \le -L \tag{41}$$

To find an appropriate solution in the region $-L \le Z \le L$ somewhat more consideration is required. The cosine of equation 36 may be written as $\cos(kL) = \frac{1}{2}\left(e^{ikL} + e^{-ikL}\right)$, and it may be seen that when the product of these terms is taken with e^{ikZ}, the value of the integral diverges over the large arc whether the arc is taken in the upper or

lower half plane. However, when the exponentials are considered separately, the integral involving $\frac{1}{2}e^{ikL}$ converges in the upper half plane, and the integral involving $\frac{1}{2}e^{-ikL}$ converges in the lower half plane. Thus these separate integrals may be evaluated, and the desired result obtained by summing the solutions. Carrying out the evaluation in detail, it is found that the residues on the real axis contribute also, so that the radial velocity is given by

$$\frac{U}{W^{(0)}} = A\left[\frac{U_1(i\frac{\pi r}{2L})}{U_1(i\frac{\pi r_h}{2L})}\cos\frac{\pi z}{2L} - \frac{\pi}{L}\sum_{n=1}^{\infty}\frac{\cosh(\xi_n z)}{\xi_n^2+(\frac{\pi}{2L})^2}e^{-\xi_n L}V_1(\xi_n r)\right] \qquad -L\le z\le L \tag{42}$$

Where $U_1(i\frac{\pi r}{2L})$ and $U_1(i\frac{\pi r}{2L})$ are the linear combinations of Bessel functions of order one

$$U_1(i\tfrac{\pi r}{2L}) = J_1(i\tfrac{\pi r}{2L})Y_1(i\tfrac{\pi r_t}{2L}) - J_1(i\tfrac{\pi r_t}{2L})Y_1(i\tfrac{\pi r}{2L}) \tag{43}$$

$$U_1(i\tfrac{\pi r_h}{2L}) = J_1(i\tfrac{\pi r_h}{2L})Y_1(i\tfrac{\pi r_t}{2L}) - J_1(i\tfrac{\pi r_t}{2L})Y_1(i\tfrac{\pi r_h}{2L}) \tag{44}$$

The continuity equation for axially symmetric flow may be written

$$\frac{\partial W}{\partial z} = -\frac{1}{r}\frac{\partial ru}{\partial r} \tag{45}$$

It is thus an elementary matter to integrate this equation to develop the expressions for the axial velocity perturbations. It follows from equation 45 that

$$\frac{W}{W^{(0)}} - 1 = -\int_{-\infty}^{z} \frac{1}{r}\frac{\partial}{\partial r}\left(r\frac{U}{W^{(0)}}\right) dz \tag{46}$$

where the appropriate representation of $\frac{U}{W^{(0)}}$ must be employed in each of the three regions. Assuming the axial velocity to be undistorted far upstream of the hub curvature, the axial velocity perturbation in the region $-\infty < z \leq -L$ may be written, using equation 40, as

$$\frac{W}{W^{(0)}} - 1 = \frac{A\pi}{L}\sum_{n=1}^{\infty} \frac{\cosh(\xi_n L)}{\xi_n^2 + \left(\frac{\pi}{2L}\right)^2} e^{\xi_n z} V_0(\xi_n r) \qquad -\infty < z \leq -L \tag{47}$$

where $V_0(\xi_n r)$ is the group of Bessel functions

$$V_0(\xi_n r) = \frac{J_0(\xi_n r) Y_1(\xi_n r_t) - J_1(\xi_n r_t) Y_0(\xi_n r)}{r_h\left[J_0(\xi_n r_h) Y_1(\xi_n r_t) - J_1(\xi_n r_t) Y_0(\xi_n r_h)\right] + r_t\left[J_1(\xi_n r_h) Y_0(\xi_n r_t) - J_0(\xi_n r_t) Y_1(\xi_n r_h)\right]} \tag{48}$$

Similarly, it is found

$$\frac{W}{W^{(0)}} - 1 = -A\,\frac{iU_0\left(i\frac{\pi r}{2L}\right)}{U_1\left(i\frac{\pi r_h}{2L}\right)}\left[1 + \sin\frac{\pi z}{2L}\right] + \frac{A\pi}{L}\sum \frac{1 + e^{-\xi_n L}\sinh(\xi_n z)}{\xi_n^2 + \left(\frac{\pi}{2L}\right)^2} V_0(\xi_n r) \tag{49}$$

Where $U_0\left(i\frac{\pi r}{2L}\right)$ is the group of Bessel functions

$$U_0\left(i\frac{\pi r}{2L}\right) = J_0\left(i\frac{\pi r}{2L}\right) Y_1\left(i\frac{\pi r_t}{2L}\right) - J_1\left(i\frac{\pi r_t}{2L}\right) Y_0\left(i\frac{\pi r}{2L}\right) \tag{50}$$

It should be noted that computation of the groups $U_0(i\frac{\pi r}{2L})$ and $U_1(i\frac{\pi r_h}{2L})$ requires that these groups be rewritten in the following form to facilitate use of the tables of functions of Jahnke and Emde [17].

$$\frac{i\,U_0(i\frac{\pi r}{2L})}{U_1(i\frac{\pi r_h}{2L})} = \frac{J_0(i\frac{\pi r}{2L})\left[-H_1^{(1)}(i\frac{\pi r_h}{2L})\right] + \left[-iJ_1(i\frac{\pi r_h}{2L})\right]\left[iH_0^{(1)}(i\frac{\pi r}{2L})\right]}{\left[-iJ_1(i\frac{\pi r_h}{2L})\right]\left[-H_1^{(1)}(i\frac{\pi r_h}{2L})\right] - \left[-iJ_1(i\frac{\pi r_h}{2L})\right]\left[-H_1^{(1)}(i\frac{\pi r_h}{2L})\right]} \tag{51}$$

Finally, downstream of the wall distortion,

$$\frac{W}{W^{(0)}} - 1 = -2A\,\frac{i\,U_0(i\frac{\pi r}{2L})}{U_1(i\frac{\pi r_h}{2L})} + \frac{A\pi}{L}\sum_{n=1}^{\infty}\frac{2 - e^{-\xi_n z}\cosh(\xi_n L)}{\xi_n^2 + (\frac{\pi}{2L})^2}\,V_0(\xi_n r) \qquad L \le z < \infty \tag{52}$$

Asymptotic Approximations. - While equations 47, 49 and 52 describe the axial velocity throughout the machine, computation is laborious because of the presence of the infinite series throughout the equations. Consideration of the axial velocity profile at infinity leads to a useful asymptotic approximation. If now the axial velocity profile is uniform and the tangential velocity vanishes (or has the distribution of a vortex) for upstream of the contraction, then the axial velocity profile for downstream will be uniform. By continuity, the uniform perturbation on the axial velocity for downstream is just

$$\frac{W}{W^{(0)}} - 1 = \frac{A\,r_h}{r_t + r_h} \tag{53}$$

and according to equation 52 it is clear then that

$$\frac{4\alpha r_n}{r_t + r_n} = -2A \frac{jU_0(j\frac{\pi r}{2L})}{U_1(j\frac{\pi r_n}{2L})} + \frac{A\pi}{L}\sum_{n=1}^{\infty} \frac{2}{\xi_n^2 + (\frac{\pi}{2L})^2} V_0(\xi_n r) \qquad (54)$$

In particular, the radial dependence of the two functions on the right side of equation 54 cancels to give a constant result. This same result could have been obtained directly by a symmetry argument about the point $z = 0$. In this case equation 49 with $z = 0$ should be used. Noting that α may be written as $\alpha = 2\frac{A_L}{\pi}\frac{1}{r_t - r_n}$, the summation of equation 54 is seen to be

$$\sum_{n=1}^{\infty} \frac{V_0(\xi_n r)}{\xi_n^2 + (\frac{\pi}{2L})^2} = \frac{1}{2(\frac{\pi}{2L})^2}\left[\frac{(j\frac{\pi}{2L})U_0(j\frac{\pi r}{2L})}{U_1(j\frac{\pi r_n}{2L})} + \frac{2r_n}{r_t^2 - r_n^2}\right] \qquad (55)$$

This summation is actually a special case of the following more general summation which is used extensively in later chapters.

$$\sum_{n=1}^{\infty} \frac{V_0(\xi_n r)}{\xi_n^2 - \beta^2} = -\frac{1}{2\beta^2}\left[\frac{\beta U_0(\beta r)}{U_1(\beta r_n)} + \frac{2r_n}{r_t^2 - r_n^2}\right] \qquad (56)$$

In equation 56, β may be any constant, real or complex. This result is relatively easy to check by Fourier-Bessel expansion of the right side.

The asymptotic approximation, then, consists of noting that the terms of principal importance in the summation are those corresponding to the first characteristic value ξ_1. Thus,

assuming that the Z dependence of the summation terms is that of the first term in the series, and using the results obtained in equations 54, 55 and 56, the axial velocity distribution may be denoted in the following approximate form:

$$\frac{W}{W^{(0)}} - 1 = A\left[\frac{i(J_0(i\frac{\pi r}{2L})}{J_1(i\frac{\pi r_h}{2L})} + \frac{4Lr_h}{\pi(r_t^2 - r_h^2)}\right]\cosh(\xi_1 L)\, e^{\xi_1 Z} \qquad -\infty < Z \leq L \tag{57}$$

$$\frac{W}{W^{(0)}} - 1 = A\left[\frac{i(J_0(i\frac{\pi r}{2L})}{J_1(i\frac{\pi r_h}{2L})} + \frac{4Lr_h}{\pi(r_t^2 - r_h^2)}\right]\left[e^{-\xi_1 L}\sinh(\xi_1 Z) - \sin\frac{\pi Z}{2L}\right]$$

$$+ \frac{A4Lr_h}{\pi(r_t^2 - r_h^2)}\left(1 + \sin\frac{\pi Z}{2L}\right) \qquad -L \leq Z \leq L \tag{58}$$

$$\frac{W}{W^{(0)}} - 1 = 2A\left[\frac{i(J_0(i\frac{\pi r}{2L})}{J_1(i\frac{\pi r_h}{2L})} + \frac{4Lr_h}{\pi(r_t^2 - r_h^2)}\right]\left[1 - \frac{1}{2}\cosh(\xi_1 L)\, e^{-\xi_1 Z}\right] + \frac{A8Lr_h}{\pi(r_t^2 - r_h^2)} \tag{59}$$

$$L \leq Z < \infty$$

The axial velocity profiles have been calculated at several axial positions using these approximate forms, and the results are shown in figure 4. It is evident from the equations that the axial velocity is antisymmetric with respect to the origin, and for this reason, only stations upstream of $Z = 0$ have been plotted. It will be noted that only the perturbation about the mean has been graphed ($\overline{W}$). The approximate velocity profiles have been compared to those obtained by computing with the series at two stations, and the results are compared in figures 5 and 6. It may be seen that the asymptotic approximations are indeed quite accurate, and are certainly incomparably easier to calculate than are the full Fourier-Bessel expansions.

The radial dependence of the solution has been graphed for several values of hub to tip ratio $\left(\frac{r_{h(0)}}{r_t}\right)$ and for two values of overall contraction in figures 7 and 8. In order to obtain a velocity profile at any given value of axial position, it is then simply necessary to select the curve for the appropriate value of α and $\left(\frac{r_h}{r_t}\right)$, and then to multiply by the appropriate factor as obtained from the dependent portions of equations 57, 58 and 59.

Throughflow With Variable Tip Radius. - When it is the tip radius rather than the root radius that varies along the direction of flow, the procedure for calculating the flow is changed only slightly. If now $\frac{dr_t}{dz} = f_t(z)$ and $\frac{dr_h}{dz} = 0$, equation 30 is replaced by

$$\hat{U}_{(r,\kappa)} = \frac{W^{(0)}}{\sqrt{2\pi}} \int_{-\infty}^{\infty} f_t(z)\, e^{-i\kappa z}\, dz \equiv\equiv W^{(0)} F_t(\kappa) \tag{60}$$

Similarly the Fourier inversion gives, corresponding to equation 33

$$\frac{U(r,z)}{W^{(0)}} = \frac{1}{\sqrt{2\pi}} \int_{-\infty}^{\infty} F_t(\kappa) \frac{J_1(i\kappa r_h) Y_1(i\kappa r) - J_1(i\kappa r) Y_1(i\kappa r_h)}{J_1(i\kappa r_h) Y_1(i\kappa r_t) - J_1(i\kappa r_t) Y_1(i\kappa r_h)}\, e^{i\kappa z}\, d\kappa \tag{61}$$

Note here that only the numerator of the bracketed term is changed from its value in equation 33 where the hub radius is varying. Hence in the ensuing contour integration, the only differences that appear from the previous case are modifications of the numerator. If, for example, the slope of the tip contour had been given as

$$f_t(z) = B\cos\frac{\pi z}{2L} \quad ; \quad |z| \le L$$
$$f_t(z) = 0 \quad ; \quad |z| \ge L \tag{62}$$

While the hub diameter remains constant, the appropriate solutions for the radial and axial velocities can be obtained by substituting the expressions

$${}_tV_1(\xi_n r) = \frac{J_1(\xi_n r_h)Y_1(\xi_n r) - J_1(\xi_n r)Y_1(\xi_n r_h)}{r_h\left[J_0(\xi_n r_h)Y_1(\xi_n r_t) - J_1(\xi_n r_t)Y_0(\xi_n r_h)\right] + r_t\left[J_1(\xi_n r_h)Y_0(\xi_n r_t) - J_0(\xi_n r_t)Y_1(\xi_n r_h)\right]}$$

$${}_tV_0(\xi_n r) = \frac{J_1(\xi_n r_h)Y_0(\xi_n r) - J_1(\xi_n r)Y_1(\xi_n r_h)}{r_h\left[J_0(\xi_n r_h)Y_1(\xi_n r_t) - J_1(\xi_n r_t)Y_0(\xi_n r_h)\right] + r_t\left[J_1(\xi_n r_h)Y_0(\xi_n r_t) - J_0(\xi_n r_t)Y_1(\xi_n r_h)\right]}$$

$${}_tU_1(i\tfrac{\pi r}{2L}) = J_1(i\tfrac{\pi r_h}{2L})Y_1(i\tfrac{\pi r}{2L}) - J_1(i\tfrac{\pi r}{2L})Y_1(i\tfrac{\pi r_h}{2L})$$

$${}_tU_0(i\tfrac{\pi r}{2L}) = J_1(i\tfrac{\pi r_h}{2L})Y_0(i\tfrac{\pi r}{2L}) - J_0(i\tfrac{\pi r}{2L})Y_1(i\tfrac{\pi r_h}{2L}) \tag{63}$$

respectively in place of the previously obtained expressions for $V_1(\xi_n r), V_0(\xi_n r), U_1(i\frac{\pi r}{2L}), U_0(i\frac{\pi r}{2L})$, equations 39, 43, 48, 50.

In addition, it should be noted that the equivalent summation to equation 55 becomes

$$\sum_{n=1}^{\infty} \frac{{}_tV_0(\xi_n r)}{\xi_n^2 + (\frac{\pi}{2L})^2} = \frac{1}{2(\frac{\pi}{2L})^2}\left[\frac{(i\frac{\pi}{2L})\,{}_tU_0(i\frac{\pi r}{2L})}{{}_tU_1(i\frac{\pi r_h}{2L})} - \frac{2r_t}{r_t^2 - r_h^2}\right] \tag{64}$$

The equations for the variation of axial velocity then become

$$\frac{W}{W^{(0)}} - 1 = B\left[\frac{{}_tU_0(i\frac{\pi r}{2L})}{{}_tU_1(i\frac{\pi r_h}{2L})} - \frac{4Lr_t}{\pi(r_t^2 - r_h^2)}\right]\cosh(\xi_1 L)\,e^{\xi_1 z} \tag{65}$$
$$-\infty < z \le -L$$

$$\frac{W}{W^{(0)}} - 1 = B\left[\frac{i_t J_0\left(i\frac{\pi r}{2L}\right)}{+J_1\left(i\frac{\pi r_h}{2L}\right)} - \frac{4L\xi_t}{\pi(\xi_t^2 - r_h^2)}\right]\left[e^{-\xi_1 L}\sinh(\xi_1 z) - \sin\frac{\pi z}{2L}\right] - \frac{B4-\xi_t}{\pi(\xi_t^2-r_h^2)}\left(1+\sin\frac{\pi z}{2L}\right) \quad (66)$$

$$-L \le z \le L$$

$$\frac{W}{W^{(0)}} - 1 = 2B\left[\frac{i_t J_0\left(i\frac{\pi r}{2L}\right)}{+J_1\left(i\frac{\pi r_h}{2L}\right)} - \frac{4L\xi_t}{\pi(\xi_t^2 - r_h^2)}\right]\left[1 - \tfrac{1}{2}\cosh(\xi_1 L)e^{-\xi_1 z}\right] - \frac{BBL\xi_t}{\pi(\xi_t^2-r_h^2)} \quad (67)$$

$$L \le z < \infty$$

It should be noted that the term B, the maximum slope of the wall, will be negative for a contracting wall shape. It is clear also that since the problem is a linear one, the situation where both hub and tip radii vary can be treated by superposition of the perturbations caused by hub variation only and tip variation only.

Hub Shape Consisting of Cosine and Exponential Curves. - Consider a particular example where the hub slope is given by

$$\begin{aligned} f_h(z) &= 0 && -\infty < z \le -L \\ f_h(z) &= A\cos\frac{\pi z}{2L} && -L \le z \le 0 \\ f_h(z) &= Ae^{-\frac{A}{c}z} \end{aligned} \quad (68)$$

as shown in figure 9. In this case the Fourier transform of the boundary shape, equation 30 yields

$$F_h(\kappa) = \frac{A}{2L}\sqrt{\frac{\pi}{2}}\left[\frac{1}{\left(\frac{\pi}{2L}\right)^2 - \kappa^2}\left(e^{i\kappa L} - i\kappa\frac{2L}{\pi}\right)\right] + \frac{A}{\sqrt{2\pi}}\frac{A/c - i\kappa}{\left(A/c\right)^2 + \kappa^2} \quad (69)$$

The radial velocity is thus given in terms of the two integrals

$$\frac{U(r,z)}{W^{(0)}} = \frac{A}{4L}\int_{-\infty}^{\infty} \frac{e^{ikL} - ik\frac{2L}{\pi}}{\left(\frac{\pi}{2L}\right)^2 - k^2} \frac{U_1(ikr)}{U_1(ikr_n)} e^{ikz}\, dk + \frac{A}{2\pi}\int_{-\infty}^{\infty} \frac{1}{A/c + ik} \frac{U_1(ikr)}{U_1(ikr_n)} e^{ikz}\, dk \qquad (70)$$

In which the groups $U_1(ikr)$ and $U_1(ikr_n)$ are directly analogous to the groups of equations 43 and 44 and are given by

$$U_1(ikr) = J_1(ikr)\,Y_1(ikr_t) - J_1(ikr_t)\,Y_1(ikr)$$

$$U_1(ikr_n) = J_1(ikr_n)\,Y_1(ikr_t) - J_1(ikr_t)\,Y_1(ikr_n) \qquad (71)$$

These integrals are evaluated in a similar manner as was the integral of equation 36. The poles of the first integral of equation 70 are located exactly as were the poles of the integral in equation 36. The second integral of equation 70 again has poles at the zeros of the denominator $U_1(\xi_n r_n) = 0$, and also has a single pole at $k = iA/c$, but does not have any poles on the real axis. This latter situation is shown in the sketch below.

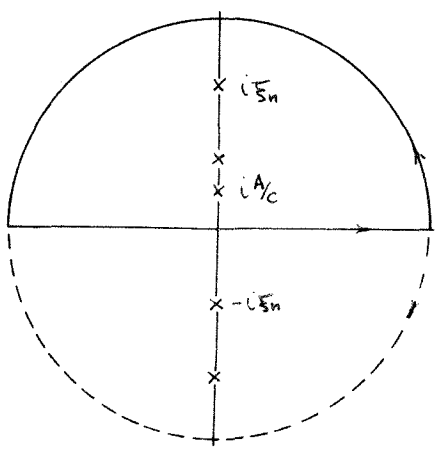

It can be seen from inspection of the integrals in equation 70, together with the previously mentioned consideration of the limiting behavior of the groups of Bessel functions, that evaluation of the portion of the first integral of equation 70 involving e^{ikL} requires that the arc of the contour be drawn in the upper half plane for $z > -L$, and be drawn in the lower half plane for $z < -L$. Similarly the portion of the first integral not involving the exponential,

and the second integral both require that the arc be drawn in the upper half plane for $z<0$, and that the arc be drawn in the lower half plane for $z>0$. Carrying out the required integrations, the radial velocity is found to be

$$\frac{u(r,z)}{W^{(0)}} = A\sum_{n=1}^{\infty}\left[\frac{\xi_n - \frac{\pi}{2L}}{\xi_n^2 + \left(\frac{\pi}{2L}\right)^2} e^{\xi_n L} - \frac{1}{\xi_n + A/c}\right] V_1(\xi_n r)\, e^{\xi_n z} \qquad -\infty < z \le -L \tag{72}$$

$$\frac{u(r,z)}{W^{(0)}} = A\,\frac{J_1\left(i\frac{\pi r}{2L}\right)}{J_1\left(i\frac{\pi r_0}{2L}\right)}\cos\frac{\pi z}{2L} + A\sum_{n=1}^{\infty}\left[\frac{\xi_n e^{\xi_n z} - \frac{\pi}{2L}e^{-\xi_n(L+z)}}{\xi_n^2 + \left(\frac{\pi}{2L}\right)^2} - \frac{e^{\xi_n z}}{\xi_n + A/c}\right] V_1(\xi_n r) \qquad -L \le z \le 0 \tag{73}$$

$$\frac{u(r,z)}{W^{(0)}} = A\,\frac{J_1(A/c\, r)}{J_1(A/c\, r_0)} e^{-A/c\, z} - A\sum_{n=1}^{\infty}\left[\frac{\xi_n + \left(\frac{\pi}{2L}\right)e^{-\xi_n L}}{\xi_n^2 + \left(\frac{\pi}{2L}\right)^2} + \frac{1}{A/c - \xi_n}\right] V_1(\xi_n r)\, e^{-\xi_n z} \qquad 0 \le z < \infty \tag{74}$$

Consideration of the equations 73 and 74 at the station leads to the evaluation of another series, the general form of which is

$$\sum_{n=1}^{\infty}\frac{\xi_n V_1(\xi_n r)}{\xi_n^2 - \beta^2} = -\frac{1}{2}\,\frac{J_1(\beta r)}{J_1(\beta r_0)} \tag{75}$$

Again, β may be any constant, real or complex. This series, like equation 56 is easy to check by Fourier-Bessel expansion. This result will be used extensively in later chapters.

The axial velocity is again computed by use of equation 46, and found to be

$$\frac{W}{W^{(0)}} - 1 = A \sum_{n=1}^{\infty} \left[\frac{\frac{\pi}{2L} e^{\xi_n L} - \xi_n}{\xi_n^2 + \left(\frac{\pi}{2L}\right)^2} + \frac{1}{\xi_n + A/C} \right] V_0(\xi_n r) e^{\xi_n z} \qquad -\infty < z \leq 0 \qquad (76)$$

$$\frac{W}{W^{(0)}} - 1 = -A \left[\left(\frac{J_0\left(i\frac{\pi r}{2L}\right)}{J_1\left(i\frac{\pi r_h}{2L}\right)} + \frac{4Lr_h}{\pi(r_t^2 - r_h^2)} \right] \sin\frac{\pi z}{2L} - \frac{A\pi}{2L} \sum_{n=1}^{\infty} \frac{e^{-\xi_n(L+z)}}{\xi_n^2 + \left(\frac{\pi}{2L}\right)^2} V_0(\xi_n r)$$

$$- A \sum_{n=1}^{\infty} \left[\frac{\xi_n}{\xi_n^2 + \left(\frac{\pi}{2L}\right)^2} - \frac{1}{\xi_n + A/C} \right] e^{\xi_n z} + \frac{A4Lr_h}{\pi(r_t^2 - r_h^2)} \left(1 + \sin\frac{\pi z}{2L}\right) \qquad -L \leq z \leq 0 \qquad (77)$$

$$\frac{W}{W^{(0)}} - 1 = A \left[\frac{J_0(A/C\, r)}{J_1(A/C\, r_h)} + \frac{2r_h}{A/C(r_t^2 - r_h^2)} \right] e^{-\frac{A}{C}z} + A \sum_{n=1}^{\infty} \frac{1}{\xi_n - A/C} V_0(\xi_n r) e^{-\xi_n z}$$

$$- A \sum_{n=1}^{\infty} \frac{\xi_n + \frac{\pi}{2L} e^{-\xi_n L}}{\xi_n^2 + \left(\frac{\pi}{2L}\right)^2} V_0(\xi_n r) e^{-\xi_n z} + \frac{A4Lr_h}{\pi(r_t^2 - r_h^2)} + \frac{2Cr_h}{r_t^2 - r_h^2} \left(1 - e^{-A/C\, z}\right) \qquad 0 \leq z < \infty \qquad (78)$$

An example set of curves has been plotted in figure 10. The geometry considered here was a hub to tip ratio of $\frac{r_h}{r_t} = 0.4$. The contraction in the "cosine" section of the hub was put equal to that in the "exponential" section, and both were given a contraction ratio $\alpha = \frac{\Delta H}{r_t - r_h}$ of $\alpha = 0.1$.

It will be noted that the magnitudes of the perturbations in the exponential section of the hub are in general somewhat smaller than those found in the cosine section. This might be expected when the behavior of the flow through the simple sinusoidal step is reviewed. In that case the flow was antisymmetric with respect to $z = 0$, and was seen to reduce in axial velocity near the hub, till the contraction was reached. It then reversed this tendency throughout the contraction,

the axial velocity speeding up throughout $-L \leq z \leq L$. This may be seen to be interpreted as the flow "seeing an obstacle" on approaching $z = -L$, and starting to flow out away from the obstruction. Within $-L \leq z \leq L$, the fluid is forced upward, however, so that an increase in velocity takes place. The effect of the exponential wall shape, however, is to combine the two disturbances, in that though the fluid sees a rising wall approaching, it is at the same time forced gradually upward, the two effects tending to cancel.

The contribution of the variation in hub radius to the distortion in axial velocity can be compared in magnitude to the distortion obtained from the effects of blade loading as given for example in reference (4) . The maximum velocity distortion for the geometry considered here, can be seen from figure 4 to be approximately $\overline{\overline{W}}_{(r,z)_{MAX}} = 0.6$. Comparison with the results of reference (4) shows that such a maximum distortion would be created by a blade row under solid body loading that imparts a tangential velocity given approximately by $\frac{V^{(0)}}{W^{(0)}} = 0.5$ at the tip radius. This corresponds to fairly high loading conditions, so that it can be seen that the effects of variation of wall radius are of much the same magnitude as are the effects of blade loading.

IV. EFFECT OF LARGE INLET ROTATION

It often happens that the flow entering a turbomachine has a large rotation associated with it. This rotation affects the magnitude and rate of formation of the velocity profiles to a large degree. In particular, the decreased decay rate of the velocity profile may invalidate the assumption often made that the inlet guide vanes are located a large distance upstream.

The effect of a "solid body" rotation at inlet is to be investigated, the inlet flow considered being described by

$$\begin{aligned} V(r_1,-\infty) &= -k\frac{\psi}{r} \equiv V^{(0)} \\ W(r_1,-\infty) &= W^{(0)} \\ U(r_1,-\infty) &= 0 \end{aligned} \tag{79}$$

The value of the stream function at infinity is given by $\psi = -\frac{W^{(0)}}{2} r^2$. With equation 79, the group in equation 19 becomes

$$-V\frac{\partial rV}{\partial \psi} = -\frac{1}{r}k^2\psi \tag{80}$$

The total head at infinity must also be investigated. The equation of motion in the radial direction equation 5 gives

$$\frac{\partial p}{\partial r} = \rho\frac{V^2}{r} = \rho k^2 \frac{W^{(0)2}}{4} r \tag{81}$$

so that the pressure distribution at infinity is seen to be

$$p = p_0 - \frac{\rho k^2 W^{(0)}}{4} \psi \tag{82}$$

in which p_0 may be considered to be the pressure at the hub.

Thus, the total head at inlet is given by

$$\begin{aligned} \frac{P}{\rho} &= \frac{p}{\rho} + \frac{1}{2}\left(V^{(0)2} + W^{(0)2} \right) \\ &= \frac{p_0}{\rho} - \frac{k^2 W^{(0)}}{2} \psi + \frac{W^{(0)2}}{2} \end{aligned} \tag{83}$$

With equations 83 and 80, equation 19 thus becomes

$$\frac{\partial}{\partial r}\left(\frac{1}{r}\frac{\partial \psi}{\partial r}\right) + \frac{\partial}{\partial z}\left(\frac{1}{r}\frac{\partial \psi}{\partial z}\right) = -\frac{k^2 W^{(0)}}{2} r - \frac{1}{r} k^2 \psi \tag{84}$$

It is again convenient to work with the radial velocity itself, and taking the derivative by z of equation 84 and making use of equation 11, it is found that

$$\frac{\partial^2 u}{\partial r^2} + \frac{1}{r}\frac{\partial u}{\partial r} + \left\{ k^2 - \frac{1}{r^2} \right\} u + \frac{\partial^2 u}{\partial z^2} = 0 \tag{85}$$

The problem of throughflow with variable hub and tip radii, and with solid body inlet is then described by equation 85 and the linearized boundary conditions, equations 22, 25, 26; that is

$$u(r, -\infty) = u(r, +\infty) = 0 \tag{22}$$

$$\frac{u}{W^{(0)}} = \frac{dr_t}{dz} \qquad \text{on} \quad r = r_t \tag{25}$$

$$\frac{u}{W^{(0)}} = \frac{dr_h}{dz} \qquad \text{on} \quad r = r_h \tag{26}$$

Once again denoting the Fourier transform of the radial velocity component by

$$\hat{u}_{(r,k)} = \frac{1}{\sqrt{2\pi}} \int_{-\infty}^{\infty} u(r,z)\, e^{-ikz}\, dz \tag{86}$$

the differential equation is obtained

$$\frac{d^2\hat{u}}{dr^2} + \frac{1}{r}\frac{d\hat{u}}{dr^2} - \left(\{k^2 - \alpha^2\} + \frac{1}{r^2}\right)\hat{u} = 0 \tag{87}$$

The boundary conditions again transform as

$$\hat{u}_{(r_t,k)} = 0 \tag{29}$$

$$\hat{u}_{(r_h,k)} = \frac{W^{(0)}}{\sqrt{2\pi}} \int_{-\infty}^{\infty} f_h(z)\, e^{-ikz}\, dz \equiv W^{(0)} F_h(k) \tag{30}$$

The differential equation 87 has solutions $J_1(i\sqrt{k^2-\alpha^2}\,r)$ and $Y_1(i\sqrt{k^2-\alpha^2}\,r)$, and with equations 29 and 30, there results

$$\hat{u}_{(r,k)} = W^{(0)} F_h(k)\, \frac{J_1(i\sqrt{k^2-\alpha^2}\,r)\, Y_1(i\sqrt{k^2-\alpha^2}\,r_t) - J_1(i\sqrt{k^2-\alpha^2}\,r_t)\, Y_1(i\sqrt{k^2-\alpha^2}\,r)}{J_1(i\sqrt{k^2-\alpha^2}\,r_h)\, Y_1(i\sqrt{k^2-\alpha^2}\,r_t) - J_1(i\sqrt{k^2-\alpha^2}\,r_t)\, Y_1(i\sqrt{k^2-\alpha^2}\,r_h)} \tag{88}$$

$$\equiv W^{(0)} F_h(k)\, \frac{U_1(i\sqrt{k^2-\alpha^2}\,r)}{U_1(i\sqrt{k^2-\alpha^2}\,r_h)} \tag{89}$$

Thus it is found that the radial velocity is given in terms of the inversion integral as

$$\frac{U(r,z)}{W^{(0)}} = \frac{1}{\sqrt{2\pi}} \int_{-\infty}^{\infty} F_n(\kappa) \frac{U_1(i\sqrt{\kappa^2-k^2}\, r)}{U_1(i\sqrt{\kappa^2-k^2}\, r_n)} e^{i\kappa z} d\kappa \qquad (90)$$

Considering the simple sinusoidal step, the Fourier transform of the boundary condition is again given by

$$F_n(\kappa) = \frac{A}{L}\sqrt{\frac{\pi}{2}} \frac{\cos(\kappa L)}{\left(\frac{\pi}{2L}\right)^2 - \kappa^2} \qquad (35)$$

The integral for the radial velocity thus becomes

$$\frac{U(r,z)}{W^{(0)}} = \frac{A}{2L} \int_{-\infty}^{\infty} \frac{\cos(\kappa L)}{\left(\frac{\pi}{2L}\right)^2 - \kappa^2} \frac{U_1(i\sqrt{\kappa^2-k^2}\, r)}{U_1(i\sqrt{\kappa^2-k^2}\, r_n)} e^{i\kappa z} d\kappa \qquad (91)$$

The poles of the integral are now found at $\kappa = \pm \frac{\pi}{2L}$, and at $i\sqrt{\kappa^2-k^2} = \xi_n$, the characteristic roots of equation 37. The limiting behaviour of the large arcs does not change from that found in evaluation of the integral in equation 36, so that integrating around the appropriate contour of the sketch shown below, the expressions for the radial velocity are found to be

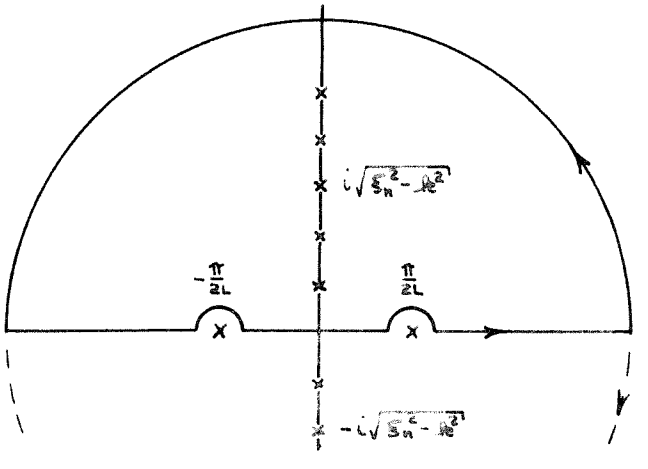

$$\frac{U(r,z)}{W^{(0)}} = -\frac{A\pi}{L}\sum_{n=1}^{\infty}\frac{S_n}{r_{1n}}\frac{\cos n\eta_{1n}L}{S_n^2-\beta^2}V_1(S_n r)\,e^{-\eta_{1n}z} \qquad -\infty < z \le -L \tag{92}$$

$$\frac{U(r,z)}{W^{(0)}} = A\left\{\frac{U_1(\beta r)}{U_1(\beta r_0)}\cos\frac{\pi z}{L} - \frac{\pi}{L}\sum_{n=1}^{\infty}\frac{S_n}{r_{1n}}\frac{\cos n\eta_{1n}z}{S_n^2-\beta^2}V_1(S_n r)\,e^{-\eta_{1n}L}\right\} \qquad -L \le z \le L \tag{93}$$

$$\frac{U(r,z)}{W^{(0)}} = -\frac{A\pi}{L}\sum_{n=1}^{\infty}\frac{S_n}{r_{1n}}\frac{\cos n\eta_{1n}L}{S_n^2-\beta^2}V_1(S_n r)\,e^{-\eta_{1n}z} \qquad L \le z < \infty \tag{94}$$

where β and η_{1n} are defined by

$$\beta = i\sqrt{\left(\frac{\pi}{2L}\right)^2 - Re^2}$$

$$\eta_{1n} = \sqrt{S_n^2 - Re^2} \tag{95}$$

Again employing equation 46, equations 92, 93 and 94 lead to the following expressions for the axial velocity

$$\frac{W}{W^{(0)}} - 1 = \frac{A\pi}{L}\sum_{n=1}^{\infty}\frac{S_n^2}{r_{1n}^2}\frac{\cos n\eta_{1n}(z-L)}{S_n^2-\beta^2}e^{-\eta_{1n}z}V_1(S_n r) \qquad -\infty < z \le -L \tag{96}$$

$$\frac{W}{W^{(0)}} - 1 = A\left[\frac{2\,U_0(\beta r)}{\frac{\pi}{2L}\,U_1(\beta r_0)} + \frac{4L r_0}{\pi\sqrt{\beta^2 r_0^2}}\right]\left[1+\sin\frac{\pi z}{2L}\right] + A\left[\frac{2}{L}\frac{U_0(\beta r)}{\beta U_1(\beta r_0)} - \frac{4L\,U_0(\pi r_0)}{\pi\,U_1(\pi r_0)}\right]$$

$$+\frac{\pi A}{L}\sum_{n=1}^{\infty}\frac{S_n^2}{r_{1n}^2}\frac{\sin n\eta_{1n}z}{S_n^2-\beta^2}e^{-\eta_{1n}L}V_1(S_n r) + \frac{A\,4L r_0}{\pi\sqrt{\beta^2 r_0^2}}\sin\frac{\pi z}{2L} \tag{97}$$

$$-L \le z \le L$$

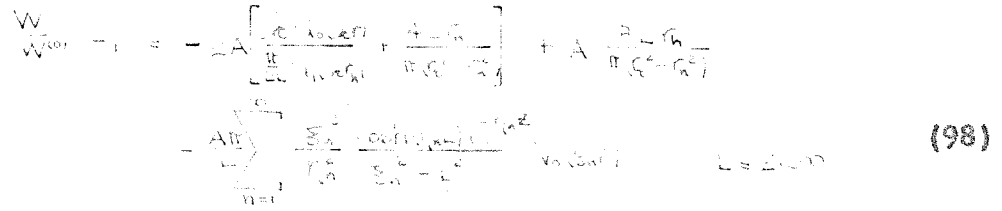

(98)

In obtaining equations 97 and 98, a slightly generalized form of equation 56 was used. That is

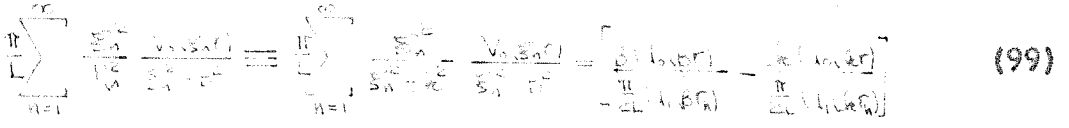

(99)

It will be noted that the equations for the radial and axial velocities all possess the factor Γ_m in the denominator of the expressions. It is, of course, obvious that this then introduces a singularity into the equations, to be found at $\lambda = \Sigma_m$, a characteristic root. Similar situations have been investigated widely, and are summarized by L. E. Fraenkel (14) and G. W. Morgan (15). In the case that the parameter λ exceeds the first critical value Σ_1, the solutions are not unique, and certain assumptions regarding the behaviour of the solution must be made. Though this phenomenon is certainly of mathematical interest, it is felt that the rotation found at the first critical value of the parameter λ is beyond that to be found in turbomachine practice, in that the rotation at this value corresponds to an angle of flow from the axial direction of almost seventy degrees for a hub-to-tip ratio of $\frac{r_h}{r_t} = 0.4$.

Equations 96, 97, and 98 have been graphed for several values of the parameter m^2 obtained from the relation $\lambda = m\Sigma_1$ and

the results are shown in figures 11, 12 and 13. The equations simplify somewhat at the value $\beta=0$, i. e., when $k = \frac{\pi}{2L}$, and this case has been included (figure 14). For this special case, the equations become

$$\frac{W}{W^{(0)}} - 1 = \frac{A\pi}{L}\sum_{n=1}^{\infty} \frac{\cosh(\eta_n L)\, e^{\eta_n z}}{\xi_n^2 - k^2} V_0(\xi_n r) \qquad -\infty < z \leq -L \tag{100}$$

$$\frac{W}{W^{(0)}} - 1 = -A\left[\frac{U_0(kr)}{U_1(kr_1)} + \frac{4Lr_1}{\pi(r_1^2 - r_1^2)}\right] + \frac{A\pi}{L}\sum_{n=1}^{\infty} \frac{\sinh(\eta z)\, e^{-\eta_n L}}{\xi_n^2 - k^2} V_0(\xi_n r)$$

$$+ A\,\frac{4Lr_1}{\pi(r_1^2 - r_1^2)}\left(1 + \sin\frac{\pi z}{2L}\right) \qquad -L \leq z \leq L \tag{101}$$

$$\frac{W}{W^{(0)}} - 1 = -2A\left[\frac{U_0(kr)}{U_1(kr_1)} + \frac{4Lr_1}{\pi(r_1^2 - r_1^2)}\right] + A\,\frac{BLr_1}{\pi(r_1^2 - r_1^2)} - \frac{A\pi}{L}\sum_{n=1}^{\infty} \frac{\cosh(\eta_n L)\, e^{-\eta_n z}}{\xi_n^2 - k^2} V_0(\xi_n r) \tag{102}$$

$$L \leq z < \infty$$

It was evident in the derivation of equation 19 that the change of vorticity with respect to the axial direction is given by the derivative by of the right side of equation 19, or of equation 84. That is, it is found that

$$\frac{\partial \eta}{\partial z} = -k^2 u \tag{103}$$

It is to be expected, then, to find a non-uniform velocity profile at outlet, and it can be seen from equation 98 that this is the case. This outlet profile is easily obtained from equilibrium theory,

and the expression will be developed, together with the expression for the outlet tangential velocity, immediately following the general development of the tangential velocity equations.

The equation of motion in the tangential direction, equation 5, for no blade forces gives

$$U \frac{\partial Vr}{\partial r} + W \frac{\partial Vr}{\partial z} = 0 \tag{104}$$

Thus

$$Vr - V^{(o)}r = -\int_{-\infty}^{z} \frac{U}{W} \frac{\partial Vr}{\partial r} dz' \tag{105}$$

Now in this case $Vr = -k\psi$ and is constant along a streamline, from equation 9. Equation 12 may thus be used to give

$$\begin{aligned} V - V^{(o)} &= -\frac{1}{r}\int_{-\infty}^{z} \frac{U}{W} \frac{\partial(-k\psi)}{\partial r} dz' \\ &= -k\int_{-\infty}^{z} U\, dz' \end{aligned} \tag{106}$$

The result of equation 106 is to be expected intuitively, for the integral $\int_{-\infty}^{z} \frac{U}{W} dz$ gives the radial distance that a stream surface moves in passing from far upstream to a point z. The angular momentum is transported along these stream surfaces so that the angular momentum which exists at a distance z downstream and radius r is not $rV^{(o)}$, but rather $V^{(o)}\left(r - \int_{-\infty}^{z} \frac{U}{W} dz'\right)$. To first order then, the angular momentum perturbation

$$-\frac{dr v^{(o)}}{dr}\int_{-\infty}^{z}\frac{u}{w}\,dz' = -r_t w^{(o)}\int_{-\infty}^{z}\frac{u}{w}\,dz' \approx -r_t\int_{-\infty}^{z} u\,dz'$$

exists due to the radial transport of the initial angular momentum.

The radial transport term given above may also be expressed conveniently in terms of the axial velocity. The radial and axial velocity are related through the continuity equation, but the integral $\int_{-\infty}^{z} u\,dz'$ which is required can be given in terms of the axial velocity by some direct physical reasoning. The stream surface bounds a constant mass of fluid between the tip and the local radius of the stream surface. It is clear then, that the surface must be displaced to accommodate a variation in mass flow $\int_{r}^{r_t}\rho(w-w^{(o)})2\pi r\,dr$ This mass flow variation is compensated by decreasing the radius of the stream surface by an amount Δr through which the mass flow is, to the first order $\rho w^{(o)} 2\pi r\,\Delta r$. The mass flow integral and this last expression must be equal for the stream surface to bound a constant mass flow. Consequently,

$$w^{(o)}\Delta r \equiv \int_{-\infty}^{z} u\,dz = \frac{1}{r}\int_{r}^{r_t}(w-w^{(o)})\,r\,dr \qquad (107)$$

Using equation 107, equation 106 may then be written in the alternative form

$$v - v^{(o)} = -\frac{r_t}{r}\int_{r}^{r_t}(w-w^{(o)})\,r\,dr \qquad (108)$$

Employing either equation 106 or equation 108, it is then

found

$$\frac{V}{W^{(o)}} - \frac{V^{(o)}}{W^{(o)}} = A\,k\,\frac{\pi}{L}\sum_{n=1}^{\infty}\frac{\xi_n}{\eta_n^2}\,\frac{\cosh(\eta_n L)\,e^{\eta_n z}}{\xi_n^2-\beta^2}\,V_1(\xi_n r) \qquad -\infty < z \le -L \tag{109}$$

$$\frac{V}{W^{(o)}} - \frac{V^{(o)}}{W^{(o)}} = -A\,k\,\frac{2L}{\pi}\left[\frac{U_1(\beta r)}{U_1(\beta r_h)}\sin\frac{\pi z}{2L} - \frac{U_1(kr)}{U_1(kr_h)}\right] + A\,\frac{k\pi}{L}\sum_{n=1}^{\infty}\frac{\xi_n}{\eta_n^2}\,\frac{\sinh(\eta_n z)\,e^{-\eta_n L}}{\xi_n^2-\beta^2}\,V_1(\xi_n r) \tag{110}$$

$$\frac{V}{W^{(o)}} - \frac{V^{(o)}}{W^{(o)}} = -A\,k\,\frac{4L}{\pi}\,\frac{U_1(kr)}{U_1(kr_h)} - A\,k\,\frac{\pi}{L}\sum_{n=1}^{\infty}\frac{\xi_n}{\eta_n^2}\,\frac{\cosh(\eta_n L)\,e^{-\eta_n z}}{\xi_n^2-\beta^2}\,V_1(\xi_n r) \tag{111}$$

The variation of axial velocity throughout the machine as described by equations 109, 110 and 111 has been plotted in figures 15, 16, 17, and 18. It should be noted that equations 109, 110 and 111 relate the local tangential velocity V to that at infinity $V^{(o)}$ along a given radius. The same value of $\frac{r - r_h(z)}{r_t - r_h(z)}$ cannot be used at both stations then, because a new location for $r_h(z)$ will be found at each station. The non-dimensional tangential velocity at inlet may be written

$$\frac{V^{(o)}}{W^{(o)}} = \frac{kr}{2} = \frac{k\,r_h(o)}{2}\,\frac{r}{r_{h(o)}} \tag{112}$$

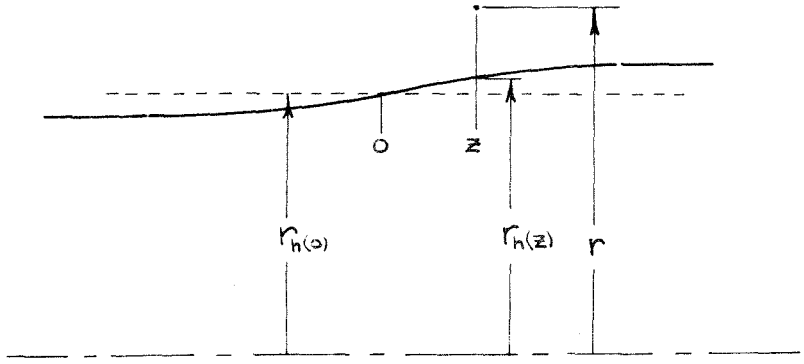

The radius at any given point is given in terms of the ratio $\frac{r - r_{h(z)}}{r_t - r_{h(z)}}$ as

$$r = r_{h(0)}\left[\left(1 - \frac{2LA}{\pi r_{h(0)}}\right)\left(1 - \frac{r - r_{h(z)}}{r_t - r_{h(z)}}\right) + \frac{r - r_{h(z)}}{r_t - r_{h(z)}}\,\frac{r_t}{r_{h(0)}}\right] \qquad -\infty < z \leq -L$$

$$r = r_{h(0)}\left[\left(1 + \frac{2LA}{\pi r_{h(0)}} \sin\frac{\pi z}{2L}\right)\left(1 - \frac{r - r_{h(z)}}{r_t - r_{h(z)}}\right) + \frac{r - r_{h(z)}}{r_t - r_{h(z)}}\,\frac{r_t}{r_{h(0)}}\right] \qquad -L \leq z \leq L$$

$$r = r_{h(0)}\left[\left(1 + \frac{2LA}{\pi r_{h(0)}}\right)\left(1 - \frac{r - r_{h(z)}}{r_t - r_{h(z)}}\right) + \frac{r - r_{h(z)}}{r_t - r_{h(z)}}\,\frac{r_t}{r_{h(0)}}\right] \qquad L \leq z < \infty \qquad (113)$$

In particular, the actual tangential velocity at any point of the machine may then be computed from the relation

$$V = \left(V - V^{(0)}\right) + V^{(0)}$$

$$= \left(V - V^{(0)}\right) + \frac{\rho_e r_{h(0)}}{2} W^{(0)} \frac{r}{r_{h(0)}} \qquad (114)$$

in which the value $\left(V - V^{(0)}\right)$ is to be obtained from equations 109, 110, 111, and the appropriate radius ratio $\frac{r}{r_{h(0)}}$ should be obtained from equation 113.

Inspection of equations 111 and 98 shows that the residual tangential and axial velocity profiles to be found infinitely far downstream are given by

$$\frac{W(r,\infty)}{W^{(o)}} - 1 = -A\,\frac{4L\,k_e}{\pi}\,\frac{U_0(kr)}{U_1(kr_h)} \tag{112}$$

$$\frac{V(r,\infty)}{W^{(o)}} - \frac{V^{(o)}}{W^{(o)}} = -A\,\frac{4L\,k_e}{\pi}\,\frac{U_1(kr)}{U_1(kr_h)} \tag{113}$$

It is apparent that these outlet profiles are a function only of the inlet conditions, and the overall contraction, rather than of the detailed wall shape. The results of equilibrium theory (13) may be utilized to obtain equations 112 and 113, in a simple manner. The value of the streamfunction downstream of the contraction is given by

$$\psi = -\int_{r_h}^{r} Wr\,dr - \frac{W^{(o)}}{2}\,r_h^2 + \frac{4AL\,r_h}{\pi}\,W^{(o)} \tag{114}$$

the last term in equation 114 arising from the increase in flow found across the annulus. When equation 114 is substituted into equation 84, there results, for zero Z variation

$$\frac{dW}{dr} = -\frac{k_e^2}{r}\int_{r_h}^{r}(W-W^{(o)})\,r\,dr + \frac{k_e^2}{r}\,\frac{4AL\,r_h}{\pi}\,W^{(o)} \tag{115}$$

Taking the derivative of both sides by r, have

$$\frac{d^2W}{dr^2} = \frac{k^2}{r^2}\int_{r_n}^{r}(W-W^{(0)})r\,dr - k^2(W-W^{(0)}) - \frac{k^2}{r^2}\frac{4AL r_n}{\pi}W^{(0)}$$

$$= -\frac{1}{r}\frac{dW}{dr} - k^2(W-W^{(0)})$$

or, finally

$$\frac{d^2(W-W^{(0)})}{dr^2} + \frac{1}{r}\frac{d(W-W^{(0)})}{dr} + k^2(W-W^{(0)}) = 0 \qquad (116)$$

The two boundary conditions necessary for complete solution of equation 116 may be obtained from the values of $\frac{dW}{dr}$ at r_n and r_t as given by equation 115. The value of the integral $\int_{r_n}^{r_t}(W-W^{(0)})r\,dr$ downstream of the contraction is $\frac{4AL r_n}{\pi}W^{(0)}$, so that the boundary conditions become

$$\left.\frac{dW}{dr}\right|_{r_t} = 0$$

$$\left.\frac{dW}{dr}\right|_{r_n} = A\frac{4L}{\pi}k^2 W^{(0)} \qquad (117)$$

The solution to equation 116 is

$$W-W^{(0)} = A\,J_0(kr) + B\,Y_0(kr) \qquad (118)$$

Equations 117 then give

$$\frac{W}{W^{(0)}} - 1 = -A\frac{4L}{\pi}k\frac{J_0(kr)}{J_1(kr_n)} \qquad (119)$$

Application of equation 108 then gives

$$\frac{V}{W^{(0)}} - \frac{V^{(0)}}{W^{(0)}} = -A \frac{4 - k_e}{\pi} \frac{J_1(kr)}{J_1(kr_h)} \qquad (120)$$

It may be seen that equations 119 and 120 agree with equations 112 and 113. The outlet profiles as given by these equations are shown in figures 18 and 19. Another interesting check has been carried out, and is indicated by the dotted line superimposed on figure 21. This dotted line represents the profile shape that would be found if the angular momentum found upstream at the hub radius were to be smeared out over the entire annulus. The curve represents a limit to the perturbations upon the flow.

It can be seen from the plotted results that the perturbations induced by the wall shape on the rotating fluid are several times larger than the perturbations induced by the wall shape on the non-rotating fluid. Examination of the equations and curves reveals that the local wall effect is much as was found in the previous chapter, but the overall displacement of the vorticity steadily introduces a velocity profile of the type shown in figure 19. Indeed, the effect of vorticity displacement is so strong that the validity of the results for the case $m = \frac{r_h}{r_1} = 0.8$ is somewhat dubious, in view of the extremely large perturbation in axial velocity found at the hub radius. This result does emphasize, however, the importance of including the rotational term in the equations.

V. WEAK ENTRANCE VANE AT ENTRY TO CONTRACTION

In this chapter, the effect of an actuator disc at the entry to the contraction is to be investigated. This configuration can be seen to give quite a close approximation to the conditions actually found in an aircraft gas turbine, because such a gas turbine would have a uniform flow approaching from upstream, and then the inlet guide vanes would impart some prescribed rotation to the flow. It is more convenient in this case to consider the origin for Z to be located at the disc itself, so that the configuration is that shown in figure 22.

The equations describing the flow now have specific regions of validity, in that the form of the differential equation changes across the actuator disc. In this example, the disc imparts a tangential velocity to the fluid of

$$V = -k\frac{\psi}{r} \tag{121}$$

Thus, the equations for the two regions are the same as equations 21 and 85. That is,

$$\frac{\partial^2 u}{\partial r^2} + \frac{\partial}{\partial r}\left(\frac{u}{r}\right) + \frac{\partial^2 u}{\partial z^2} = 0 \qquad -\infty < z < 0 \tag{122}$$

$$\frac{\partial^2 u}{\partial r^2} + \frac{\partial}{\partial r}\left(\frac{u}{r}\right) + k^2 u + \frac{\partial^2 u}{\partial z^2} = 0 \qquad 0 < z < \infty \tag{123}$$

Effect of Actuator Disc on Flow in a Parallel Walled Annulus.

It will be useful for comparison purposes to compute the effect of

the actuator disc and parallel walls only, and in this case, it is convenient to assume solutions of the form

$$U(r,z) = \sum_{n=1}^{\infty} A_n U_1(\xi_n r) e^{\xi_n z} \qquad -\infty < z < 0 \qquad (124)$$

$$U(r,z) = \sum_{n=1}^{\infty} B_n U_1(\xi_n r) e^{-\eta_n z} \qquad 0 < z < \infty \qquad (125)$$

The solutions assumed in equations 124 and 125 satisfy the boundary conditions, and it is necessary to consider the matching conditions across the disc in order to evaluate the A_n's and B_n's. The assumption of tangential forces only within the disc insures that the radial velocity is continuous across the disc so that

$$U(r,0-) = U(r,0+) = U_0 \qquad (126)$$

Equation 19 may be written for the two regions

$$-\frac{\partial W}{\partial r} + \frac{\partial U}{\partial z} = 0 \qquad -\infty < z < 0 \qquad (127)$$

$$-\frac{\partial W}{\partial r} + \frac{\partial U}{\partial z} = -\frac{1}{r}\int_{re}^{z} \psi \qquad 0 < z < \infty \qquad (128)$$

so that, noting that the axial velocity is continuous across the disc, there results

$$\left.\frac{\partial U}{\partial z}\right|_{0+} - \left.\frac{\partial U}{\partial z}\right|_{0-} = -\frac{1}{r}\int_{re}^{z} \psi_{(0)} = \int_{re}^{z} \frac{W_{(0)} r}{2} - \int_{re}^{z}\int_{-\infty}^{0} U_1 \, dz \qquad (129)$$

Equation 126 leads immediately to $A_n = B_n$, and application of equation 129 then gives

$$\sum_{n=1}^{\infty} \frac{A_n}{\xi_n}\left(\eta_n^2 + \xi_n \eta_n\right) U_1(\xi_n r) = -\frac{k^2 W^{(0)}}{2} r \tag{130}$$

The right side of equation 130 may be expanded in terms of the orthogonal functions $V_1(\xi_n r)$ to give

$$\sum_{n=1}^{\infty} \frac{A_n}{\xi_n}\left(\eta_n^2 + \xi_n \eta_n\right) U_1(\xi_n r) = -k^2 W^{(0)} \frac{\pi}{2} \sum_{n=1}^{\infty} \left(r_t^2 W_0(\xi_n r_t) - r_n^2 W_0(\xi_n r_n)\right) V_1(\xi_n r)$$

or

$$A_n = -\frac{\pi}{2} \frac{k^2 W^{(0)} \xi_n \left(r_t^2 W_0(\xi_n r_t) - r_n^2 W_0(\xi_n r_n)\right)}{\eta_n^2 + \xi_n \eta_n} \frac{V_1(\xi_n r)}{U_1(\xi_n r)} \tag{131}$$

where

$$W_0(\xi_n r) = J_1(\xi_n r_n) Y_0(\xi_n r) - Y_1(\xi_n r_n) J_0(\xi_n r) \tag{132}$$

It should be noted that the ratio $\frac{V_1(\xi_n r)}{U_1(\xi_n r)}$ appearing in equation 131 is, of course, independent of r . However, the form given here is the most convenient, for substitution of A_n into equations 124 and 125 gives immediately

$$U(r,z) = -k^2 W^{(0)} \frac{\pi}{2} \sum_{n=1}^{\infty} \frac{\xi_n \left(r_t^2 W_0(\xi_n r_t) - r_n^2 W_0(\xi_n r_n)\right) e^{\xi_n z}}{\eta_n^2 + \xi_n \eta_n} V_1(\xi_n r) \qquad -\infty < z \leq 0 \tag{133}$$

$$U(r,z) = -k^2 W^{(0)} \frac{\pi}{2} \sum_{n=1}^{\infty} \frac{\xi_n \left(r_t^2 W_0(\xi_n r_t) - r_n^2 W_0(\xi_n r_n)\right) e^{-\eta_n z}}{\eta_n^2 + \xi_n \eta_n} V_1(\xi_n r) \qquad 0 \leq z < \infty \tag{134}$$

Application of the continuity equation, 45 , then gives

$$\frac{W(r,z)}{W^{(0)}} - 1 = \kappa^2 \frac{\pi}{2} \sum_{n=1}^{\infty} \frac{\xi_n \left(r_t^2 W_0(\xi_n r_t) - r_n^2 W_0(\xi_n r_n) \right) e^{\xi_n z}}{\eta_n^2 + \xi_n r_n} V_0(\xi_n r) \qquad -\infty < z \leq 0 \tag{135}$$

$$\frac{W(r,z)}{W^{(0)}} - 1 = \kappa^2 \frac{\pi}{2} \sum_{n=1}^{\infty} \frac{\xi_n}{\xi_n^2 - \kappa^2} \left[1 - \frac{\xi_n e^{-\eta_n z}}{\xi_n + \eta_n} \right] \left(r_t^2 W_0(\xi_n r_t) - r_n^2 W_0(\xi_n r_n) \right) V_0(\xi_n r) \qquad 0 \leq z < \infty \tag{136}$$

The tangential velocity is again obtained through use of equation 105, though in this case the integration starts from $z = 0$.

$$V - V^{(0)} = -\frac{1}{r} \int_0^z \frac{U}{W} \frac{\partial r V}{\partial r} dz' = -\kappa \int_0^z u \, dz' \tag{137}$$

in which $$V^{(0)} = \kappa W^{(0)} \left[\frac{r}{2} + \frac{\pi}{2} \kappa^2 \sum_{n=1}^{\infty} \frac{r_t^2 W_0(\xi_n r_t) - r_n^2 W_0(\xi_n r_n)}{\eta_n^2 + \xi_n \eta_n} V_1(\xi_n r) \right] \tag{138}$$

From equation 137, there then results

$$V - V^{(0)} = \kappa^2 \frac{\pi}{2} \sum_{n=1}^{\infty} \frac{\xi_n \left(r_t^2 W_0(\xi_n r_t) - r_n^2 W_0(\xi_n r_n) \right)}{\eta_n^2 (\xi_n + \eta_n)} \left(1 - e^{-\eta_n z} \right) V_1(\xi_n r) \tag{139}$$

Graphical results of these equations have been obtained for values of $m^2 = \frac{\kappa^2}{\xi_1^2}$, of 0.025 and 0.1 . (figures 23, 24, 25, 26, and 27.)

Actuator Disc at Entrance to Contraction. Returning to the problem of the actuator disc at entrance to the contraction, we have that the expression for radial velocity will be valid for only one region of the flow, so that it is necessary to describe transform variables for each region. Thus, write

$$\hat{u}_{(r,\kappa)_+} = \frac{1}{\sqrt{2\pi}}\int_0^\infty u_{(r,z)_+} e^{-i\kappa z}\, dz \tag{140}$$

$$\hat{u}_{(r,\kappa)_-} = \frac{1}{\sqrt{2\pi}}\int_{-\infty}^0 u_{(r,z)_-} e^{-i\kappa z}\, dz \tag{141}$$

The corresponding inversion formulae are

$$\begin{aligned} u_{(r,z)_+} &= \frac{1}{\sqrt{2\pi}}\int_{-\infty}^\infty \hat{u}_{(r,\kappa)_+} e^{i\kappa z}\, d\kappa \qquad 0 < z < \infty \\ &= 0 \qquad\qquad -\infty < z < 0 \end{aligned} \tag{142}$$

$$\begin{aligned} u_{(r,z)_-} &= \frac{1}{\sqrt{2\pi}}\int_{-\infty}^\infty \hat{u}_{(r,\kappa)_-} e^{i\kappa z}\, d\kappa \qquad -\infty < z < 0 \\ &= 0 \qquad\qquad 0 < z < \infty \end{aligned} \tag{143}$$

When the transformation of equation 123 is taken, using the definition of equation 140, the values of the as yet unknown conditions at $z=0$ remain, and the equation for the transform variable becomes

$$\frac{d^2\hat{u}}{dr^2} + \frac{1}{r}\frac{d\hat{u}}{dr} + \left((k^2-\kappa^2) - \frac{1}{r^2}\right)\hat{u} = \frac{1}{\sqrt{2\pi}}\left[\left.\frac{\partial u}{\partial z}\right|_{z=0+} + i\kappa\left(u_{z=0+}\right)\right] \tag{144}$$

The boundary conditions downstream of the disc are now

$$\frac{u(r_t,z)}{W^{(o)}} = \frac{dr_t}{dz} = 0 \qquad -\infty < z < \infty \tag{145}$$

$$\frac{u(r_h,z)}{W^{(o)}} = \frac{dr_h}{dz} = A \sin\frac{\pi z}{2L} \qquad 0 \le z \le 2L$$

$$= 0 \qquad 2L \le z < \infty \tag{146}$$

The transformed boundary conditions may then be written

$$\hat{u}_{(r_t,k)_+} = 0 \tag{147}$$

$$\hat{u}_{(r_h,k)_+} = \frac{AW^{(o)}}{\sqrt{2\pi}} \int_0^{2L} \sin\frac{\pi z}{2L}\, e^{-ikz}\, dz$$

$$= \frac{AW^{(o)}}{L}\sqrt{\frac{\pi}{2}}\, \frac{\cos(Lk)\, e^{-iLk}}{\left(\frac{\pi}{2L}\right)^2 - k^2} \tag{148}$$

Solution for Downstream Transform Variable. The problem for the solution of the downstream transform variable in terms of conditions at the actuator disc is thus described by equations 144, 147 and 148. The solution to the homogeneous form of equation 144 is easily found to be

$$\hat{u}_{hom.} = \hat{u}_{(r_h,k)} \frac{J_1(r\sqrt{k^2 - \lambda^2})}{J_1(r_h\sqrt{k^2 - \lambda^2})} \tag{149}$$

The effect of the inhomogeneous term may be determined by first finding the Green's function for the equation and then integrating

the result. We thus want the solution to the equation

$$\frac{d^2\hat{u}}{dr^2} + \frac{1}{r}\frac{d\hat{u}}{dr} + \left\{(\omega^2 - k^2) - \frac{1}{r^2}\right\}\hat{u} = \delta(r - r_0) \tag{150}$$

together with the boundary conditions, and matching conditions

$$\hat{u}_{(r_t)} = \hat{u}_{(r_n)} = 0 \tag{151}$$

$$\begin{aligned} \hat{u}_{(r_0)_+} &= \hat{u}_{(r_0)_-} \\ \left.\frac{d\hat{u}}{dr}\right|_{r_{0+}} - \left.\frac{d\hat{u}}{dr}\right|_{r_{0-}} &= 1 \end{aligned} \tag{152}$$

Denoting the solutions to equation 150, $K(r;r_0)_+$ and $K(r;r_0)_-$ valid in the regions $r>r_0$ and $r<r_0$ respectively, it is then found that

$$K(r;r_0)_+ = -\frac{\pi r_0}{2}\frac{W_1(i\sqrt{k^2-\omega^2}\,r_0)}{U_1(i\sqrt{k^2-\omega^2}\,r_n)}U_1(i\sqrt{k^2-\omega^2}\,r) \tag{153}$$

$$K(r;r_0)_- = -\frac{\pi r_0}{2}\frac{U_1(i\sqrt{k^2-\omega^2}\,r_0)}{U_1(i\sqrt{k^2-\omega^2}\,r_n)}W_1(i\sqrt{k^2-\omega^2}\,r) \tag{154}$$

in which $W_1(i\sqrt{k^2-\omega^2}\,r_0)$ is the linear combination of Bessel functions

$$W_1(i\sqrt{k^2-\omega^2}\,r_0) = J_1(i\sqrt{k^2-\omega^2}\,r_n)Y_1(i\sqrt{k^2-\omega^2}\,r_0) - J_1(i\sqrt{k^2-\omega^2}\,r_0)Y_1(i\sqrt{k^2-\omega^2}\,r_n) \tag{155}$$

The full solution to equation 144 is thus given by

$$\hat{u}_{(r,\kappa)} = \hat{u}_{hom.} + \int_{r_n}^{r} \frac{1}{\sqrt{2\pi}} \left[\left. \frac{\partial u}{\partial z} \right|_{z=0+} + i\kappa U_{z=0+} \right] K(r;r_0)_+ dr_0 + \int_{r}^{r_t} \frac{1}{\sqrt{2\pi}} \left[\left. \frac{\partial u}{\partial z} \right|_{z=0+} + i\kappa U_{z=0+} \right] K(r;r_0)_+ dr_0$$

$$= \hat{u}_{(r_n,\kappa)} \frac{U_1(\sqrt{\kappa^2 - \bar{\omega}^2} r)}{U_1(\sqrt{\kappa^2 - \bar{\omega}^2} r_n)} - \frac{1}{2}\sqrt{\frac{\pi}{2}} \int_{r_n}^{r} \frac{U_1(\sqrt{\kappa^2 - \bar{\omega}^2} r)}{U_1(\sqrt{\kappa^2 - \bar{\omega}^2} r_n)} \left[\left. \frac{\partial u}{\partial z} \right|_{z=0+} + i\kappa U_{z=0+} \right] r_0 W_1(\sqrt{\kappa^2 - \bar{\omega}^2} r_0) \, dr_0$$

$$- \frac{1}{2}\sqrt{\frac{\pi}{2}} \int_{r}^{r_t} \frac{W_1(\sqrt{\kappa^2 - \bar{\omega}^2} r)}{U_1(\sqrt{\kappa^2 - \bar{\omega}^2} r_n)} \left[\left. \frac{\partial u}{\partial z} \right|_{z=0+} + i\kappa U_{z=0+} \right] r_0 U_1(\sqrt{\kappa^2 - \bar{\omega}^2} r_0) \, dr_0 \qquad (156)$$

Solution Valid Upstream For the solution valid upstream, the definition of equation 141, together with equation 122, leads to

$$\frac{d^2\hat{u}}{dr^2} + \frac{1}{r}\frac{d\hat{u}}{dr} - \left(\kappa^2 + \frac{1}{r^2}\right)\hat{u} = \frac{-1}{\sqrt{2\pi}} \left[\left. \frac{\partial u}{\partial z} \right|_{0-} + i\kappa U_{0-} \right] \qquad (157)$$

In this case, of upstream flow, $\frac{dr_t}{dz} = \frac{dr_n}{dz} = 0$ so that the solution to the homogeneous portion of equation 157 is identically zero. The inhomogeneous solution is evaluated in the same way as was equation 144, leading to

$$\hat{U}(r,K)_{-} = \frac{1}{2}\sqrt{\frac{\pi}{2}}\int_{r_n}^{r}\frac{J_1(iKr)}{J_1(iKr_n)}\left[\left(\frac{\partial U}{\partial z}\right)_{0-} + iKU_{0-}\right] r_0 W_1(iKr_0)\,dr_0$$

$$+ \frac{1}{2}\sqrt{\frac{\pi}{2}}\int_{r}^{r_t}\frac{W_1(iKr)}{J_1(iKr_n)}\left[\left(\frac{\partial U}{\partial z}\right)_{0-} + iKU_{0-}\right] r_0 J_1(iKr_0)\,dr_0 \qquad (158)$$

Equations 158 and 156 may now be substituted into equations 143 and 142 to obtain the desired expressions for the radial velocity. In particular, the inversion integral for the upstream velocity becomes

$$U(r,z)_{-} = \frac{1}{4}\int_{-\infty}^{\infty}\left[\int_{r_n}^{r}\frac{J_1(iKr)}{J_1(iKr_n)}\left[\left(\frac{\partial U}{\partial z}\right)_{0-} + iKU_{0-}\right] r_0 W_1(iKr_0)\,dr_0 + \int_{r}^{r_t}\frac{W_1(iKr)}{J_1(iKr_n)}\left[\left(\frac{\partial U}{\partial z}\right)_{0-} + iKU_{0-}\right] r_0 J_1(iKr_0)\,dr_0\right] e^{iKz}\,dK \qquad (159)$$

Investigation of the limiting behaviour of the integrand of equation 159 shows that the inversion integral is convergent for negative values of z when the contour of the large arc is taken in the lower half plane. The only residues appearing are again roots of the equation $J_1(\xi_n r_n) = 0$, so that interchanging the order of integration, the equation for the radial velocity becomes

$$U(r,z)_{-} = -\sqrt{\frac{\pi}{2}}\sum_{n=1}^{\infty}\left[\int_{r_n}^{r} V_1(\xi_n r)\left[\left(\frac{\partial U}{\partial z}\right)_{0-} + \xi_n U_{0-}\right] r_0 W_1(\xi_n r_0)\,dr_0\right. \qquad (160)$$

$$\left. + \int_{r}^{r_t} V_1(\xi_n r)\left[\left(\frac{\partial U}{\partial z}\right)_{0-} + \xi_n U_{0-}\right]\frac{W_1(\xi_n r)}{J_1(\xi_n r)}\, r_0 J_1(\xi_n r_0)\,dr_0\right]$$

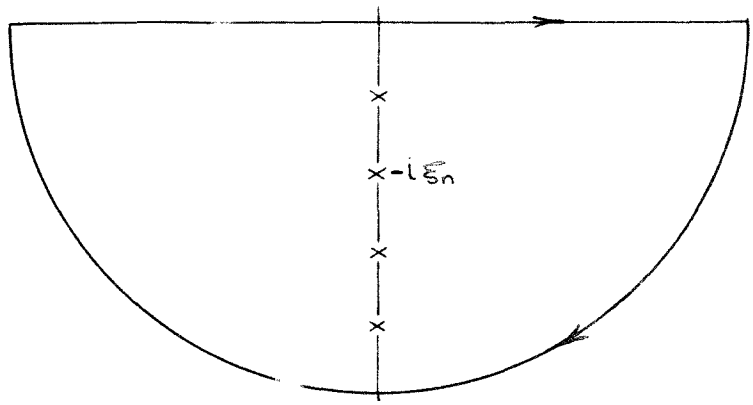

Now, $W_1(\xi_n r)$ and $U_1(\xi_n r)$ are eigenfunctions with the same eigenvalue, and it thus follows that the ratio of the two is independent of the value n. This can, of course, be checked by expanding the groups and rearranging the terms. It is convenient then to write

$$\frac{W_1(\xi_n r)}{U_1(\xi_n r)} U_1(\xi_n r_0) = \frac{W_1(\xi_n r_0)}{U_1(\xi_n r_0)} U_1(\xi_n r_0) = W_1(\xi_n r_0)$$ which then gives for the upstream radial velocity

$$U_1(r,z)_- = -\frac{\pi}{2} \sum_{n=1}^{\infty} \int_{r_n}^{r_c} \left[\left. \frac{\partial U}{\partial z} \right|_{0-} + \xi_n U_0 \right] r_0 W_1(\xi_n r_0)\, dr_0\, V_1(\xi_n r)\, e^{\xi_n \epsilon} \qquad (161)$$

Inversion of Downstream Velocity. Considering now the inversion integral for the downstream velocity, equations 156 and 142 give

$$U(r,z)_+ = \frac{1}{\sqrt{2\pi}}\int_{-\infty}^{\infty} \hat{U}_{(r_n,\kappa)} \frac{J_1(i\sqrt{\kappa^2-\alpha^2}\,r)}{J_1(i\sqrt{\kappa^2-\alpha^2}\,r_n)} e^{i\kappa z}\, d\kappa$$

$$- \frac{1}{4}\int_{-\infty}^{\infty}\left[\int_{r_n}^{r} \frac{J_1(i\sqrt{\kappa^2-\alpha^2}\,r)}{J_1(i\sqrt{\kappa^2-\alpha^2}\,r_n)}\left[\left.\frac{\partial U}{\partial z}\right|_{0+} + i\kappa U_{0+}\right] r_0 W_1(i\sqrt{\kappa^2-\alpha^2}\,r_0)\, dr_0\right.$$

$$\left. + \int_{r}^{r_t} \frac{W_1(i\sqrt{\kappa^2-\alpha^2}\,r)}{J_1(i\sqrt{\kappa^2-\alpha^2}\,r_n)}\left[\left.\frac{\partial U}{\partial z}\right|_{0+} + i\kappa U_{0+}\right] r_0 J_1(i\sqrt{\kappa^2-\alpha^2}\,r_0)\, dr_0\right] \qquad (162)$$

The same procedure as was used to obtain equation 161 then leads to the result

$$U(r,z)_+ = \frac{1}{\sqrt{2\pi}}\int_{-\infty}^{\infty} \hat{U}_{(r_n,\kappa)} \frac{J_1(i\sqrt{\kappa^2-\alpha^2}\,r)}{J_1(i\sqrt{\kappa^2-\alpha^2}\,r_n)} e^{i\kappa z}\, d\kappa + \frac{\pi}{2}\int_{r_n}^{r_t}\left[\left.\frac{\partial U}{\partial z}\right|_{0+} - r_{(n} U_{0+}\right] r_0 W_1(s_n r_0)\, dr_0\, V_1(s_n r)\, \frac{\bar{s}_n}{r_{(n}} e^{-r_{(n}z} \qquad (163)$$

It is most convenient, for the present, to leave the inversion of the homogeneous portion of the solution in symbolic form, so that a more general result may be obtained which will be more directly applicable to different wall shapes. For the present, then, the group shall be denoted by

$$\frac{1}{\sqrt{2\pi}}\int_{-\infty}^{\infty} \hat{U}_{(r_n,\kappa)} \frac{J_1(i\sqrt{\kappa^2-\alpha^2}\,r)}{J_1(i\sqrt{\kappa^2-\alpha^2}\,r_n)} e^{i\kappa z}\, d\kappa \equiv \Delta \qquad (164)$$

In the particular case described by equation 148, the value of Δ is found to be

$$\Delta = -AW^{(0)}\frac{\pi}{L}\sum_{n=1}^{\infty}\frac{\cosh[\eta_n(L-z)]}{\xi_n^2-\beta^2}\frac{\xi_n}{\eta_n}e^{-\eta_n L}V_1(\xi_n r) + AW^{(0)}\sin\frac{\pi z}{2L}\frac{I_1(\beta r)}{I_1(\beta r_h)} \qquad (165)$$

$0 \le z \le 2L$

$$\Delta = -AW^{(0)}\frac{\pi}{L}\sum_{n=1}^{\infty}\frac{\cosh(\eta_n L)}{\xi_n^2-\beta^2}\frac{\xi_n}{\eta_n}e^{-(z-L)\eta_n}V_1(\xi_n r) \qquad (166)$$

$2L \le z < \infty$

which may be seen to be simply the result of equations 93 and 94 translated from $z=0$ at the center of the contraction to $z=0$ at entrance to the contraction.

The unknown quantities $\left.\frac{\partial u}{\partial z}\right|_{0+}$, $\left.\frac{\partial u}{\partial z}\right|_{0-}$, u_{0+}, u_{0-} must be evaluated from the matching conditions at the disc, equations 126 and 129.

<u>Application of Matching Conditions.</u> Conditions on either side of the disc are given by

$$u(r,0)_- = -\frac{\pi}{L}\sum_{n=1}^{\infty}\int_{r_h}^{r_t}\left[\left.\frac{\partial u}{\partial z}\right|_{0-} + \xi_n u_{0-}\right] r_0 W_1(\xi_n r_0)\,dr_0\, V_1(\xi_n r) \qquad (167)$$

$$u(r,0)_+ = \frac{\pi}{L}\sum_{n=1}^{\infty}\int_{r_h}^{r_t}\left[\left.\frac{\partial u}{\partial z}\right|_{0+} - \eta_n u_{0+}\right] r_0 W_1(\xi_n r_0)\,dr_0\, V_1(\xi_n r)\frac{\xi_n}{\eta_n} + \Delta_0 \qquad (168)$$

$$\left.\frac{\partial u}{\partial z}\right|_{0-} = -\frac{\pi}{2}\sum_{n=1}^{\infty}\int_{r_n}^{r_t}\left[\left.\frac{\partial u}{\partial z}\right|_{0-} + \xi_n u_{0-}\right] r_0 W_1(\xi_n r_0)\, dr_0\, V_1(\xi_n r)\, \xi_n \tag{169}$$

$$\left.\frac{\partial u}{\partial z}\right|_{0+} = -\frac{\pi}{2}\sum_{n=1}^{\infty}\int_{r_n}^{r_t}\left[\left.\frac{\partial u}{\partial z}\right|_{0+} - r_{(n)}^2 u_{0+}\right] r_0 W_1(\xi_n r_0)\, dr_0\, V_1(\xi_n r)\, \xi_n + \frac{\partial \Delta_0}{\partial z} \tag{170}$$

where Δ_0 is the value of Δ at $z=0$, and

$\frac{\partial \Delta_0}{\partial z}$ is the value of $\frac{\partial \Delta}{\partial z}$ at $z=0$

From equations 161 and 129, there results

$$\left.\frac{\partial u}{\partial z}\right|_{0+} - \left.\frac{\partial u}{\partial z}\right|_{0-} = \frac{2}{\kappa^2}\frac{W^{(0)} r}{2} + \frac{2}{\kappa^2}\frac{\pi}{2}\sum_{n=1}^{\infty}\int_{r_n}^{r_t}\left[\left.\frac{\partial u}{\partial z}\right|_{0-} + \xi_n u_{0-}\right] r_0 W_1(\xi_n r_0)\, dr_0 \frac{V_1(\xi_n r)}{\xi_n} \tag{171}$$

Equating equation 167 to equation 168, obtains

$$\frac{\pi}{2}\sum_{n=1}^{\infty}\int_{r_n}^{r_t}\left[\frac{\xi_n}{r_{(n)}}\left.\frac{\partial u}{\partial z}\right|_{0+} + \left.\frac{\partial u}{\partial z}\right|_{0-}\right] r_0 W_1(\xi_n r_0)\, dr_0\, V_1(\xi_n r) = -\Delta_0 \tag{172}$$

Equations 169, 170, and 171 give

$$\frac{\pi}{2}\sum_{n=1}^{\infty}\int_{r_n}^{r_t}\left[\xi_n \left.\frac{\partial u}{\partial z}\right|_{0+} - \frac{r_{(n)}^2}{\xi_n}\left.\frac{\partial u}{\partial z}\right|_{0-} - \left(r_{(n)}^2 + \xi_n r_{(n)}\right) u_0\right] r_0 W_1(\xi_n r_0)\, dr_0\, V_1(\xi_n r) = \frac{\partial \Delta_0}{\partial z} \tag{173}$$

Equations 171, 172 and 173 thus give three equations for the three unknowns, U_o , $\left.\frac{\partial U}{\partial z}\right|_{o+}$, $\left.\frac{\partial U}{\partial z}\right|_{o-}$. The solution of these three equations requires evaluation of the integral

$$\int_{r_h}^{r_t} \sum_{m=1}^{\infty} V_1(\xi_m r_o)\, W_1(\xi_n r_o)\, r_o\, dr_o \equiv \int_{r_h}^{r_t} \sum_{m=1}^{\infty} \frac{r_o\, U_1(\xi_m r_o)}{r_h U_o(\xi_m r_h) + r_t W_o(\xi_m r_t)}\, W_1(\xi_n r_o)\, dr_o \qquad (174)$$

here the expression $V_1(\xi_m r_o)$ has been expanded into the group $\frac{U_1(\xi_m r_o)}{r_h U_o(\xi_m r_h) + r_t W_o(\xi_m r_t)}$, which follows from the original definition of $V_1(\xi_m r)$, equation 39.

Equation 174 then becomes, with the aid of the orthogonality of the functions $W_1(\xi_n r)$

$$\int_{r_h}^{r_t} \sum_{m=1}^{\infty} V_1(\xi_m r_o)\, W_1(\xi_n r_o)\, r_o\, dr_o = \int_{r_h}^{r_t} \sum_{m=1}^{\infty} \frac{U_1(\xi_m r)}{W_1(\xi_m r)} \frac{1}{r_h U_o(\xi_m r_h) + r_t W_o(\xi_m r_t)}\, W_1(\xi_m r_o)\, W_1(\xi_n r_o)\, r_o\, dr_o$$

$$= \frac{U_1(\xi_n r)}{W_1(\xi_n r)} \frac{1}{r_h (U_o(\xi_n r_h) + r_t W_o(\xi_n r_t)} \left[r_t^2 W_o^2(\xi_n r_t) - r_h^2 W_o^2(\xi_n r_h) \right]$$

$$= r_t W_o(\xi_n r_t) \frac{U_1(\xi_n r)}{W_1(\xi_n r)} \qquad (175)$$

As previously discussed, the ratio $\frac{U_1(\xi_n r)}{W_1(\xi_n r)}$ is a constant, and it would seem appropriate to choose $r = r_t$ as a most suitable reference value. In this case, the ratio becomes indeterminant,

but the application of L'Hopital's rule leads to

$$r_t W_0(\xi_n r_t) \frac{J_1(\xi_n r)}{W_1(\xi_n r)} = r_t W_0(\xi_n r_t) \frac{J_0(\xi_n r_t)}{W_0(\xi_n r_t)}$$

$$= r_t \left(-\frac{2}{\pi \xi_n r_t} \right) = -\frac{2}{\pi \xi_n} \tag{176}$$

The summation of equation 174 has thus been shown to reduce simply to

$$\int_{r_n}^{r_t} \sum_{m=1}^{\infty} V_1(\xi_n r_0) W_1(\xi_n r_0) r_0 \, dr_0 = -\frac{2}{\pi \xi_n} \tag{177}$$

One further integral is required for the solution of equations 171, 172, and 173:

$$\int_{r_n}^{r_t} r_0^2 W_1(\xi_n r_0) \, dr_0 = -\frac{1}{\xi_n} \left[r_t^2 W_0(\xi_n r_t) - r_n^2 W_0(\xi_n r_n) \right] \tag{178}$$

Utilising the results of equations 177 and 178, there then results

$$\frac{\pi}{2} \sum_{n=1}^{\infty} \left[\frac{\xi_1 + \eta_n - \frac{k^2}{2\xi_n}}{\eta_n} \int_{r_n}^{r_t} \left. \frac{\partial u}{\partial z} \right|_{0-} r_0 W_1(\xi_n r_0) \, dr_0 - \frac{1}{2} \frac{k^2}{\eta_n} \int_{r_n}^{r_t} J_0 r_0 W_1(\xi_n r_0) \, dr_0 \right] V_1(\xi_n r)$$

$$= \frac{\pi}{4} \sum_{n=1}^{\infty} \frac{k^2 W^{(0)}}{\eta_n} \left[r_t^2 W_0(\xi_n r_t) - r_n^2 W_0(\xi_n r_n) \right] V_1(\xi_n r) \quad - \Delta \tag{179}$$

$$\frac{\pi}{2}\sum_{n=1}^{\infty}\left[\frac{k^2}{2\xi_n}\int_{r_n}^{r_t}\left.\frac{\partial u}{\partial z}\right|_{0-} r_0 W_1(\xi_n r_0)\,dr_0 - \left(\xi_n^2 - \frac{k^2}{2} + \xi_n\eta_n\right)\int_{r_n}^{r_t} u_0 r_0 W_1(\xi_n r_0)\,dr_0\right] V_1(\xi_n r)$$

$$= -\frac{\pi}{4}\sum_{n=1}^{\infty} k^2 W^{(0)}\left[r_t^2 W_0(\xi_n r_t) - r_n^2 W_0(\xi_n r_n)\right] V_1(\xi_n r) + \frac{\partial \Delta_0}{\partial z} \qquad (180)$$

In order to solve for the terms u_0 and $\left.\frac{\partial u}{\partial z}\right|_{0-}$, it is now necessary to expand the function Δ in terms of the characteristic group $V_1(\xi_n r)$ so that the individual terms of the series in equations 179 and 180 may be equated. Denoting the n^{th} coefficient of the series for the function Δ taken at $z=0$, and the function $\frac{\partial \Delta}{\partial z}$ taken at $z=0$ by Δ_0 and $\left.\frac{\partial \Delta_0}{\partial z}\right|_n$ respectively, equations 179 and 180 combine to give

$$\int_{r_n}^{r_t}\left[\left.\frac{\partial u}{\partial z}\right|_{0-} + \xi_n u_0\right] r_0 W_1(\xi_n r_0)\,dr_0 = -\frac{2\xi_n}{\xi_n + \eta_n}\frac{1}{\pi}\Delta_{0n} - \frac{2\xi_n}{\eta_n^2 + \xi_n\eta_n}\frac{1}{\pi}\left.\frac{\partial \Delta_0}{\partial z}\right|_n$$

$$+ \frac{\xi_n k^2 W^{(0)}}{\eta_n^2 + \xi_n\eta_n}\left[r_t^2 W_0(\xi_n r_t) - r_n^2 W_0(\xi_n r_n)\right] \qquad (181)$$

Use of equations 171, 179 and 180 then leads to

$$\int_{r_n}^{r_t}\left[\left.\frac{\partial u}{\partial z}\right|_{0+} - \eta_n u_0\right] r_0 W_1(\xi_n r_0)\,dr_0$$

$$= \left[-k^2 W^{(0)}\left[r_t^2 W_0(\xi_n r_t) - r_n^2 W_0(\xi_n r_n)\right] - \frac{2}{\pi}\frac{\eta_n^2}{\xi_n}\Delta_{0n} + \frac{2}{\pi}\left.\frac{\partial \Delta_0}{\partial z}\right|_n\right]\frac{1}{\xi_n + \eta_n} \qquad (182)$$

Substituting equations 181 and 182 into equations 161 and 163 respectively, the expressions for the radial velocities are found.

$$U(r,z)_- = \sum_{n=1}^{\infty}\left[\Delta_n + \frac{1}{\eta_n}\left.\frac{\partial \Delta_0}{\partial z}\right|_n - \frac{\pi}{2}\frac{k^2 W^{(0)}}{\eta_n}\left[r_t^2 W_0(\xi_n r_t) - r_h^2 W_0(\xi_n r_h)\right]\right]\frac{\xi_n e^{\xi_n z}}{\xi_n + \eta_n} V_1(\xi_n r) \qquad (183)$$

$$U(r,z)_+ = \sum_{n=1}^{\infty}\left[\left.\frac{\partial \Delta_0}{\partial z}\right|_n - \frac{\eta_n^2}{\xi_n}\Delta_n - \frac{\pi}{2}k^2 W^{(0)}\left[r_t^2 W_0(\xi_n r_t) - r_h^2 W_0(\xi_n r_h)\right]\right]\frac{\xi_n e^{-\eta_n z}}{\eta_n^2 + \xi_n \eta_n} V_1(\xi_n r) + \Delta \qquad (184)$$

Expressions for Axial Velocity. The expressions for the function Δ could now be inserted in equations 183 and 184 to obtain the explicit forms for the radial velocity, but it is more convenient to continue with this notation and obtain the corresponding expressions for axial velocity. The continuity equation, 45, gives

$$W(r,z) - W^{(0)} = -\sum_{n=1}^{\infty}\left[\Delta_n + \frac{1}{r_n}\left.\frac{\partial \Delta_0}{\partial z}\right|_n - \frac{\pi}{2}\frac{k^2 W^{(0)}}{\eta_n}\left[r_t^2 W_0(\xi_n r_t) - r_h^2 W_0(\xi_n r_h)\right]\right]\frac{\xi_n e^{\xi_n z}}{\xi_n + \eta_n} V_0(\xi_n r) \qquad (185)$$

$$-\infty < z \leq 0$$

$$W(r,z) - W^{(0)} = \sum_{n=1}^{\infty}\left[-\left.\frac{\partial\Delta^{(0)}}{\partial z}\right|_n + \frac{\pi}{2}k^2 W^{(0)}\left[r_t^2 W_0(\xi_n r_t) - r_n^2 W_0(\xi_n r_n)\right]\right]\frac{\xi_n}{\eta_n^2} V_0(\xi_n r)$$

$$+\sum_{n=1}^{\infty}\left[\left.\frac{\partial\Delta^{(0)}}{\partial z}\right|_n - \frac{\eta_n^2}{\xi_n}\Delta_{0_n} - \frac{\pi}{2}k^2 W^{(0)}\left[r_t^2 W_0(\xi_n r_t) - r_n^2 W_0(\xi_n r_n)\right]\right]\frac{\xi_n^2 e^{-\eta_n z}}{(\xi_n+\eta_n)\eta_n^2} V_0(\xi_n r)$$

$$-\int_0^z \frac{1}{r}\frac{\partial r\Delta}{\partial r}\,dz \qquad 0 \le z < \infty \tag{186}$$

It should be noted in equation 186 that the function Δ changes form from $z < 2L$ to $z > 2L$. With the boundary conditions of equations 145 and 146, the function Δ is as given in equations 165 and 166, and from these equations there results

$$\Delta_n \equiv\equiv -W^{(0)}\frac{A\pi}{L}\frac{\cosh(\eta_n L)}{\xi_n^2 - \beta^2}\frac{\xi_n}{\eta_n}e^{-\eta_n L} \tag{187}$$

$$\left.\frac{\partial\Delta}{\partial z}\right|_n \equiv\equiv -W^{(0)}\frac{A\pi}{L}\frac{\cosh(\eta_n L)}{\xi_n^2 - \beta^2}\xi_n e^{-\eta_n L} \tag{188}$$

Substituting equations 187 and 188 into equations 185 and 186, and including the value of $\int_0^z \frac{1}{r}\frac{\partial r\Delta}{\partial r}\,dz$ as obtained from equations 165, 166, the results are obtained

$$\frac{W(r,z)}{W^{(0)}} - 1 = \sum_{n=1}^{\infty}\left[A\frac{2\pi}{L}\frac{\cosh(\eta_n L)}{\xi_n^2 - \beta^2}\xi_n e^{-\eta_n L} + \frac{\pi}{2}k^2\left[r_t^2 W_0(\xi_n r_t) - r_n^2 W_0(\xi_n r_n)\right]\right]\frac{\xi_n e^{\xi_n z}}{\eta_n^2 + \eta_n\xi_n}V_0(\xi_n r) \tag{189}$$

$$\frac{W(r,z)}{W^{(0)}} - 1 = -A\frac{\pi}{L}\sum_{n=1}^{\infty}\frac{\xi_n^2}{\eta_n^2}\frac{\sinh\{\eta_n(L-z)\}}{\xi_n^2-\beta^2}e^{-\eta_n L}V_0(\xi_n r) - \frac{A2L}{\pi}\left[\frac{k\,U_0(kr)}{U_1(kr_h)} - \frac{\beta\,U_0(\beta r)}{U_1(\beta r_h)}\right]\cos\frac{\pi z}{2L}$$

$$+\frac{\pi}{2}k^2\sum_{n=1}^{\infty}\left[r_t^2 W_0(\xi_n r_t) - r_h^2 W_0(\xi_n r_h)\right]\left[1-\frac{\xi_n e^{-\eta_n z}}{\xi_n+\eta_n}\right]\frac{\xi_n V_0(\xi_n r)}{\eta_n^2} - Ak^2\frac{\pi}{L}\sum_{n=1}^{\infty}\frac{\xi_n^2 e^{-\eta_n(L+z)}}{(\eta_n^2+\xi_n\eta_n)^2}\frac{\cosh(\eta_n L)}{\xi_n^2-\beta^2}V_0(\xi_n r) \qquad (190)$$

$$0 \le z \le 2L$$

$$\frac{W(r,z)}{W^{(0)}} - 1 = -A\frac{\pi}{L}\sum_{n=1}^{\infty}\frac{\xi_n^2}{\eta_n^2}\frac{\cosh(\eta_n L)}{\xi_n^2-\beta^2}e^{-\eta_n(z-L)}V_0(\xi_n r) - A\frac{4L}{\pi}\frac{k\,U_0(kr)}{U_1(kr_h)}$$

$$+\frac{\pi}{2}k^2\sum_{n=1}^{\infty}\left[r_t^2 W_0(\xi_n r_t) - r_h^2 W_0(\xi_n r_h)\right]\left[1-\frac{\xi_n e^{-\eta_n z}}{\xi_n+\eta_n}\right]\frac{\xi_n V_0(\xi_n r)}{\eta_n^2} - Ak^2\frac{\pi}{L}\sum_{n=1}^{\infty}\frac{\xi_n^2 e^{-\eta_n(L+z)}}{(\eta_n^2+\xi_n\eta_n)^2}\frac{\cosh(\eta_n L)}{\xi_n^2-\beta^2}V_0(\xi_n r) \qquad (191)$$

The tangential velocity follows from equation 137, and is found to be

$$\frac{V}{W^{(0)}} - \frac{V^{(0)}}{W^{(0)}} = k\left[\frac{A\pi}{L}\sum_{n=1}^{\infty}\frac{\xi_n}{\eta_n^2}\frac{\sinh(\eta_n L)-\sinh\{\eta_n(L-z)\}}{\xi_n^2-\beta^2}e^{-\eta_n L}V_1(\xi_n r)\right.$$

$$+\frac{\pi}{2}\sum_{n=1}^{\infty}\left[\frac{2Ak^2}{L}\frac{e^{-\eta_n L}}{(\xi_n+\eta_n)^2}\frac{\cosh(\eta_n L)}{\xi_n^2-\beta^2} + \frac{k^2}{\xi_n+\eta_n}\left[r_t^2 W_0(\xi_n r_t) - r_h^2 W_0(\xi_n r_h)\right]\right]\frac{\xi_n}{\eta_n^2}\left(1-e^{-\eta_n z}\right)V_1(\xi_n r)$$

$$\left. - A\frac{2L}{\pi}\left[1-\cos\frac{\pi z}{2L}\right]\frac{U_1(\beta r)}{U_1(\beta r_h)}\right] \qquad 0 \le z \le 2L \qquad (192)$$

$$\frac{V}{W^{(0)}} - \frac{V^{(0)}}{W^{(0)}} = k\left[-\frac{A\pi}{L}\sum_{n=1}^{\infty}\frac{\xi_n}{r_n^2}\frac{\cosh(r_{nL})}{\xi_n^2-\beta^2}e^{-r_{nL}}\left(1+e^{-r_n(z-2L)}\right)V_1(\xi_n r) - \frac{4AL}{\pi}\frac{U_1(kr)}{U_1(kr_n)}\right.$$

$$\left.+\frac{\pi}{2}\sum_{n=1}^{\infty}\left[\frac{2A}{L}\frac{k^2}{(\xi_n+r_{nL})^2}\frac{e^{-r_{nL}}}{\xi_n^2-\beta^2}\cosh(r_{nL}) + \frac{k^2}{\xi_n+r_{nL}}\left[r_t^2 W_0(\xi_n r_t) - r_n^2 W_0(\xi_n r_n)\right]\right]\frac{\xi_n}{r_n^2}\left(1-e^{-r_n z}\right)V_1(\xi_n r)\right] \qquad (193)$$

$$2L \le z < \infty$$

The results of equations 189 to 193 have been plotted for the ratio $m^2 = \frac{k^2}{\xi_1^2}$ of 0.025 and 0.1 (figures 28, 29, 30 and 31). The effect of the wall only on the axial velocity which would have been present with the disc and parallel walls (equations 135, 136, figures 23 and 24) has been plotted separately and is shown in figures 32 and 33. It will be observed that the effects of wall shape are of the same order as are the effects of the actuator disc.

The equations for axial velocity given above contain several special cases, and comparison to previously obtained results gives some simple checks of the results above. If the slope A is allowed to go to zero, the results should be the same as given in equations 135 and 136, and as is easily seen, this is the case. The effects of the rotation can be removed by allowing k to go to zero, in which case equations 189, 190 and 191 reduce to equations 47, 49 and 52, except for the change in location of origin. It should be noted in the last case that the ratio $\frac{k\,U_0(kr)}{U_1(kr_n)}$ becomes $\frac{-2r_n}{r_t^2 - r_n^2}$ in the limit as k approaches zero. Inspection of the equations reveals that the outlet velocity profile as given by equation 191 is simply the sum of the profiles given by equations 136 and 102. Indeed, the only inter-

action between the two flows represented by these equations is the term

$$-A\frac{k^2\pi}{L}\sum_{n=1}^{\infty}\frac{\xi_n^2\, e^{-\eta_n(L+z)}}{(\eta_n^2+\xi_n\eta_n)^2}\,\frac{\cosh(\eta_n r)}{\xi_n^2-\beta^2}\,V_0(\xi_n r)$$

which can be seen to decrease strongly both with decreasing k and with distance from the actuator disc. The composite result of the entrance vane and shaped wall is thus very nearly the sum of the results for the actuator disc and parallel walls, and for the simple sinusoidal step and rotation at inlet, for the values of $m^2=\frac{k^2}{\xi_1^2}$, considered here. The entrance vane tends to introduce a large positive axial velocity perturbation far downstream at the hub radius, but this effect is somewhat compensated for by the opposite effect induced by the increasing wall radius. This opposition of the two effects relocates the maximum velocity perturbation.

VI. STRONG ENTRANCE VANE AT ENTRY TO CONTRACTION

In actual flows, the rotation may be quite large, and it would thus be of interest to investigate the effect of wall shape as coupled with inlet guide vane, a little more closely. In the derivation of equations 189, 190 and 191, the boundary condition of tangential flow over the hub was approximated by assuming $\frac{U}{W} \approx \frac{U}{W^{(0)}}$, but if large rotation is allowed, the more reasonable approximation would be $\frac{U}{W} \approx \frac{U}{W^{(0)}}$, where W_K is taken to be the axial velocity at the hub in the presence of actuator disc and parallel walls only. The effect of this modified boundary condition is to change the value of the function Δ , and this effect will now be discussed.

With the condition that $U(r_h, z) = W_{fc} A \sin \frac{\pi z}{2L}$, it follows that

$$\hat{U}_{(r_h,\kappa)_+} = \frac{A}{\sqrt{2\pi}} \int_0^{2L} W_{fc} \sin \frac{\pi z}{2L} \, e^{-i\kappa z} \, dz \qquad (194)$$

Equation 136 gives

$$W_{fc} = W^{(0)} + r_{fc}^2 \frac{\pi}{2} \sum_{m=1}^{\infty} \frac{\xi_m}{\mu_m^2} \left[1 - \frac{\xi_m e^{-\mu_m z}}{\xi_m + \mu_m} \right] \left[r_t^2 W_0(\xi_m r_t) - r_h^2 W_0(\xi_m r_h) \right] V_0(\xi_m r_h)$$

$$= W_{(r_h,\infty)} - \sum_{m=1}^{\infty} B_m e^{-\mu_m z} \qquad (195)$$

in which the constants B_m and μ_m are given by

$$B_m = r_{fc}^2 \frac{\pi}{2} \frac{\xi_m^2}{\mu_m^2} \frac{r_t^2 W_0(\xi_m r_t) - r_h^2 W_0(\xi_m r_h)}{\xi_m + \mu_m} V_0(\xi_m r_h)$$

$$\mu_m \equiv r_{(n)} = \sqrt{\xi_m^2 - \kappa^2} \qquad (196)$$

The portion of the inversion integral involving $W_{(r_n,\infty)}$ will remain of the same form as equation 148, but the summation of equation 195 must be considered in detail. The integral becomes

$$\hat{U}_{(r_n,K)_+} = \frac{A}{\sqrt{2\pi}}\int_0^{2L} W_{(r_n,\infty)} \sin\frac{\pi z}{2L}\, e^{-iKz}\, dz - \frac{A}{\sqrt{2\pi}}\int_0^{2L} \sum_{m=1}^{\infty} B_m \sin\frac{\pi z}{2L}\, e^{-(\mu_m + iK)z}\, dz$$

$$= \frac{A W_{(r_n,\infty)}}{L}\sqrt{\frac{\pi}{2}}\,\frac{\cos(LK)\, e^{-iKL}}{\left(\frac{\pi}{2L}\right)^2 - K^2} - \frac{A}{2L}\sqrt{\frac{\pi}{2}}\sum_{m=1}^{\infty}\frac{B_m\left[1 + e^{-(\mu_m+iK)2L}\right]}{\mu_m^2 + \mu_m(2iK) + \left(\frac{\pi}{2L}\right)^2 - K^2} \tag{197}$$

The definition of Δ, equation 164, then gives

$$\Delta = \frac{A W_{(r_n,\infty)}}{2L}\int_{-\infty}^{\infty}\frac{\cos(LK)}{\left(\frac{\pi}{2L}\right)^2 - K^2}\,\frac{U_1(i\sqrt{K^2-k^2}\,r)}{U_1(i\sqrt{K^2-k^2}\,r_n)}\, e^{iK(z-L)}\, dK$$

$$-\frac{A}{4L}\int_{-\infty}^{\infty}\sum_{m=1}^{\infty}\frac{B_m\left[1 + e^{-(\mu_m+iK)2L}\right]}{\mu_m^2 + \mu_m(2iK) + \left(\frac{\pi}{2L}\right)^2 - K^2}\,\frac{U_1(i\sqrt{K^2-k^2}\,r)}{U_1(i\sqrt{K^2-k^2}\,r_n)}\, e^{iKz}\, dK \tag{198}$$

The first integral gives exactly the results of equations 165 and 166, except that $W_{(r_n,\infty)}$ replaces $W^{(0)}$. Investigation of the limiting behaviour of the integrand of the second integral shows that the arc of the contour in the complex plane must be taken in the upper half plane for $z > 2L$. In this case, the singularities at $K = i\mu_m \pm \frac{\pi}{2L}$ do not contribute, because the numerator goes to zero at the same time. The only contributions come from the zeroes of $U_1(i\sqrt{K^2-k^2}\,r_n)$, and there is thus obtained

$$\Delta = \frac{A\pi}{2L}\sum_{n=1}^{\infty}\left[\sum_{m=1}^{\infty}\frac{B_m\left[1 + e^{-(\mu_m-\eta_{(n)})2L}\right]}{(\mu_m-\eta_{(n)})^2 + \left(\frac{\pi}{2L}\right)^2}\right]\frac{\xi_n}{\eta_n}\, e^{-\eta_n z}\, V_1(\xi_n r)$$

$$-\frac{A W_{(r_n,\infty)}\pi}{L}\sum_{n=1}^{\infty}\frac{\cosh\eta_{(n-L)}}{\xi_n^2 - B^2}\,\frac{\xi_n}{\eta_n}\, e^{-(z-L)\eta_n}\, V_1(\xi_n r) \tag{199}$$

$$2L \le z < \infty$$

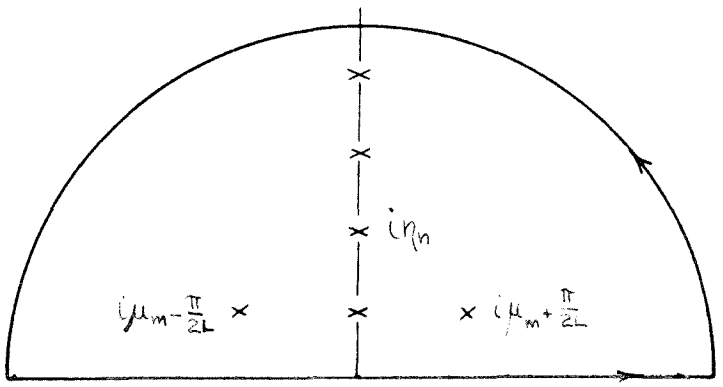

When the region $0 \le z \le 2L$ is considered, it is found necessary to take the contour in the lower half plane for the portion of the second integral involving $e^{-(\mu_m + ik)2L}$, but the other part of the integral must still be taken with the contour in the upper half plane. In this case, the two singularities off axis contribute, and the expression for Δ becomes

$$\Delta = -AW_{(r_h,\infty)}\frac{\pi}{L}\sum_{n=1}^{\infty}\frac{\cosh[\eta_n(L-z)]}{\xi_n^2-\beta^2}\frac{\xi_n}{\eta_n}e^{-\eta_n L}V_1(\xi_n r) + AW_{(r_h,\infty)}\sin\frac{\pi z}{2L}\frac{U_1(\beta r)}{U_1(\beta r_w)}$$

$$+\frac{A\pi}{2L}\sum_{n=1}^{\infty}\left[\sum_{m=1}^{\infty}\frac{B_m e^{-\eta_n z}}{(\mu_m-\eta_n)^2+\left(\frac{\pi}{2L}\right)^2}+\frac{B_m e^{-\mu_m 2L-\eta_m(2L-z)}}{(\mu_m+\eta_n)^2+\left(\frac{\pi}{2L}\right)^2}\right]\frac{\xi_n}{\eta_n}V_1(\xi_n r)$$

$$+A\sum_{m=1}^{\infty}\frac{B_m}{2L}\left[\frac{U_1(\xi_{m-}r)}{U_1(\xi_{m-}r_h)}e^{\frac{i\pi}{2L}z}-\frac{U_1(\xi_{m+}r)}{U_1(\xi_{m+}r_h)}e^{\frac{i\pi}{2L}z}\right]e^{-\mu_m z} \qquad 0\le z\le 2L \qquad (200)$$

here

$$\gamma_{m-} = \left[\mu_m^2 + k^2 - \left(\frac{\pi}{2L}\right)^2 + i\mu_m \frac{\pi}{L} \right]^{1/2} = \bar{\gamma}_{m+}$$

$$\gamma_{m+} = \left[\mu_m^2 + k^2 - \left(\frac{\pi}{2L}\right)^2 - i\mu_m \frac{\pi}{L} \right]^{1/2} = \bar{\gamma}_{m-} \qquad (201)$$

The results of equations 199 and 200 may now be combined with equations 185 and 186 to obtain the desired expressions for axial velocity. The summations of equations 56 and 75 are useful in expanding the complex conjugate group of equation 200 into a series that becomes purely real when multiplied by the coefficient $\frac{1}{2i}$. The expressions for axial velocity become

$$W_{(r,z)} - W^{(0)} = \sum_{n=1}^{\infty} \left[A W_{(r_n,\infty)} \frac{2\pi}{L} \frac{\cosh(\eta_n L)}{\xi_n^2 - \theta^2} \xi_n e^{-\eta_n L} + \frac{\pi}{2} k^2 W^{(0)} \left[r_t^2 W_0(\xi_n r_t) - r_n^2 W_0(\xi_n r_n) \right] \right] \frac{\xi_n e^{\xi_n z}}{\eta_n^2 + \xi_n \eta_n} V_0(\xi_n r)$$

$$- \frac{A\pi}{L} \sum_{n=1}^{\infty} \left[\sum_{m=1}^{\infty} B_m \left[\frac{(\mu_m - \eta_n)^2 + \left(\frac{\pi}{2L}\right)^2}{\left[\eta_n^2 - \mu_m^2 + \left(\frac{\pi}{2L}\right)^2 \right] + \left(\mu_m \frac{\pi}{L}\right)^2} + \frac{e^{-(\mu_m + \eta_n)2L}}{(\mu_m + \eta_n)^2 + \left(\frac{\pi}{2L}\right)^2} \right] \right] \frac{\xi_n^2 e^{\xi_n z}}{\eta_n^2 + \xi_n \eta_n} V_0(\xi_n r)$$

$$-\infty < z \leq 0 \qquad (202)$$

$$W(r,z) - W^{(0)} = -A\frac{W(r_n,\infty)\pi}{L}\sum_{n=1}^{\infty}\frac{\xi_n^2}{\eta_n^2}\frac{e^{-\eta_n L}}{\xi_n^2-\beta^2}\left[\sinh\{\eta_n(L-z)\} + \frac{\xi_c^2\cosh(\eta_n L)}{(\xi_n+\eta_n)L}e^{-\eta_n z}\right]V_0(\xi_n r)$$

$$+ A\frac{2L\,W(r_n,\infty)}{\pi}\left[\frac{\beta J_0(\beta r)}{J_1(\beta r_n)} - \frac{\xi_c J_0(\xi_c r)}{J_1(\xi_c r_n)}\right] - A\frac{2L\,W(r_n,\infty)}{\pi}\left[1-\cos\frac{\pi z}{2L}\right]\left[\frac{\beta J_0(\beta r)}{J_1(\beta r_n)} + \frac{2r_n}{\xi_c^2-r_n^2}\right]$$

$$+ \frac{\pi}{2}\xi_c^2 W^{(0)}\sum_{n=1}^{\infty}\left[r_c^2 W_0(\xi_n r_c) - r_n^2 W_0(\xi_n r_n)\right]\left[1 - \frac{\xi_n e^{-\eta_n z}}{\xi_n+\eta_n}\right]\frac{\xi_n}{\eta_n^2}V_0(\xi_n r) - \frac{A\pi}{L}\sum_{n=1}^{\infty}\left[\sum_{m=1}^{\infty}\frac{B_m}{\mu_m^2+\left(\frac{\pi}{2L}\right)^2}\right]\frac{\xi_c^2}{\eta_n^2}V_0(\xi_n r)$$

$$+ \frac{A\pi}{L}\sum_{n=1}^{\infty}\left[\sum_{m=1}^{\infty}\frac{B_m\left[\xi_n\eta_n^2 + 2\eta_n\mu_m + \xi_n\left(\mu_m^2+\left(\frac{\pi}{2L}\right)^2\right)\right]}{\left[\left(\mu_m^2-\eta_n^2-\left(\frac{\pi}{2L}\right)^2\right)^2 + \left(\mu_m\frac{\pi}{L}\right)^2\right]}\right]\frac{\xi_n^2 e^{-\eta_n z}}{\eta_n^2(\xi_n+\eta_n)}V_0(\xi_n r)$$

$$- \frac{A\pi}{2L}\sum_{n=1}^{\infty}\left[\sum_{m=1}^{\infty}\frac{B_m e^{-(\eta_n+\mu_m)2L}}{(\eta_n+\mu_m)^2+\left(\frac{\pi}{2L}\right)^2}\right]\left[e^{\eta_n z} - \frac{\xi_c^2}{(\xi_n+\eta_n)^2}e^{-\eta_n z}\right]\frac{\xi_n^2}{\eta_n^2}V_0(\xi_n r)$$

$$- A\sum_{n=1}^{\infty}\left[\sum_{m=1}^{\infty}B_m e^{-\mu_m}\frac{2\left[\mu_m\sin\frac{\pi z}{2L} + \frac{\pi}{2L}\cos\frac{\pi z}{2L}\right]\left[\left(\mu_m^2+\beta^2\right)\left(\mu_m^2-\eta_n^2-\left(\frac{\pi}{2L}\right)^2\right) + \left(\eta_n\frac{\pi}{L}\right)^2\right] + \xi_n^2\left[2\mu_m^2\frac{\pi}{L}\cos\frac{\pi z}{2L} - \left(\frac{\pi}{L}\right)^2\sin\frac{\pi z}{2L}\right]}{\left[\mu_m^2+\left(\frac{\pi}{2L}\right)^2\right]\left[\left(\mu_m^2-\eta_n^2-\left(\frac{\pi}{2L}\right)^2\right)^2 + \left(\mu_m\frac{\pi}{L}\right)^2\right]}\right]V_0(\xi_n r)$$

$0 \le z \le 2L$

(203)

$$W(r,z) - W^{(0)} = -\frac{A\pi}{L} W_{V(r_1,\infty)} \sum_{n=1}^{\infty} \frac{\xi_n^2}{\eta_n^2} \frac{\cosh(\eta_n L)}{\xi_n^2 - \beta^2} \left[e^{-\eta_n(z-L)} + \frac{k^2}{(\xi_n + \eta_n)^2} e^{-\eta_n(L+z)} \right] V_1(\xi_n r)$$

$$+ \frac{\pi}{2} k^2 W^{(0)} \sum_{n=1}^{\infty} \frac{\xi_n}{\eta_n^2} \left[1 - \frac{\xi_n e^{-\eta_n z}}{\xi_n + \eta_n} \right] \left[r_t^2 W_0(\xi_n r_t) - r_n^2 W_0(\xi_n r_n) \right] V_0(\xi_n r) - W_{(r_1,\infty)} \frac{A4L}{\pi} \left[\frac{k U_0(kr)}{J_1(kr_n)} + \frac{2 r_n}{r_t^2 - r_n^2} \right]$$

$$+ \frac{A\pi}{L} \sum_{n=1}^{\infty} \left[\sum_{m=1}^{\infty} \frac{B_m \left[\xi_n \eta_n^2 + 2\mu_m \eta_n^2 + \xi_n \left(\mu_m^2 + \left(\frac{\pi}{2L}\right)^2 \right) \right]}{\left[\left(\mu_m^2 - \eta_n^2 - \left(\frac{\pi}{2L}\right)^2 \right)^2 + \left(\mu_m \frac{\pi}{L} \right)^2 \right]} \right] \frac{\xi_n^2 e^{-\eta_n z}}{\eta_n^2 (\xi_n + \eta_n)} V_0(\xi_n r) - \frac{A\pi}{L} \sum_{n=1}^{\infty} \left[\sum_{m=1}^{\infty} \frac{B_m}{\mu_m^2 + \left(\frac{\pi}{2L}\right)^2} \right] \frac{k^2}{\eta_n^2} V_0(\xi_n r)$$

$$- \frac{A\pi}{2L} \sum_{n=1}^{\infty} \left[\sum_{m=1}^{\infty} \frac{B_m e^{-(\mu_m + \eta_n)2L}}{(\mu_m + \eta_n)^2 + \left(\frac{\pi}{2L}\right)^2} \right] \left[e^{\eta_n 2L} - \frac{k^2}{(\xi_n + \eta_n)^2} e^{-\eta_n z} \right] \frac{\xi_n^2}{\eta_n^2} V_0(\xi_n r)$$

$$+ \frac{A\pi}{L} \sum_{n=1}^{\infty} \left[\sum_{m=1}^{\infty} \frac{B_m e^{-\mu_m 2L} \left[2\mu_m^2 \xi_n^2 + \left(\mu_m \frac{\pi}{L}\right)^2 + (\mu_m^2 + \beta^2)\left(\mu_m^2 - \eta_n^2 - \left(\frac{\pi}{2L}\right)^2 \right) \right]}{\left[\mu_m^2 + \left(\frac{\pi}{2L}\right)^2 \right] \left[\left(\mu_m^2 - \eta_n^2 - \left(\frac{\pi}{2L}\right)^2 \right)^2 + \left(\mu_m \frac{\pi}{L} \right)^2 \right]} \right] V_0(\xi_n r)$$

$$- \frac{A\pi}{2L} \sum_{n=1}^{\infty} \left[\sum_{m=1}^{\infty} \frac{B_m e^{-(\mu_m - \eta_n)2L}}{(\mu_m - \eta_n)^2 + \left(\frac{\pi}{2L}\right)^2} \right] \left[e^{-\eta_n 2L} - e^{-\eta_n z} \right] \frac{\xi_n^2}{\eta_n^2} V_0(\xi_n r)$$

$$2L \le z < \infty \qquad (204)$$

These equations for the axial velocity contain only the perturbation about the mean flow. Finally, the expressions for the tangential velocity are obtained from equations 200, 199, 184 and 137. The resulting expressions are

$$V - V^{(0)} = k_e^3 \sum_{n=1}^{\infty} \left[\frac{\pi A}{L} W_{(r_1,\infty)} \frac{\cosh(\eta_n L)}{\xi_n^2 - \beta^2} \frac{e^{-\eta_n L}}{\xi_n + \eta_n} + W^{(0)} \left[r_t^2 W_0(\xi_n r_t) - r_n^2 W_0(\xi_n r_n) \right] \right] \frac{\xi_n}{\eta_n^2} \frac{1 - e^{-\eta_n z}}{\xi_n + \eta_n} V_1(\xi_n r)$$

$$+ \frac{A\pi k_e}{L} W_{(r_1,\infty)} \sum_{n=1}^{\infty} \frac{\xi_n}{\eta_n^2} \frac{\sinh\{\eta_n L\} - \sinh\{\eta_n (L-z)\}}{\xi_n^2 - \beta^2} e^{-\eta_n L} V_1(\xi_n r) - A k_e \frac{2}{\pi} W_{(r_1,\infty)} \left[1 - \cos\frac{\pi z}{2L} \right] \frac{U_1(\beta r)}{U_1(\beta r_1)}$$

$$- \frac{A\pi k_e}{2L} \sum_{n=1}^{\infty} \left[\sum_{m=1}^{\infty} \frac{B_m e^{-(\mu_m + \eta_n) 2L}}{(\mu_m + \eta_n)^2 + \left(\frac{\pi}{2L}\right)^2} \right] \left[\left(1 - e^{\eta_n z}\right) - \frac{k_e^2}{(\xi_n + \eta_n)^2} \left(1 - e^{-\eta_n z}\right) \right] \frac{\xi_n}{\eta_n^2} V_1(\xi_n r)$$

$$+ \frac{A\pi k_e}{L} \sum_{n=1}^{\infty} \left[\sum_{m=1}^{\infty} \frac{B_m \left[\xi_n \eta_n^2 + 2\mu_m \eta_n^2 + \xi_n \mu_m^2 + \xi_n \left(\frac{\pi}{2L}\right)^2 \right]}{\left[\left(\eta_n^2 - \mu_m^2 + \left(\frac{\pi}{2L}\right)^2\right)^2 + \left(\mu_m \frac{\pi}{L}\right)^2 \right]} \right] \frac{\xi_n \left(1 - e^{-\eta_n z}\right)}{\eta_n^2 (\xi_n + \eta_n)} V_1(\xi_n r)$$

$$+ 2A k_e \sum_{n=1}^{\infty} \left[\sum_{m=1}^{\infty} \frac{B_m \left[\left\{ \eta_n^2 - \mu_m^2 + \left(\frac{\pi}{2L}\right)^2 \right\} \left\{ \frac{\pi}{2L} - e^{-\mu_m z} \left(\mu_m \sin\frac{\pi z}{2L} + \frac{\pi}{2L} \cos\frac{\pi z}{2L} \right) \right\} - \mu_m \frac{\pi}{L} \left\{ \mu_m - e^{-\mu_m z} \left(\mu_m \cos\frac{\pi z}{2L} - \frac{\pi}{2L} \sin\frac{\pi z}{2L} \right) \right\} \right]}{\left[\mu_m^2 + \left(\frac{\pi}{2L}\right)^2 \right] \left[\left(\eta_n^2 - \mu_m^2 + \left(\frac{\pi}{2L}\right)^2\right)^2 + \left(\mu_m \frac{\pi}{L}\right)^2 \right]} \right] \xi_n V_1(\xi_n r)$$

$$0 \le z \le 2L \qquad (205)$$

$$V - V^{(0)} = k_e^3 \sum_{n=1}^{\infty} \left[\frac{\pi A}{L} W_{(r_1,\infty)} \frac{\cosh(\eta_n L)}{\xi_n^2 - \beta^2} \frac{e^{-\eta_n L}}{\xi_n + \eta_n} + W^{(0)} \left[r_t^2 W_0(\xi_n r_t) - r_n^2 W_0(\xi_n r_n) \right] \right] \frac{\xi_n}{\eta_n^2} \frac{1 - e^{-\eta_n z}}{\xi_n + \eta_n} V_1(\xi_n r)$$

$$- \frac{A\pi k_e}{L} W_{(r_1,\infty)} \sum_{n=1}^{\infty} \frac{\xi_n}{\eta_n^2} \frac{\cosh(\eta_n L)}{\xi_n^2 - \beta^2} e^{-\eta_n L} \left(1 + e^{-\eta_n (z-2L)}\right) V_1(\xi_n r) - W_{(r_1,\infty)} \frac{4L}{\pi} \frac{U_1(kr)}{U_1(kr_1)}$$

$$- \frac{A\pi k_e}{2L} \sum_{n=1}^{\infty} \left[\sum_{m=1}^{\infty} \frac{B_m e^{-(\mu_m + \eta_n) 2L}}{(\mu_m + \eta_n)^2 + \left(\frac{\pi}{2L}\right)^2} \right] \left[\left(1 - e^{\eta_n 2L}\right) - \frac{k_e^2}{(\xi_n + \eta_n)^2} \left(1 - e^{-\eta_n z}\right) \right] \frac{\xi_n}{\eta_n^2} V_1(\xi_n r)$$

$$+ \frac{A\pi k_e}{L} \sum_{n=1}^{\infty} \left[\sum_{m=1}^{\infty} \frac{B_m \left[\xi_n \eta_n^2 + 2\mu_m \eta_n^2 + \xi_n \mu_m^2 + \xi_n \left(\frac{\pi}{2L}\right)^2 \right]}{\left[\left(\eta_n^2 - \mu_m^2 + \left(\frac{\pi}{2L}\right)^2\right)^2 + \left(\mu_m \frac{\pi}{L}\right)^2 \right]} \right] \frac{\xi_n \left(1 - e^{-\eta_n z}\right)}{\eta_n^2 (\xi_n + \eta_n)} V_1(\xi_n r)$$

$$+ 2A k_e \sum_{n=1}^{\infty} \left[\sum_{m=1}^{\infty} \frac{B_m \frac{\pi}{2L} \left\{ 1 + e^{-\mu_m 2L} \right\} \left\{ \eta_n^2 - 3\mu_m^2 + \left(\frac{\pi}{2L}\right)^2 \right\}}{\left[\mu_m^2 + \left(\frac{\pi}{2L}\right)^2 \right] \left[\left(\eta_n^2 - \mu_m^2 + \left(\frac{\pi}{2L}\right)^2\right)^2 + \left(\mu_m \frac{\pi}{L}\right)^2 \right]} \right] \xi_n V_1(\xi_n r)$$

$$- \frac{A\pi k_e}{2L} \sum_{n=1}^{\infty} \left[\sum_{m=1}^{\infty} \frac{B_m e^{-\mu_m 2L}}{(\mu_m - \eta_n)^2 + \left(\frac{\pi}{2L}\right)^2} \right] \frac{\xi_n}{\eta_n^2} \left(1 - e^{-\eta_n (z-2L)}\right) V_1(\xi_n r) \qquad 2L \le z < \infty \qquad (206)$$

The complete expression given by equations 202, 203 and 204 has been calculated for the value $m^2 = \frac{k^2}{s_1^2}$ of 0.1 and the effect of the modification of the boundary condition on the axial velocity both at the disc and infinitely far downstream is shown in figure 34. It can be seen that for the geometry and rotation given here, the effect is quite small, amounting to about 20 % of the total wall effect, but if the slope and overall contraction of the wall were increased, this variation could well become significant.

VII. HEAVILY LOADED ENTRANCE VANE FOLLOWED BY LIGHTLY LOADED ROTOR

The effect of a lightly loaded rotor behind a heavily loaded entrance vane will be considered. It is assumed that because of the low loading of the rotor, the interaction between it and the wall will be negligible, so that the effect of adding a loaded rotor to the flow induced by an actuator disc within parallel walls may be computed, and the effect of actuator disc only subtracted out. The difference may then be added to the previously obtained results including effect of wall, to obtain the overall flow.

"Free vortex" blade loading will be assumed in this case, that is, the blade imparts a rotation given by

$$\Delta V = \frac{C}{r}$$

The increase in total head across the blade row, is from equation 10

$$\Delta \frac{P}{\rho} = \omega \Delta V r = \omega C \qquad (207)$$

for all streamlines.

The tangential velocity in the region behind the blade row is thus described by

$$rV = -k\psi + C \qquad (208)$$

so that equation 19 becomes for this region

$$\frac{\partial}{\partial r}\left(\frac{1}{r}\frac{\partial \psi}{\partial r}\right) + \frac{\partial}{\partial z}\left(\frac{1}{r}\frac{\partial \psi}{\partial z}\right) = \frac{k}{r}\left(-k\psi + C\right) \tag{209}$$

Taking the derivative by z, it is found that the equation reduces to equation 85. The effect of the blade row is felt through the matching conditions, however, because subtracting equation 209 from equation 84 gives

$$\left.\frac{\partial u}{\partial z}\right|_{\nu+} - \left.\frac{\partial u}{\partial z}\right|_{\nu-} = \frac{C k}{r}$$

in which ν is the value of z at the rotor.

The problem is thus defined by the equations

$$\frac{\partial^2 u}{\partial r^2} + \frac{\partial}{\partial r}\left(\frac{u}{r}\right) + \frac{\partial^2 u}{\partial z^2} = 0 \qquad -\infty < z \leq 0 \tag{210}$$

$$\frac{\partial^2 u}{\partial r^2} + \frac{\partial}{\partial r}\left(\frac{u}{r}\right) + k^2 u + \frac{\partial^2 u}{\partial z^2} = 0 \qquad 0 \leq z < \infty \tag{211}$$

and the matching conditions

$$\left.\frac{\partial u}{\partial z}\right|_{0+} - \left.\frac{\partial u}{\partial z}\right|_{0-} = \frac{k^2 w^{(0)} r}{2} - k^2 \int_{-\infty}^{0} u\, dz \quad , \quad u_{0+} = u_{0-} \tag{212}$$

$$\left.\frac{\partial u}{\partial z}\right|_{\nu+} - \left.\frac{\partial u}{\partial z}\right|_{\nu-} = \frac{C k}{r} \quad , \quad u_{\nu+} = u_{\nu-} \tag{213}$$

The solutions valid in each of the three regions are of the form

$$U(r,z) = \sum_{n=1}^{\infty} A_n V_1(\xi_n r)\, e^{-\xi_n z} \qquad -\infty < z \le 0 \qquad (214)$$

$$U(r,z) = \sum_{n=1}^{\infty} \left[B_n e^{\eta_n z} + C_n e^{-\eta_n z} \right] V_1(\xi_n r) \qquad 0 \le z \le \nu \qquad (215)$$

$$U(r,z) = \sum_{n=1}^{\infty} D_n V_1(\xi_n r)\, e^{-\eta_n z} \qquad \nu \le z < \infty \qquad (216)$$

Application of the matching condition equation 213 requires expansion of $\frac{1}{r}$ in terms of the characteristic functions $V_1(\xi_n r)$. It is easily shown that

$$\frac{1}{r} = \pi \sum_{n=1}^{\infty} \left[W_0(\xi_n r_t) - W_0(\xi_n r_n) \right] V_1(\xi_n r) \qquad (217)$$

and

$$r = \pi \sum_{n=1}^{\infty} \left[r_t^2 W_0(\xi_n r_t) - r_n^2 W_0(\xi_n r_n) \right] V_1(\xi_n r) \qquad (218)$$

With these expansions, the four constants A_n, B_n, C_n and D_n may be evaluated by application of the four matching conditions, equations 212 and 213. The results for the radial velocity then become

$$U(r,z) = -\frac{\pi}{2}\sum_{n=1}^{\infty}\left[C_n k e^{-\eta_n \nu}\left[W_0(\xi_n r_t) - W_0(\xi_n r_n)\right]\left[1 + \frac{k^2}{(\xi_n+\eta_n)^2}\right] + \frac{\xi_n k^2 W^{(0)}}{\xi_n+\eta_n}\left[r_t^2 W_0(\xi_n r_t) - r_n^2 W_0(\xi_n r_n)\right]\right]\frac{V_1(\xi_n r)}{\eta_n} e^{\xi_n z}$$

$$-\infty < z \le 0 \qquad (219)$$

$$U(r,z) = -\frac{\pi}{2}\sum_{n=1}^{\infty}\left[C_n k e^{-\eta_n \nu}\left[W_0(\xi_n r_t) - W_0(\xi_n r_n)\right]\left[e^{\eta_n z} + \frac{k^2}{(\xi_n+\eta_n)^2} e^{-\eta_n z}\right] + \frac{\xi_n k^2 W^{(0)}}{\xi_n+\eta_n}\left[r_t^2 W_0(\xi_n r_t) - r_n^2 W_0(\xi_n r_n)\right] e^{-\eta_n z}\right]\frac{V_1(\xi_n r)}{\eta_n}$$

$$0 \le z \le \nu \qquad (220)$$

$$U(r,z) = -\frac{\pi}{2}\sum_{n=1}^{\infty}\left[C_n k\left[W_0(\xi_n r_t) - W_0(\xi_n r_n)\right]\left[e^{-\eta_n (z-\nu)} + \frac{k^2}{(\xi_n+\eta_n)^2} e^{-\eta_n (z+\nu)}\right] + \frac{\xi_n k^2 W^{(0)}}{\xi_n+\eta_n}\left[r_t^2 W_0(\xi_n r_t) - r_n^2 W_0(\xi_n r_n)\right] e^{-\eta_n z}\right]\frac{V_1(\xi_n r)}{\eta_n}$$

$$\nu \le z < \infty \qquad (221)$$

The axial velocity equations follow by straightforward application of the continuity equation and give

$$W(r,z) - W^{(0)} = \frac{\pi}{2}\sum_{n=1}^{\infty}\left[C_n k e^{-\eta_n \nu}\left[W_0(\xi_n r_t) - W_0(\xi_n r_n)\right]\left[1 + \frac{k^2}{(\xi_n+\eta_n)^2}\right] + \frac{\xi_n k^2 W^{(0)}}{\xi_n+\eta_n}\left[r_t^2 W_0(\xi_n r_t) - r_n^2 W_0(\xi_n r_n)\right]\right]\frac{V_0(\xi_n r)\, e^{\xi_n z}}{\eta_n}$$

$$-\infty < z \le 0 \qquad (222)$$

$$W_{(r,z)} - W^{(o)} = \frac{\pi}{2} \sum_{n=1}^{\infty} \left[C k e^{-\eta_n \nu} \left[W_o(\xi_n r_t) - W_o(\xi_n r_n) \right] \left[e^{\eta_n z} - \frac{k^2}{(\xi_n + \eta_n)^2} e^{-\eta_n z} \right] \right.$$

$$\left. + \frac{k^2 W^{(o)}}{\xi_n + \eta_n} \left[r_t^2 W_o(\xi_n r_t) - r_n^2 W_o(\xi_n r_n) \right] \left[\eta_n + \xi_n (1 - e^{-\eta_n z}) \right] \right] \frac{\xi_n}{\eta_n^2} V_o(\xi_n r)$$

$$0 \le z \le \nu \qquad (223)$$

$$W_{(r,z)} - W^{(o)} = \frac{\pi}{2} \sum_{n=1}^{\infty} \left[C k \left[W_o(\xi_n r_t) - W_o(\xi_n r_n) \right] \left[2 - e^{-\eta_n (z-\nu)} - \frac{k^2}{(\xi_n + \eta_n)^2} e^{-\eta_n (z+\nu)} \right] \right.$$

$$\left. + \frac{k^2 W^{(o)}}{\xi_n + \eta_n} \left[r_t^2 W_o(\xi_n r_t) - r_n^2 W_o(\xi_n r_n) \right] \left[\eta_n + \xi_n (1 - e^{-\eta_n z}) \right] \right] \frac{\xi_n}{\eta_n^2} V_o(\xi_n r)$$

$$\nu \le z < \infty \qquad (224)$$

Finally, application of equation 106 to equations 220 and 221 gives the expressions for tangential velocity as

$$V - V^{(o)} = k \frac{\pi}{2} \sum_{n=1}^{\infty} \left[C k \left[W_o(\xi_n r_t) - W_o(\xi_n r_n) \right] \left[e^{-\eta_n (\nu - z)} - e^{-\eta_n \nu} + \frac{k^2 e^{-\eta_n \nu}}{(\xi_n + \eta_n)^2} (1 - e^{-\eta_n z}) \right] \right.$$

$$\left. + \frac{\xi_n k^2 W^{(o)}}{\xi_n + \eta_n} \left[r_t^2 W_o(\xi_n r_t) - r_n^2 W_o(\xi_n r_n) \right] \left[1 - e^{-\eta_n z} \right] \right] \frac{V_1(\xi_n r)}{\eta_n^2}$$

$$0 \le z \le \nu \qquad (225)$$

$$V - V^{(o)} = k \frac{\pi}{2} \sum_{n=1}^{\infty} \left[C k \left[W_o(\xi_n r_t) - W_o(\xi_n r_n) \right] \left[2 - e^{-\eta_n (z-\nu)} - e^{-\eta_n \nu} + \frac{k^2 e^{-\eta_n \nu}}{(\xi_n + \eta_n)^2} (1 - e^{-\eta_n z}) \right] \right.$$

$$\left. + \frac{\xi_n k^2 W^{(o)}}{\xi_n + \eta_n} \left[r_t^2 W_o(\xi_n r_t) - r_n^2 W_o(\xi_n r_n) \right] \left[1 - e^{-\eta_n z} \right] \right] \frac{V_1(\xi_n r)}{\eta_n^2} + \frac{C}{r}$$

$$\nu \le z < \infty \qquad (226)$$

As discussed previously, the effect of the blade only is to be determined, so that the expressions for the velocity perturbations from the actuator disc and parallel walls only, equations 135 and 136 must be subtracted from the appropriate equations above. The results follow quickly, and are given by

$$\Delta\left(W_{(r,z)} - W^{(0)}\right) = \frac{\pi}{2}\sum_{n=1}^{\infty} C_n k\, e^{-\eta_n \nu}\left[W_0(\xi_n r_t) - W_0(\xi_n r_h)\right]\left[1 + \frac{k^2}{(\xi_n+\eta_n)^2}\right]\frac{V_0(\xi_n r)}{\eta_n} e^{\xi_n z}$$

$$-\infty < z \leq 0 \qquad (227)$$

$$\Delta\left(W_{(r,z)} - W^{(0)}\right) = \frac{\pi}{2}\sum_{n=1}^{\infty} C_n k\, e^{-\eta_n \nu}\left[W_0(\xi_n r_t) - W_0(\xi_n r_h)\right]\left[e^{\eta_n z} - \frac{k^2}{(\xi_n+\eta_n)^2} e^{-\eta_n z}\right]\frac{\xi_n}{\eta_n^2} V_0(\xi_n r)$$

$$0 \leq z \leq \nu \qquad (228)$$

$$\Delta\left(W_{(r,z)} - W^{(0)}\right) = \frac{\pi}{2}\sum_{n=1}^{\infty} C_n k\left[W_0(\xi_n r_t) - W_0(\xi_n r_h)\right]\left[2 - e^{-\eta_n (z-\nu)} - \frac{k^2}{(\xi_n+\eta_n)^2} e^{-\eta_n (z+\nu)}\right]\frac{\xi_n}{\eta_n^2} V_0(\xi_n r)$$

$$\nu \leq z < \infty \qquad (229)$$

The results of equations 227, 228 and 229 are shown in figures 35 and 36 for the values $m^2 = 0.1$, $C = 0.2 W^{(0)} r_h$ and $m^2 = 0.025$, $C = 0.1 W^{(0)} r_h$, with the blade positioned at $\nu = \frac{1}{2}$. The entire solution, including effects of actuator disc at inlet, loaded blade row and variable wall are obtained by adding the curves of figures 35 and 36 to those of figures 28 and 29. The final results are shown in figures 37 and 38.

The effects of the loaded blade row only on the tangential velocity are obtained in a similar manner to the above, and the resultant equations become

$$\Delta(V-V^{(0)}) = C k^2 \frac{\pi}{2} \sum_{n=1}^{\infty} \left[W_0(\xi_n r_t) - W_0(\xi_n r_h) \right] \left[e^{-\eta_n(\nu - z)} - e^{-\eta_n \nu} + \frac{k^2 e^{-\eta_n \nu}}{(\xi_n + \eta_n)^2} \left(1 - e^{-\eta_n z}\right) \right] \frac{V_1(\xi_n r)}{\eta_n^2}$$

$$0 \le z \le \nu \qquad (230)$$

$$\Delta(V-V^{(0)}) = C k^2 \frac{\pi}{2} \sum_{n=1}^{\infty} \left[W_0(\xi_n r_t) - W_0(\xi_n r_h) \right] \left[2 - e^{-\eta_n (z-\nu)} - e^{-\eta_n \nu} + \frac{k^2 e^{-\eta_n \nu}}{(\xi_n + \eta_n)^2} \left(1 - e^{-\eta_n z}\right) \right] \frac{V_1(\xi_n r)}{\eta_n^2}$$

$$+ \frac{C}{r} \qquad \nu \le z < \infty \qquad (231)$$

The change in tangential velocity as given by these equations is shown in figure 39 for $m^2 = 0.1$, $C = 0.2 W^{(0)} r_h$. The zero order term $\frac{C}{r}$ has not been included in the figure, but must be added on once downstream of the blade row. The effect of the blade row on the tangential velocity can be seen to be very small, except for the zero order term $\frac{C}{r}$, and in the case $m^2 = 0.025$ the results were found to be negligibly small, the maximum perturbation being $\Delta(V-V^{(0)}) = .003 W^{(0)}$

For the magnitudes of blade loading chosen in these examples, the change in flow conditions caused by the rotating blade row being superimposed on the flow from the inlet guide vanes is slightly less than that of the inlet guide vanes alone, the maximum perturbations in axial velocity being respectively $.26 W^{(0)}$ and $.35 W^{(0)}$ for $m^2 = 0.1$, $C = 0.2 W^{(0)} r_h$, and $.064 W^{(0)}$ and $.075 W^{(0)}$ for $m^2 = 0.025$, $C = 0.1 W^{(0)} r_h$. It is evident from the equation that the effect of the rotor on the axial

velocity vanishes when the approaching rotation is removed. This is to be expected from the fact that the rotor imparts a free vortex motion to the flow, which would be a radial equilibrium condition if the approaching flow was irrotational. For a given rotor input, C, the relative distortion caused by the inlet guide vanes increases more rapidly with increasing rotation, k, than does the distortion caused by the addition of the rotor. This is, of course, a result of the fact that the distortion caused by the inlet guide vanes behaves as the square of the parameter k, but the rotor distortion changes almost linearly with k. In the event that the rotor loading was considered to become very large, the interaction between it and the distortion caused by the variable hub radius would have to be considered, and a solution similar to that given in Chapter VI should be carried out.

VIII. CONCLUDING REMARKS

The results of the foregoing analysis illustrate that the velocity perturbations introduced by the varying wall geometry of a turbomachine can be of the same magnitude as the perturbations introduced by the flade rows themselves, the velocity distortions being larger, the greater the curvature of the wall. The method of obtaining appropriate analytic expressions for the effect of wall shape under several inlet flow conditions and for arbitrary wall geometry has been developed. The two examples of wall shape illustrated here by no means exhaust the possible choices of geometry which lead to easy analytic solutions, and the more general form of solution given in Chapter VI allows comparatively rapid determination of the analytic solution, once a wall geometry is chosen.

The actual conditions to be found in a turbomachine are closely approximated by the configuration investigated here; that of a heavily loaded set of inlet guide vanes followed by a varying wall radius. The axial velocity distortion induced by the inlet guide vanes increases rapidly as the inlet guide vane loading is increased. This is to be expected from energy considerations, in that for this case the total head is constant for all streamlines, so that the introduction of a large tangential velocity at the tip radius brings about a compensating increase in axial velocity along the hub radius. It was shown in the development of the equations for the inlet guide vanes loading considered here, that the equations for the flow were linear, so that when linear boundary conditions, such as a parallel walled annulus,

are given, the distortions induced may be allowed to become large. This observation led to the use of the approximate boundary condition that the flow over the variable wall is that found with entrance guide vanes and parallel walls only. In this case then, the overall velocity distortions can be quite large, so long as the effect of the wall is such as to not invalidate the assumption of linearity.

The equations encountered throughout are quite complex, and the need for some approximate forms similar to those developed for the case of non-rotating flow over a varying wall radius, Chapter III, is evident. In particular, the equations obtained for the wall perturbation of the flow induced by the entrance guide vanes are extremely lengthy, and some further investigations of these exact analytical expressions could possibly yield some welcome approximations. With such approximations, it would then be reasonable to extend the analysis to the case where the rotating blade row is also heavily loaded, so that the interaction between it and the variable wall radius should be included. It is clear that the calculations to be carried out under the assumptions of perfect fluid and infinite blade number need be carried out only to an accuracy justified within the limits of these physical approximations, and the use of convenient mathematical approximations within such limits is therefore reasonable.

The effects of compressibility have not been included in the foregoing analysis, because it is felt that though a significant portion of the change in radius of the compressor walls is to compensate for the change in density of the fluid, the general flow pattern about the mean flow is not so greatly changed so that the incompressible flow pat-

terms give most of the necessary information. The analysis could thus obviously be extended to cover flow in water pumps in which the compressibility is not a factor.

The mixed flow compressor, or pump, in which both the hub radius and tip radius increase throughout the machine, should also be amenable to a similar analysis as was given here, though care should be taken that the variation in wall radius is not such as to invalidate the linearizing assumptions.

REFERENCES

(1) Ruden, P., "Untersuchungen uber einstufige Axialgeblase," Luftfahrtforschung, Vo. 14, no. 7 (1937) pp. 325-346 and Vo. 14, no. 9, (1937) pp. 458-473. (Translated as NACA Technical Note No. 1062.)

(2) Traupel, Walter, Neve Allegemeine Theorie der Mehrstufigen Axialen Turbomaschine, Leemann and Company, (Zurich), (1942).

(3) Bowen, John T., Sabersky, Rolf H., and Rannie, W. Duncan, "Theoretical and Experimental Investigations of Axial Flow Compressors," Summary Report, Contract N6-ori-102, Task Order IV, Office of Naval Research, and Mechanical Engineering Laboratory, California Institute of Technology, (January, 1949).

(4) Marble, Frank E., "The Flow of a Perfect Fluid Through an Axial Turbomachine with Prescribed Blade Loading," Journal of Aeronautical Sciences, Vol. 15, no. 8, (August 1948), pp. 473-485

(5) Marble, Frank E., "Some Problems Concerning the Three-Dimensional Flow in Axial Turbomachines," Presented at Annual Meeting, Institute of Aeronautical Sciences, (January 1949), Preprint No. 182.

(6) Marble, Frank E. and Michelson, I., "Analytical Investigation of Some Three-Dimensional Flow Problems in Turbomachines," NACA Technical Note 2614, (March 1952)

(7) Railly, J. W., "The Flow of an Incompressible Fluid Through an Axial Turbo-Machine with Any Number of Rows," The Aeronautical Quarterly, Vol. III, (September 1951)

(8) Horlock, J. H., "Some Actuator Disc Theories for the Flow of Air Through Axial Turbo-Machines," R and M 3030, (1952).

(9) Horlock, J. H., "The Compressible Flow Through Actuator Discs," The Aeronautical Quarterly, Vol. IX, (May 1958), pp. 110-130

(10) Wu, Chung-Hua, "General Through-Flow Theory of Fluid Flow With Subsonic or Supersonic Velocity in Turbomachines of Arbitrary Hub and Casing Shapes," NACA Technical Note 2302, (March 1951)

(11) Wu, Chung-Hua and Brown, Curtis A., "Method of Analysis for Compressible Flow Past Arbitrary Turbomachine Blades on General Surface of Revolution," 42 p. diagrams NACA Technical Note 2407 (July 1951)

(12) Bragg, Stephen L. and Hawthorne, William R., "Some Exact Solutions of the Flow Through Annular Cascade Actuator Discs," Journal of the Aeronautical Sciences, Vol. 17, no. 4, (April 1950), pp. 243-249

(13) Marble, Frank E., "Three Dimensional Flow in Turbomachines," (To be published in High Speed Aerodynamics and Jet Propulsion, Volume X, Princeton Press.)

(14) Fraenkel, L. E., "On the Flow of a Rotating Fluid Past Bodies in a Pipe," Royal Society of London Proceedings, Series A, Volume 233 (January 1956), pp. 506-526

(15) Morgan, G. W., "A Study of Motions in a Rotating Liquid," Royal Society of London Proceedings, Series A, Volume 206 (March 1951), pp. 108-130

(16) Copson, E. T., An Introduction to the Theory of Functions of a Complex Variable, (Oxford, Clarendon Press) (1935), pp. 335-336

(17) Jahnke, Eugene and Emde, Fritz, Tables of Functions, (Dover Publications, New York), (1943), pp. 125-265

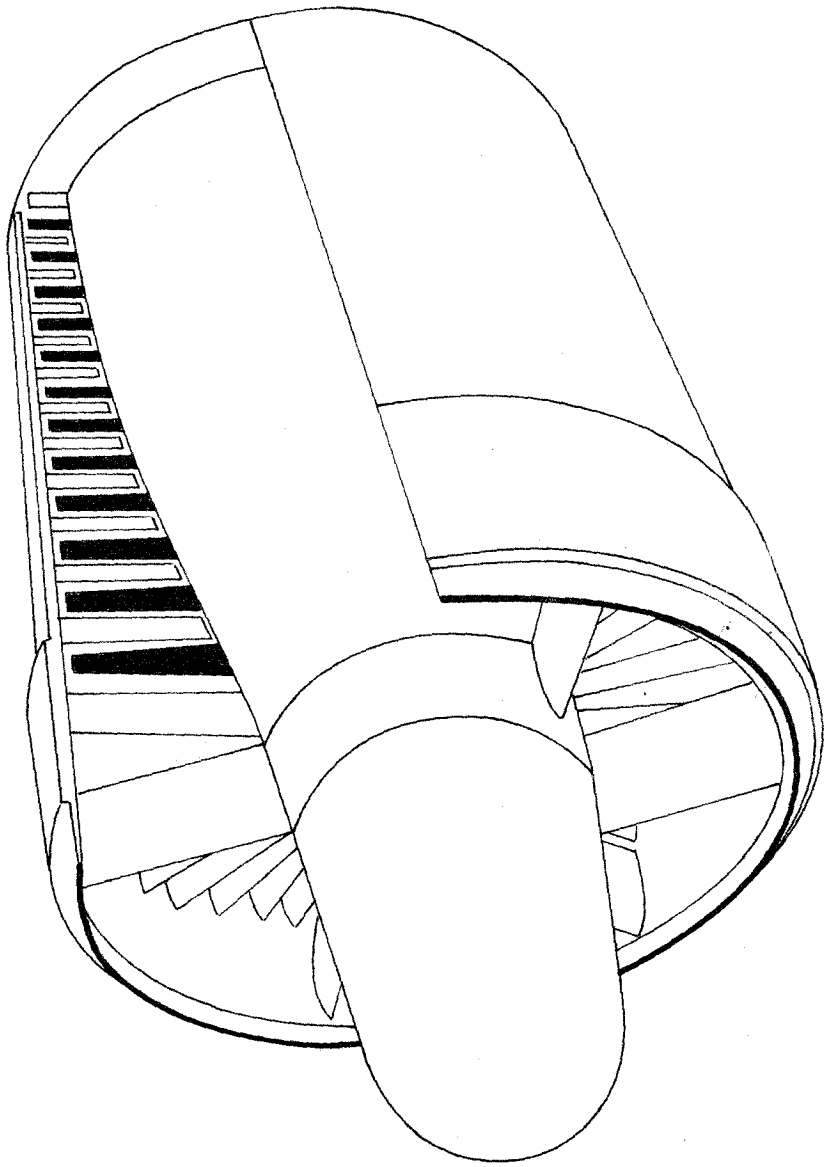

Figure 1. Typical Aircraft Gas Turbine Compressor

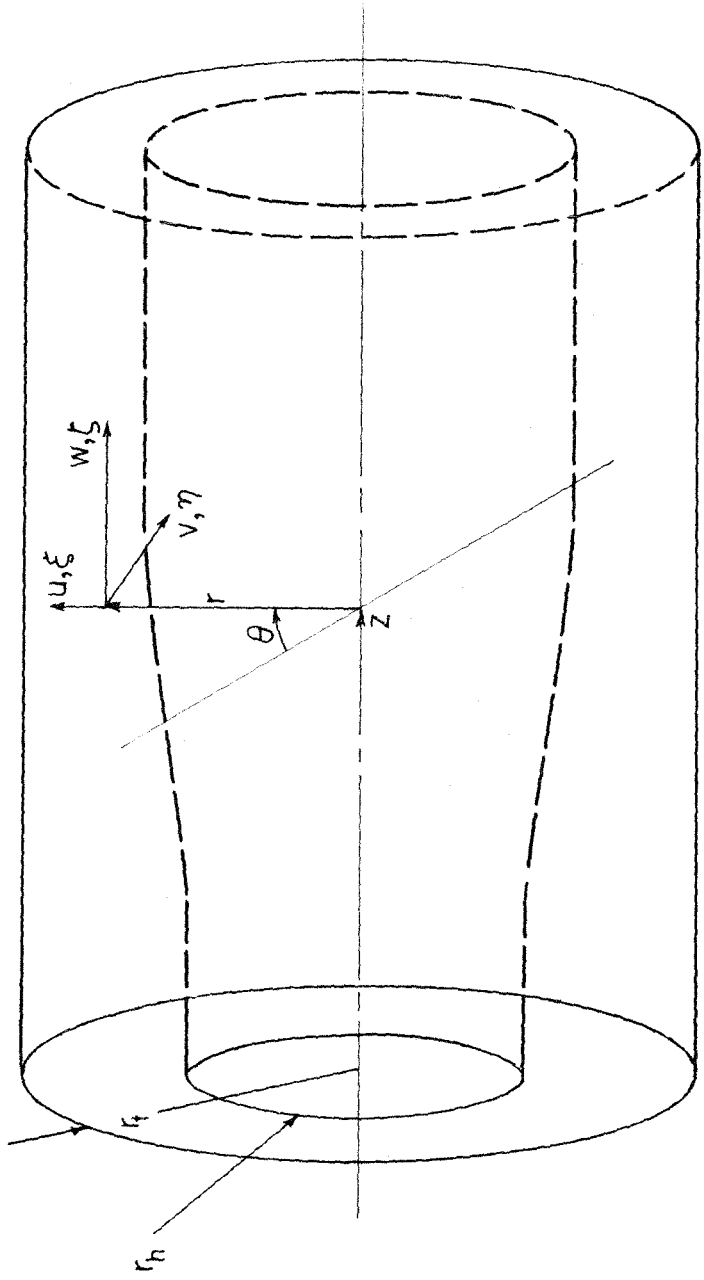

Figure 2. Coordinate System and Velocity Components in Axial Turbomachine.

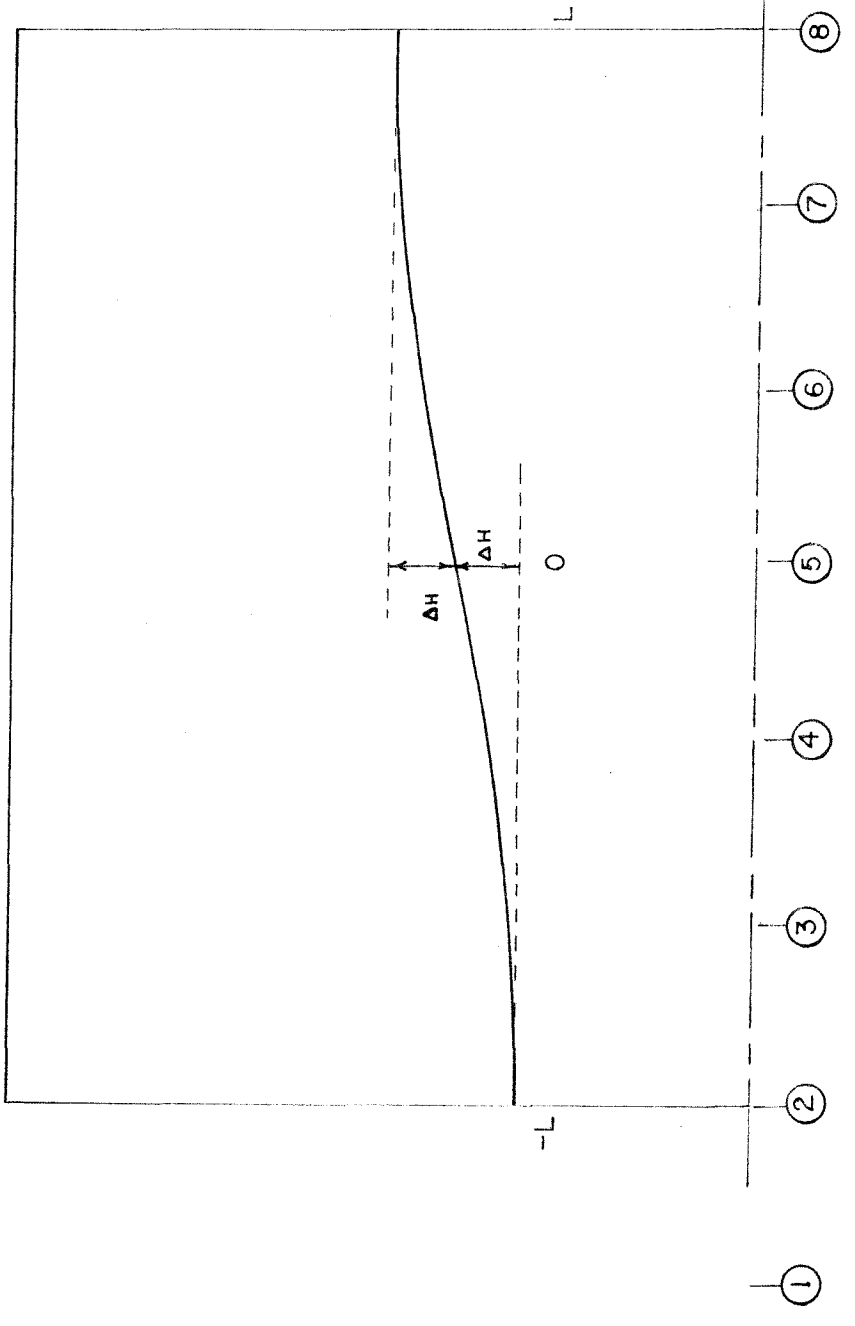

Figure 3. Example Wall Geometry Considered. Contraction Ratio $\propto = \frac{\Delta H}{r_t - r_h} = 0.15$
Simple Sinusoidal Step. Hub/Tip Ratio $\frac{r_h}{r_t} = 0.4$

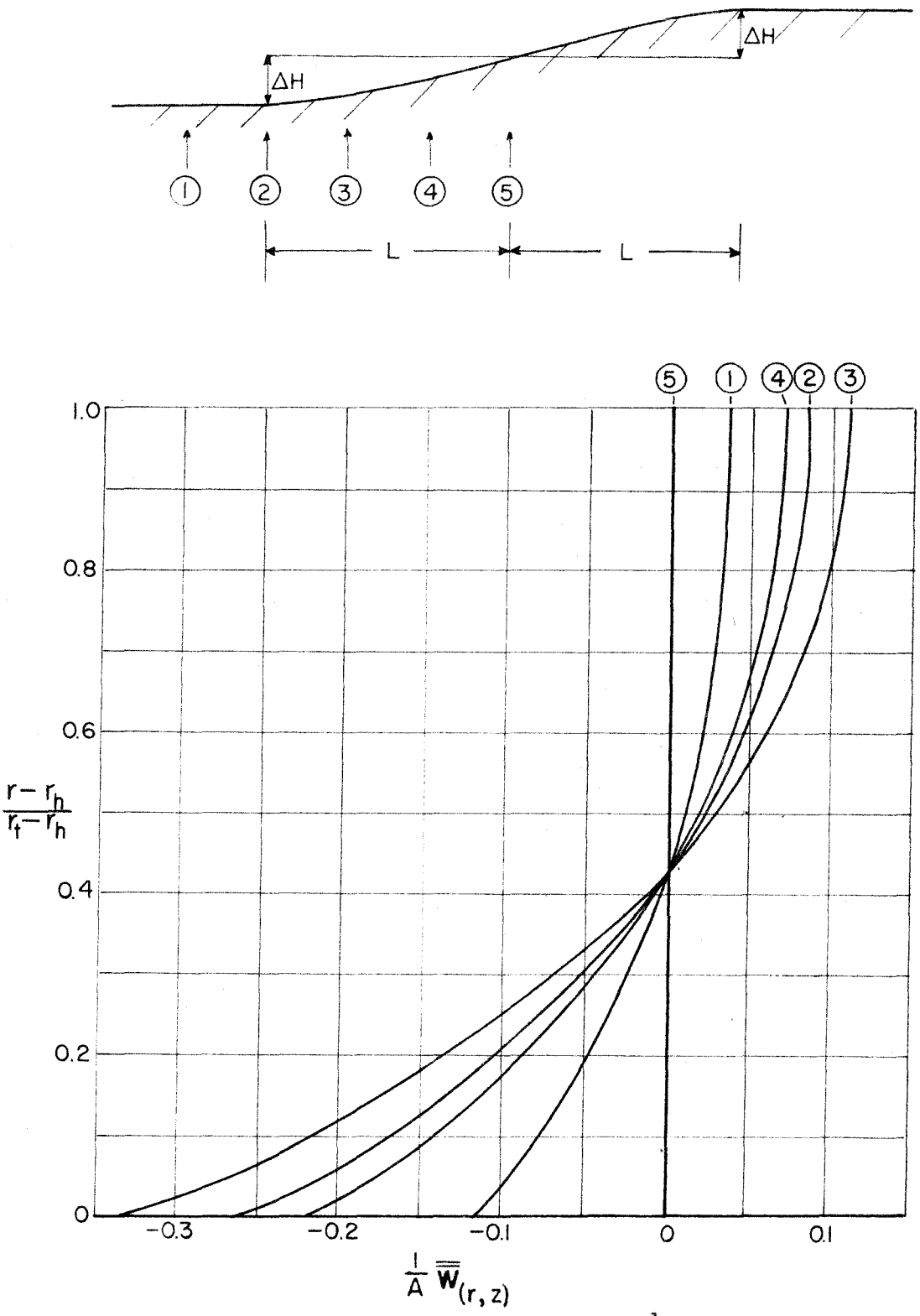

Fig. 4 Axial Velocity Profiles About Mean Flow $\frac{1}{A}\overline{\overline{W}}$ Contraction Ratio = 0.1 Simple Sinusoidal Step Hub tip ratio $\frac{r_h}{r_t}$ = 0.4

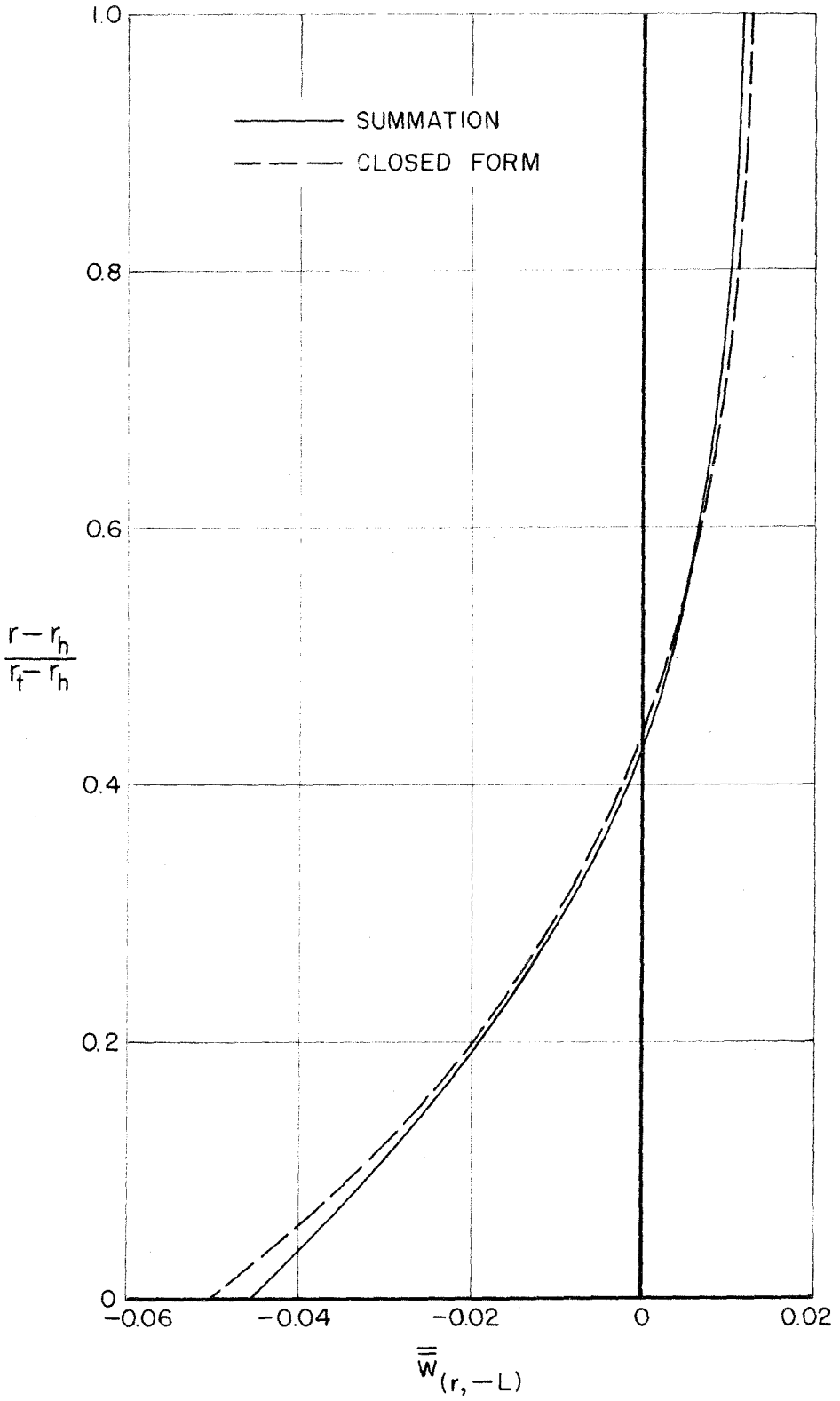

Fig. 5 Comparison of Closed Form Approximation to Exact Solution At Station (2), z = -L

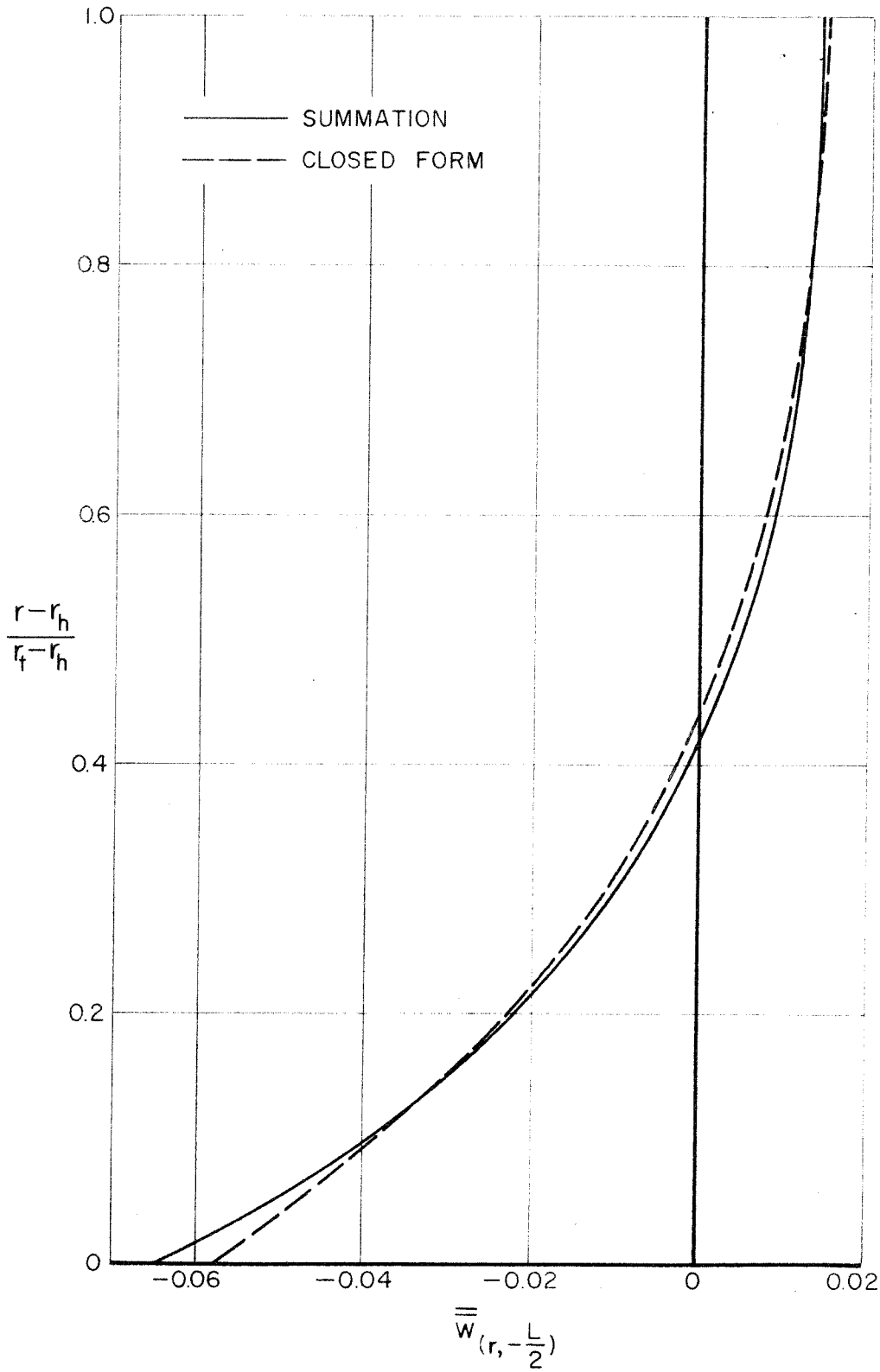

Fig. 6 Comparison of Closed Form Approximation to Exact Solution

$$z = -\frac{L}{2}$$

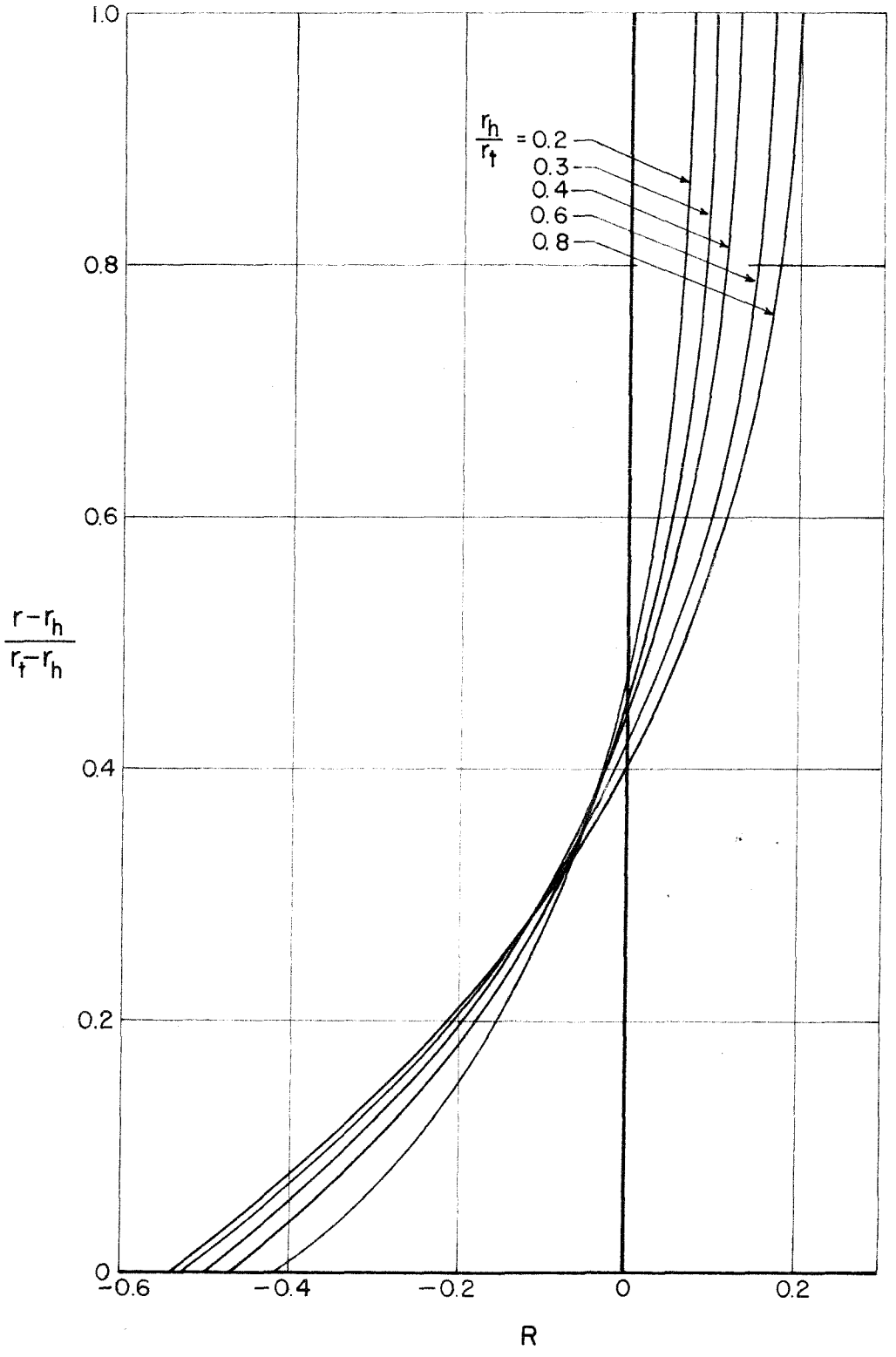

Fig. 7 Radially Dependent Portion of Solution Contraction Ratio, $\alpha = 0.1$

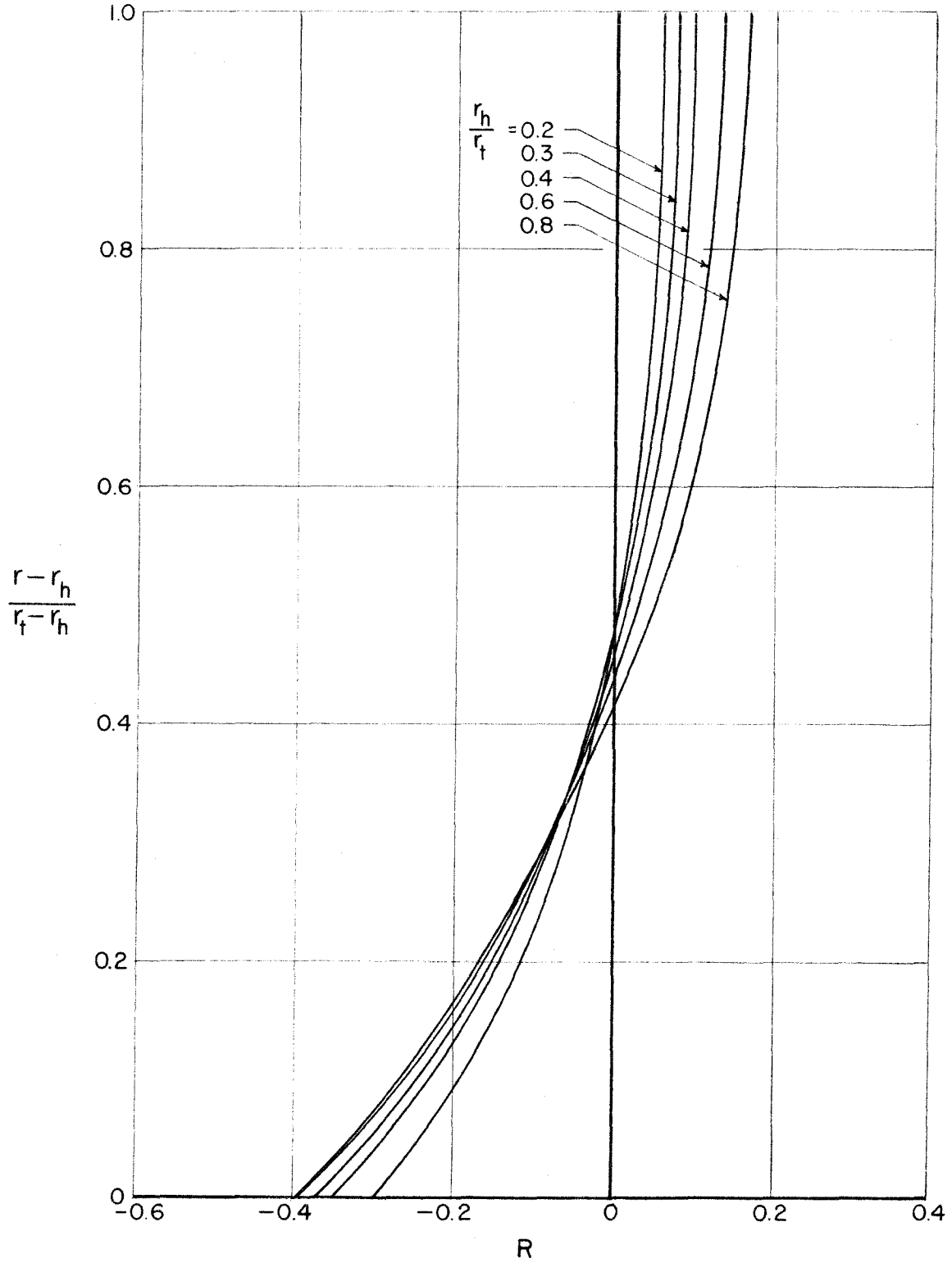

Figure 8 Radially Dependent Portion of Solution

Contraction Ratio α = 0.15

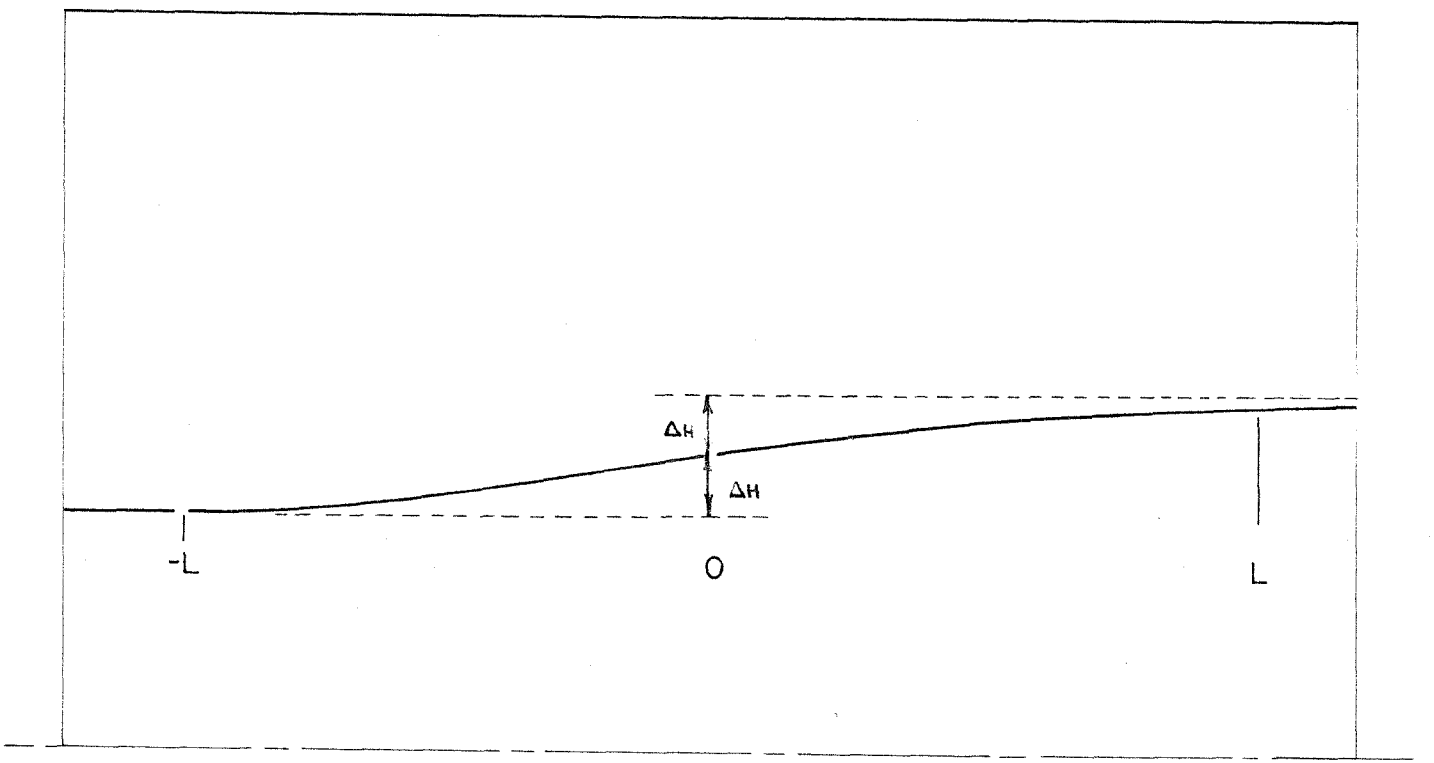

Figure 9. Example Wall Geometry Considered. Contraction Ratio α = 0.15, Hub/Tip Ratio $\frac{r_h}{r_t}$ = 0.4. Hub Shape Consisting of Cosine and Exponential Curve.

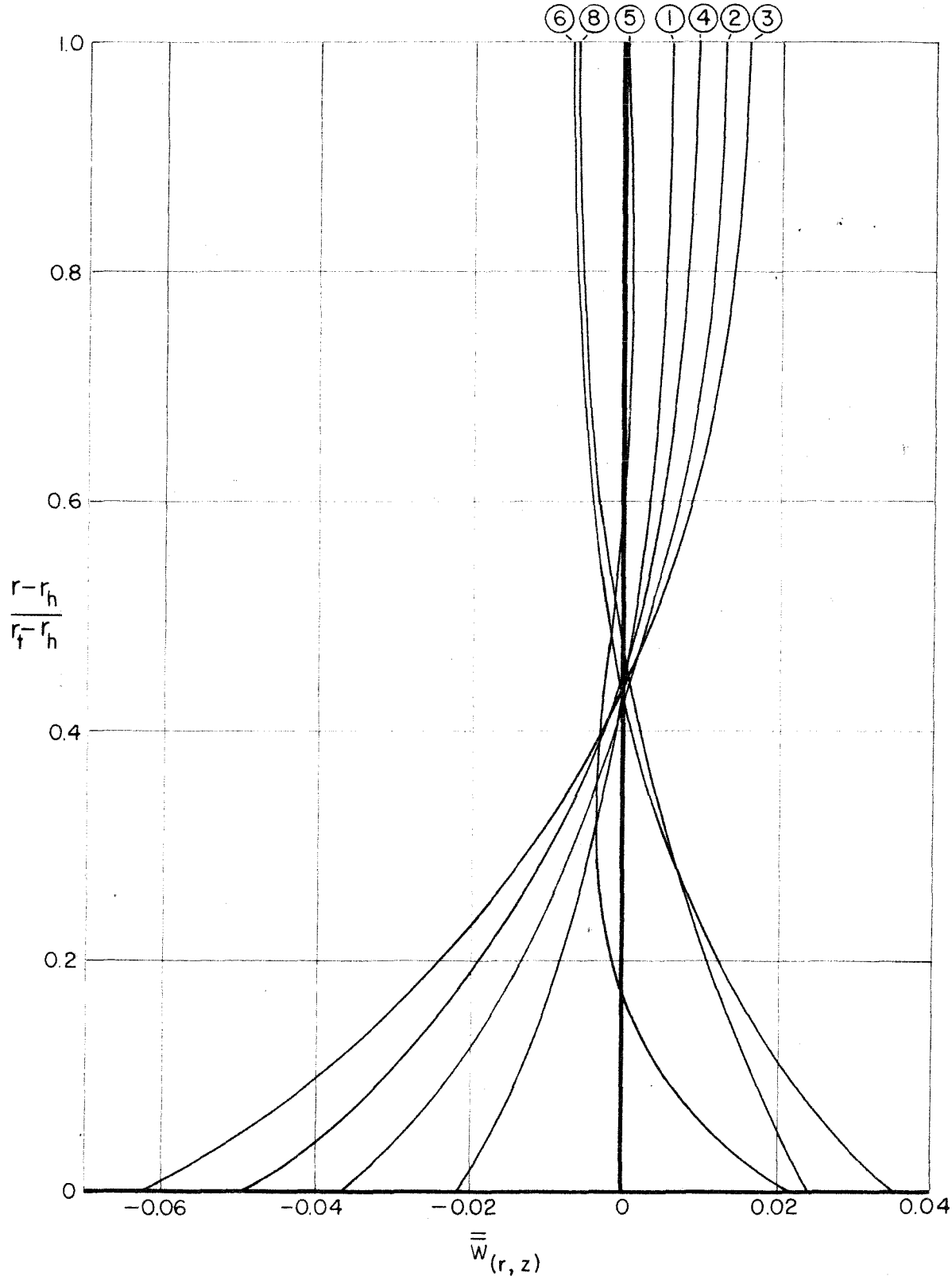

Fig. 10 Axial Velocity Profiles About Mean Flow $\bar{\bar{W}}$. Contraction Ratio $\alpha = 0.1$. Hub tip Ratio $\frac{r_h}{r_t} = 0.4$. Cosine and Exponential Curve.

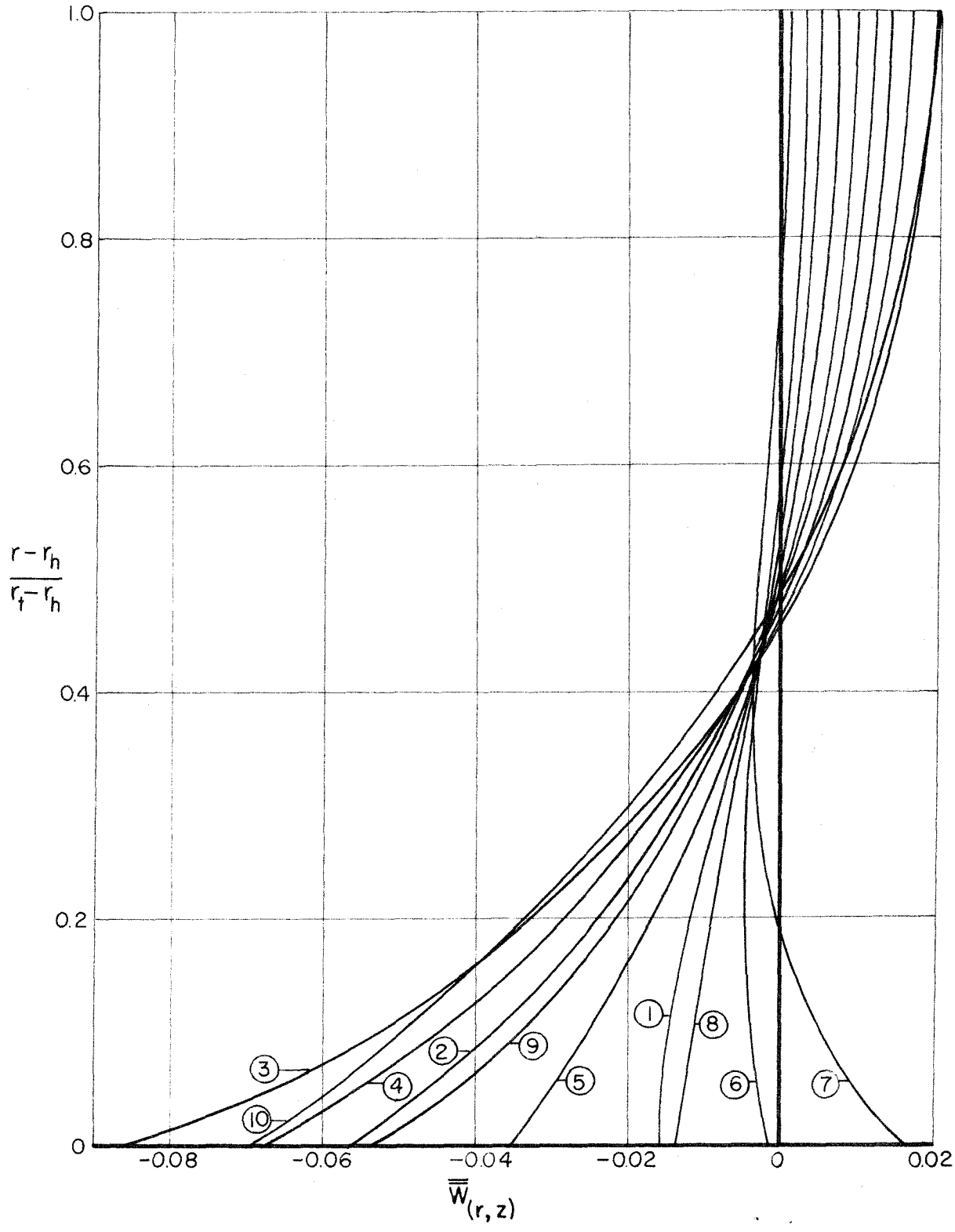

Figure 11 Axial Velocity Profiles About Mean Flow $m^2 = 0.1$

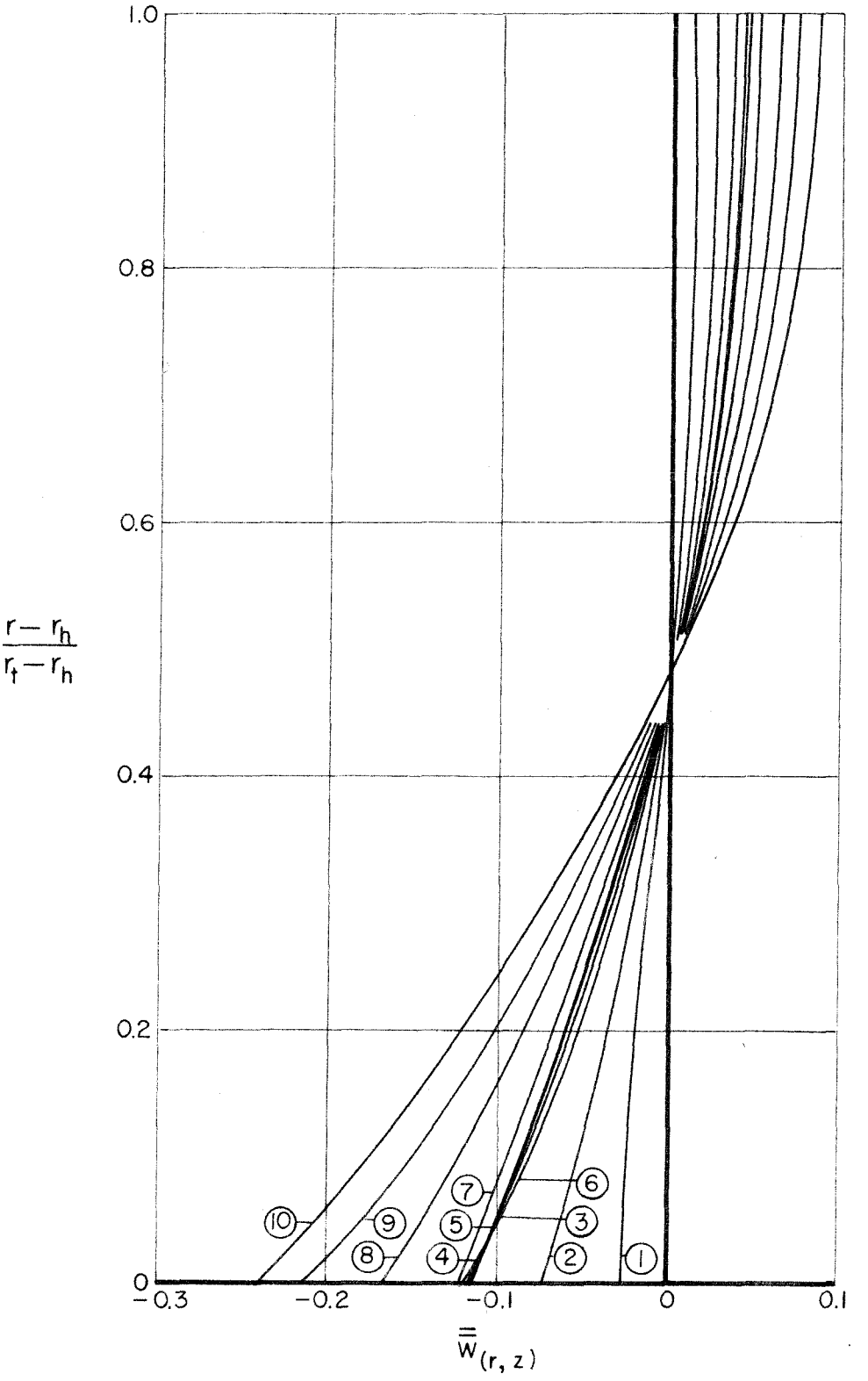

Figure 12. Axial Velocity Profiles About Mean Flow $m^2 = 0.3$

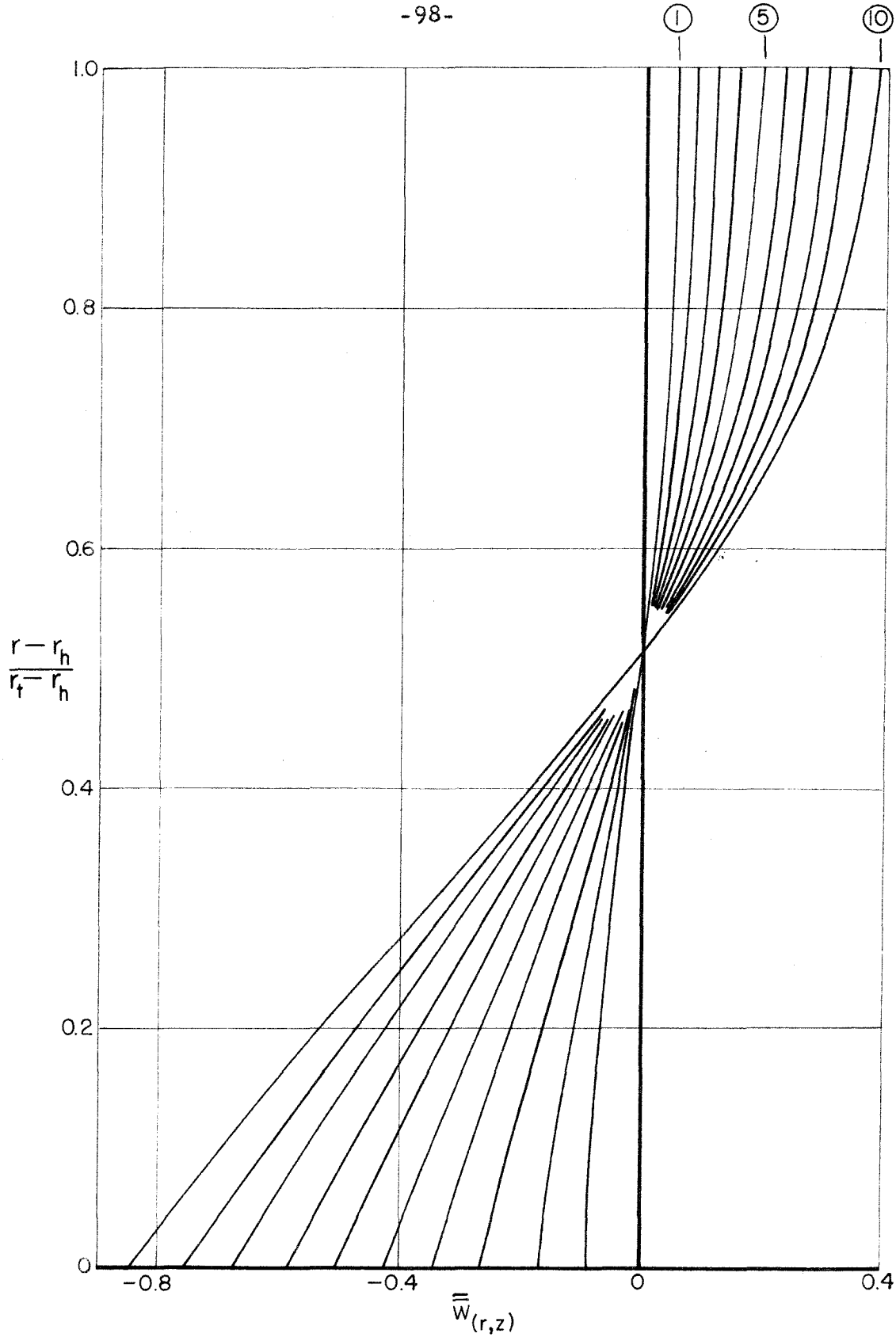

Figure 13. Axial Velocity Profile About Mean Flow. $m^2 = 0.64$

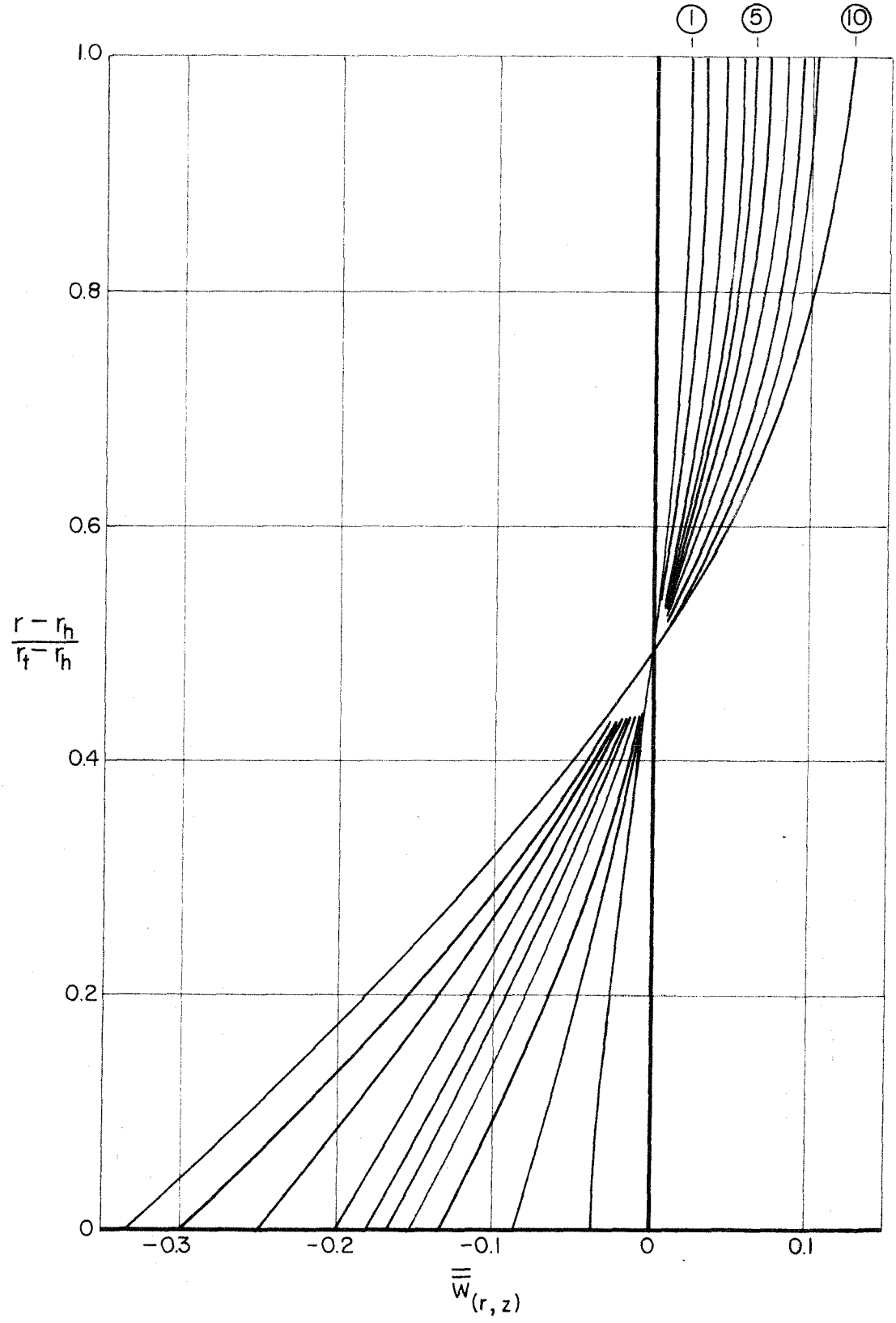

Figure 14. Axial Velocity Profiles About Mean Flow. $k = (\frac{\pi}{2L})$

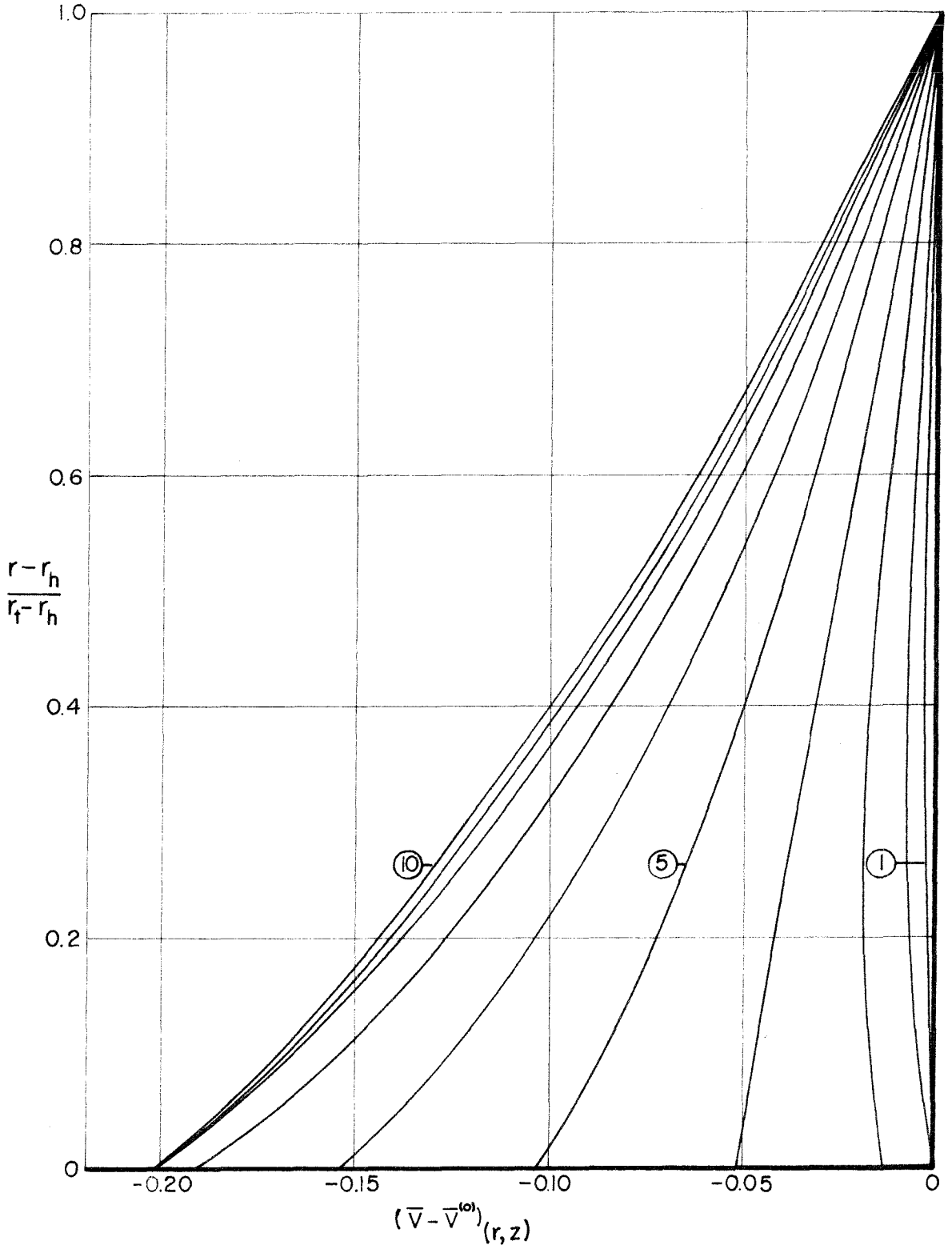

Figure 15. Change in Tangential Velocity. $m^2 = 0.1$

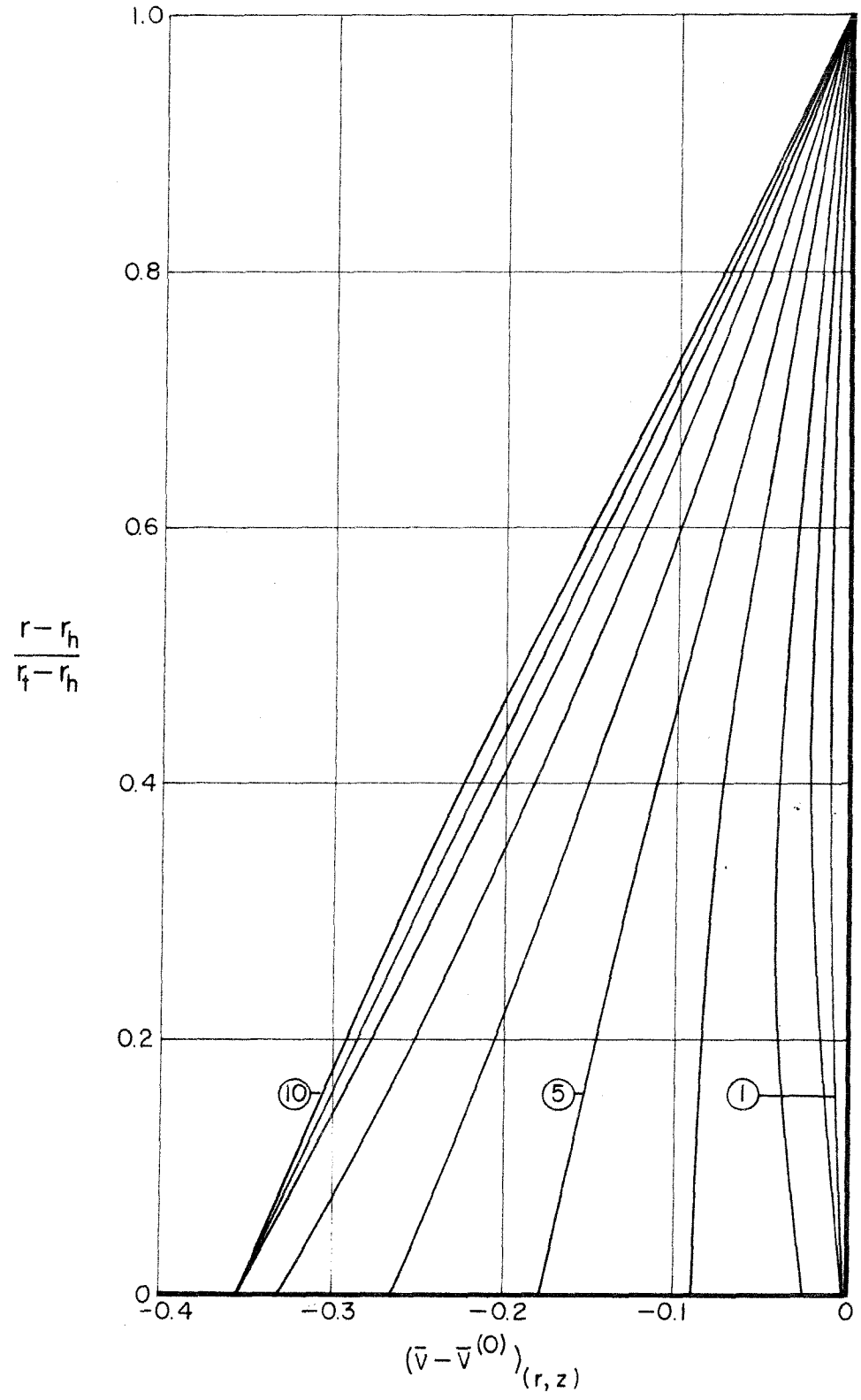

Figure 16. Change in Tangential Velocity. $m^2 = 0.3$

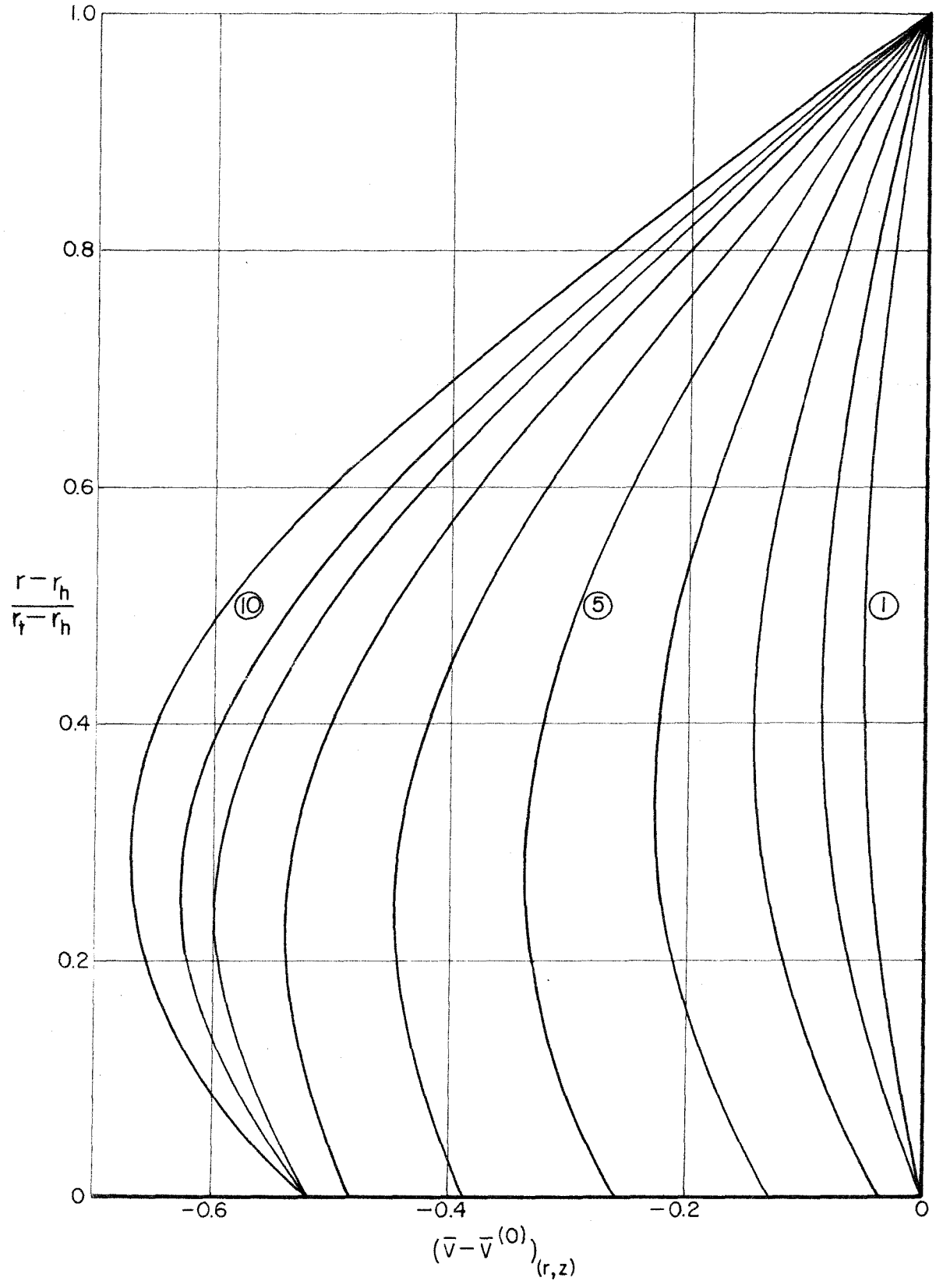

Figure 17. Change in Tangential Velocity. $m^2 = 0.64$

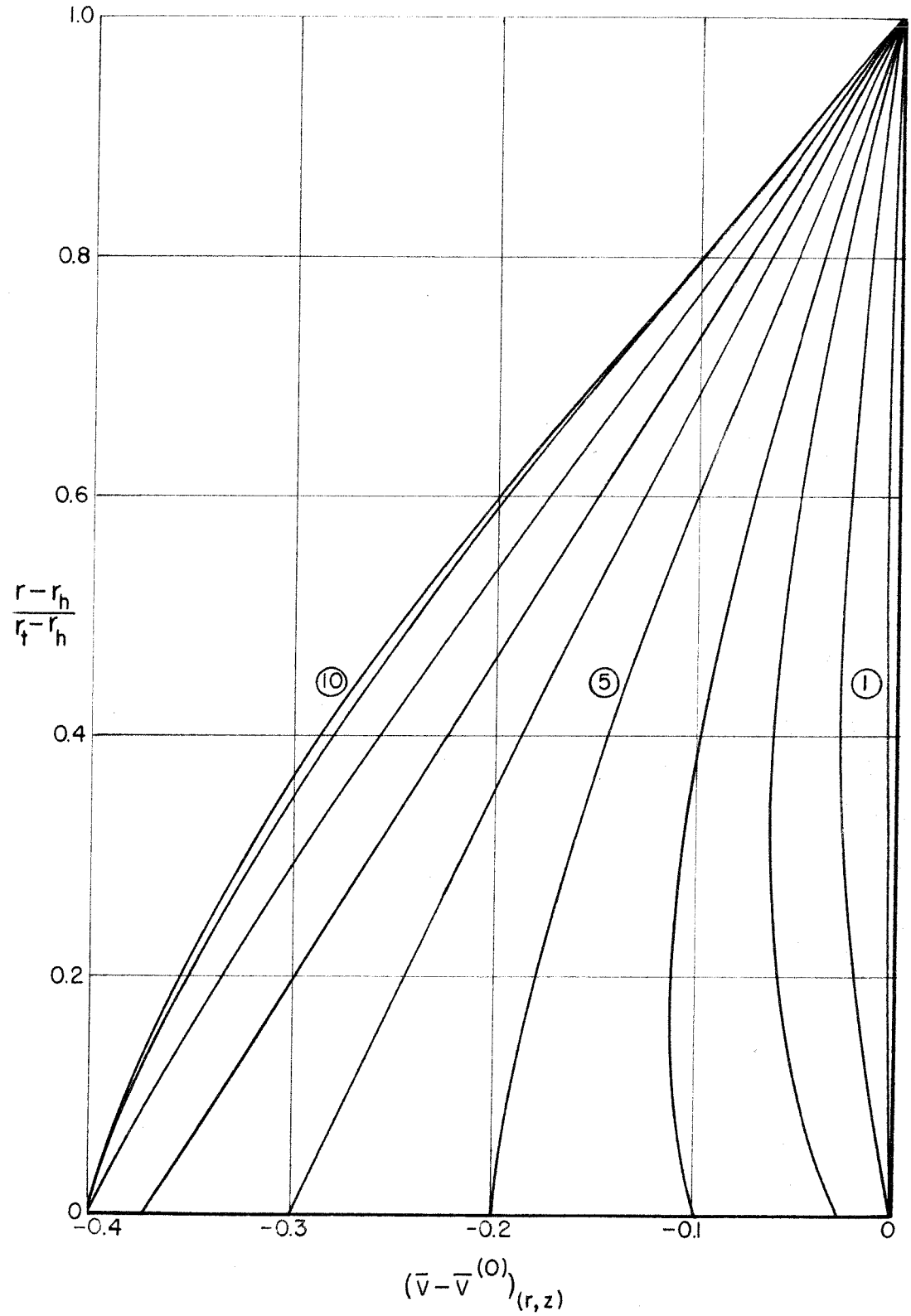

Figure 18. Change in Tangential Velocity. $k = (\frac{\pi}{2L})$

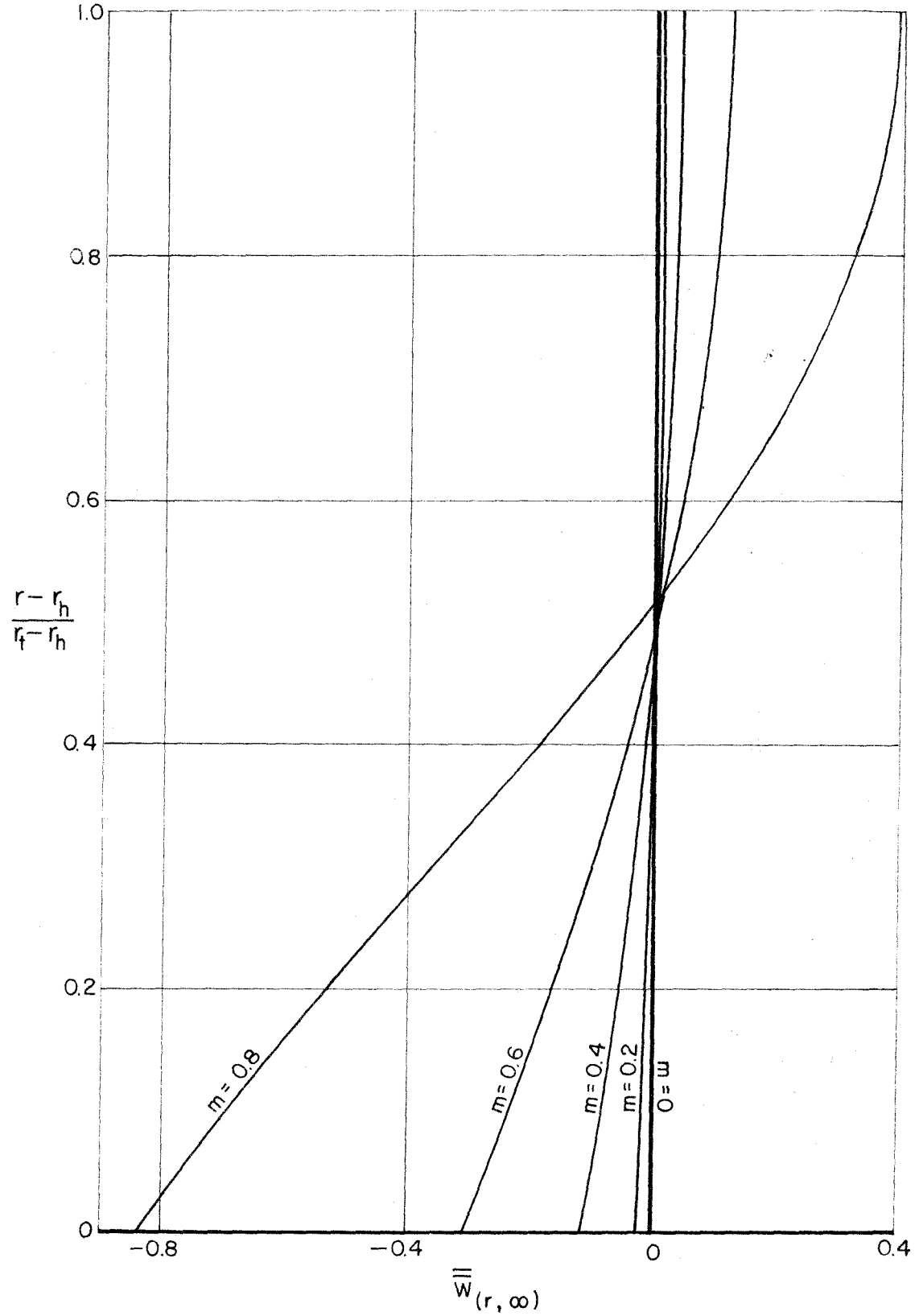

Fig. 19. Outlet Axial Velocity Profiles About Mean Flow as Function of Fraction of Rotation of Critical Value. $m = \frac{k}{\xi_1}$

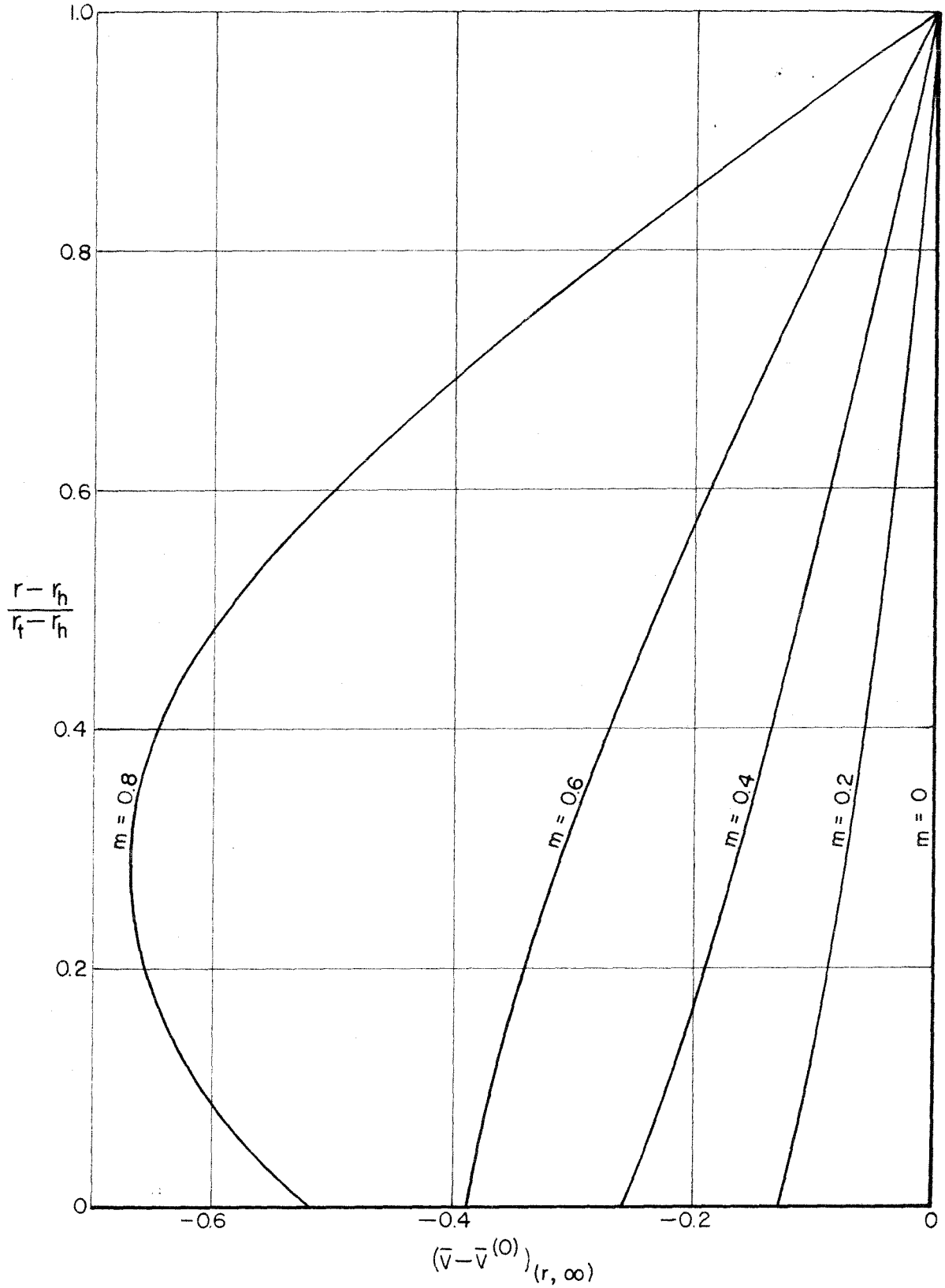

Figure 20. Outlet Changes in Tangential Velocity as Function of Fraction of Rotation of Critical Value. $m = \frac{k}{\xi_1}$

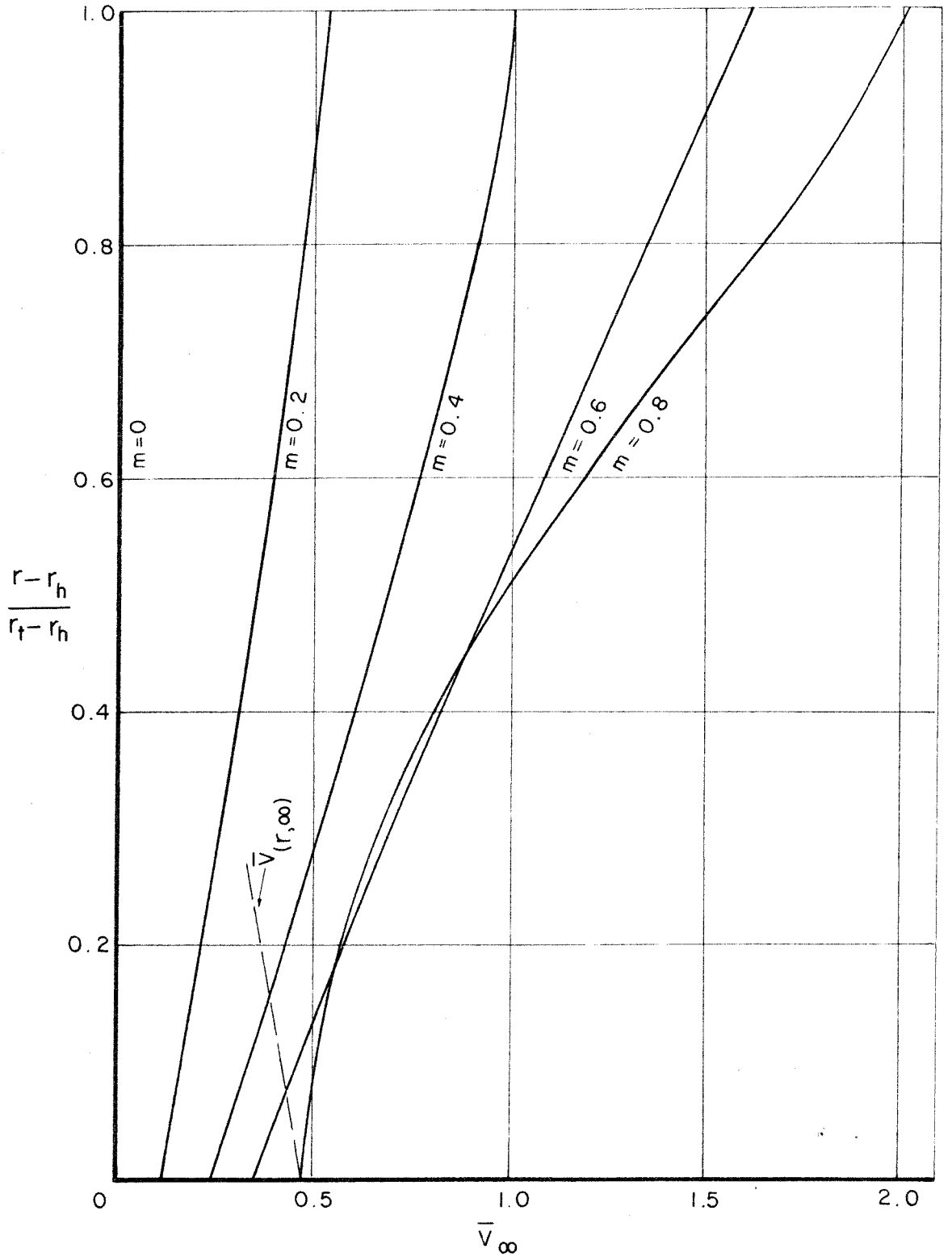

Fig. 21. Outlet Tangential Velocity as Function of Fraction of Rotation of Critical Value. $m = \frac{k}{\xi_1}$

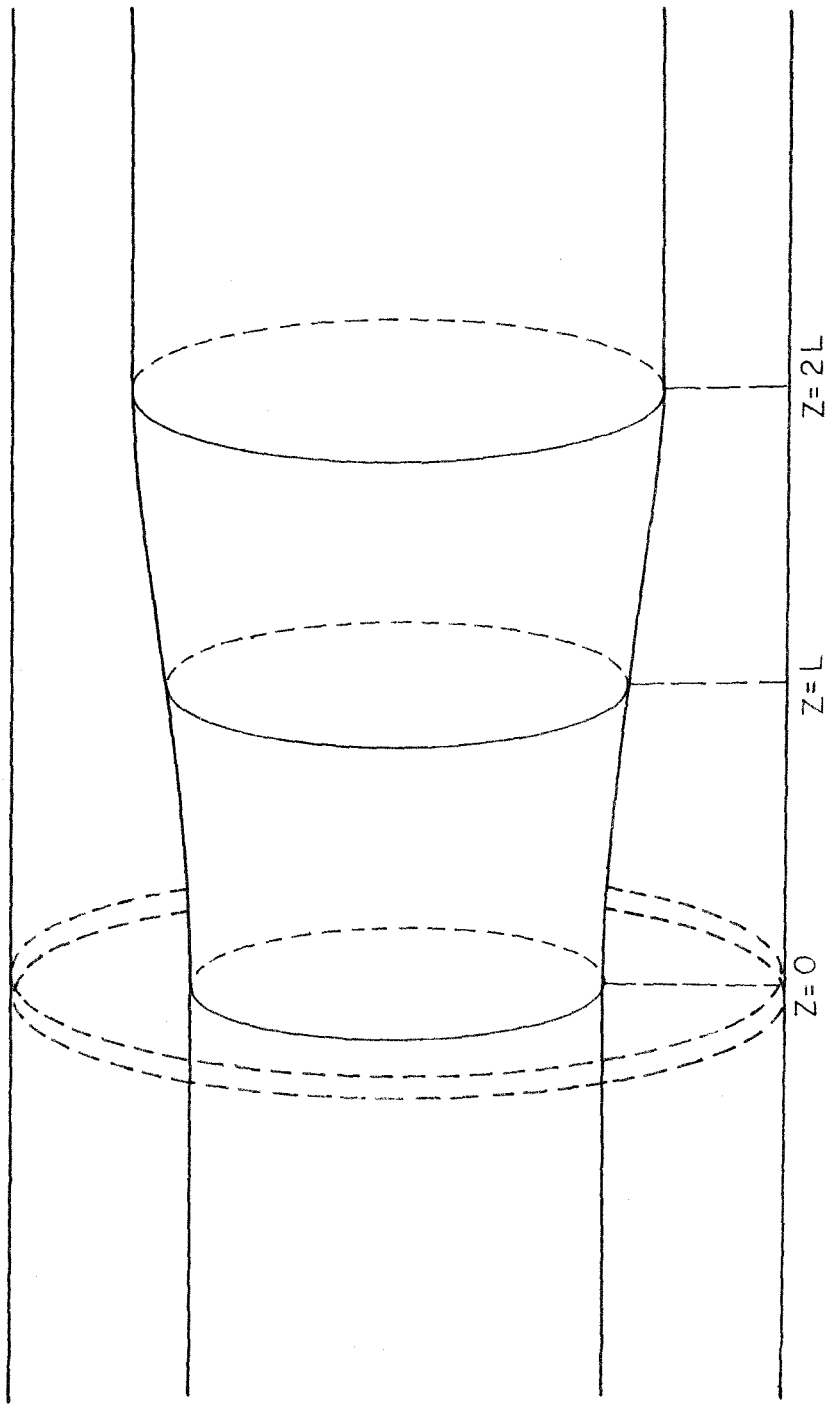

Figure 22. Entrance Vane at Entry to Contraction

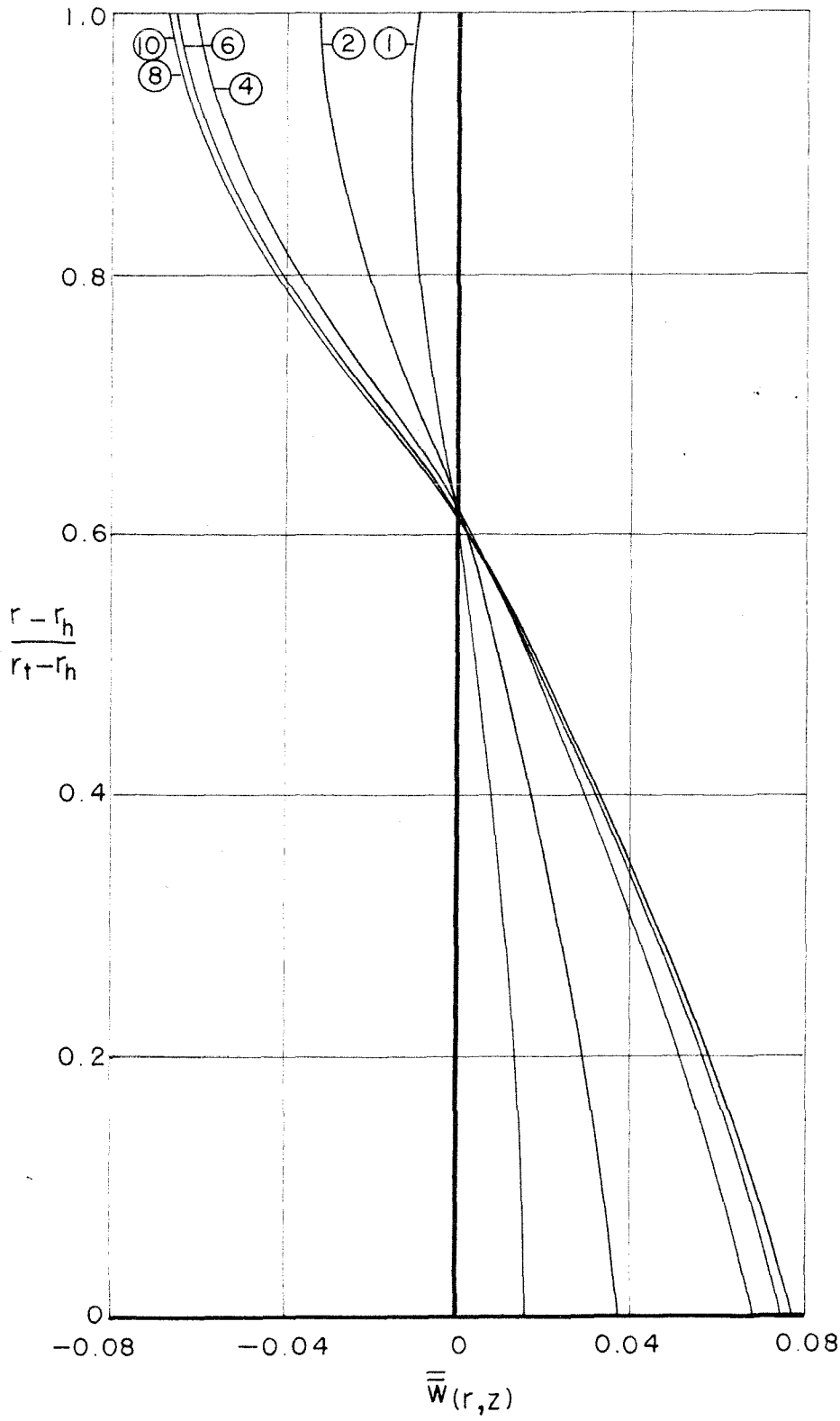

Fig. 23. Actuator Disc and Parallel Walls. Axial Velocity.
$m^2 = 0.025$

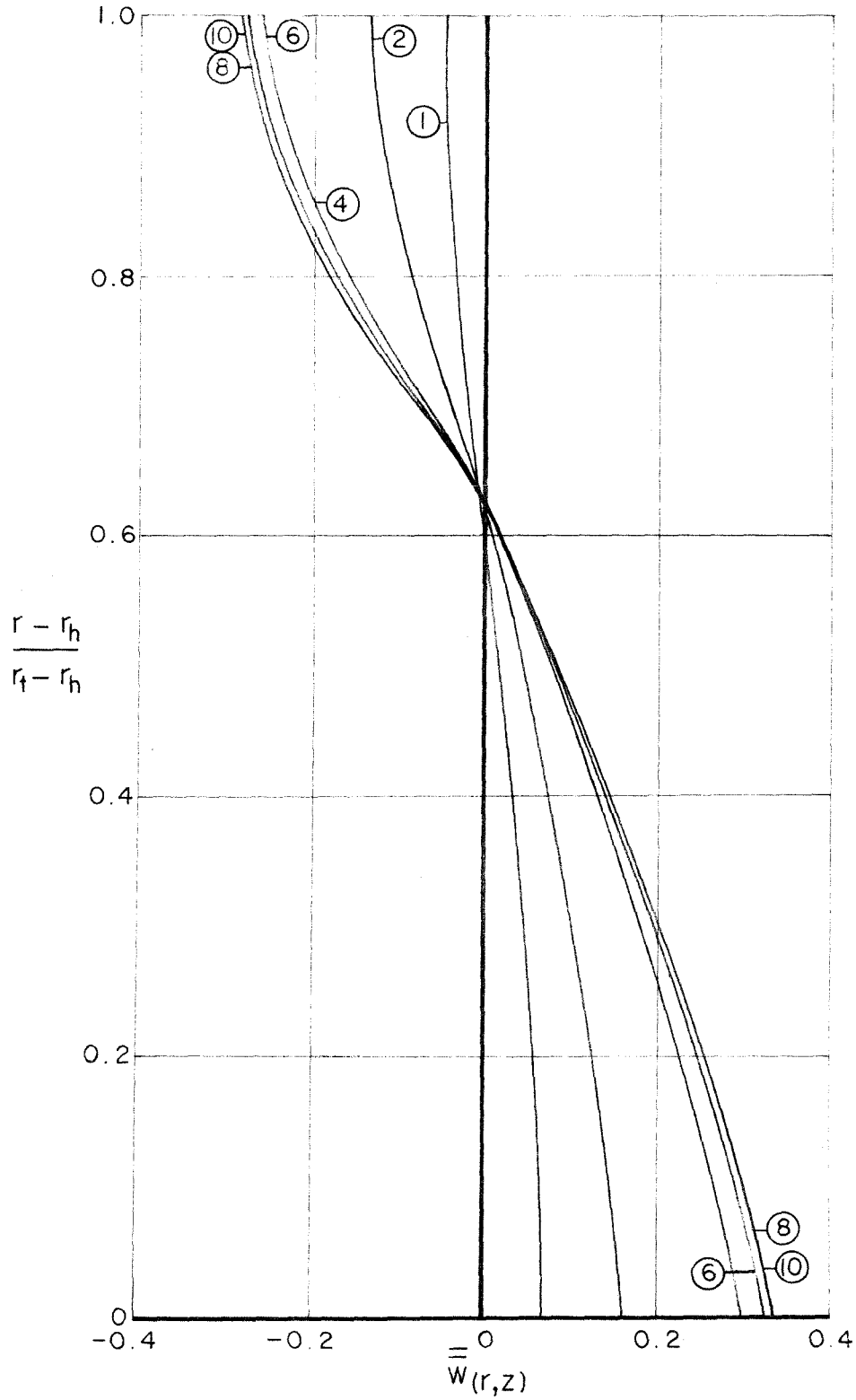

Fig. 24. Actuator Disc and Parallel Walls. Axial Velocity. $m^2 = 0.1$

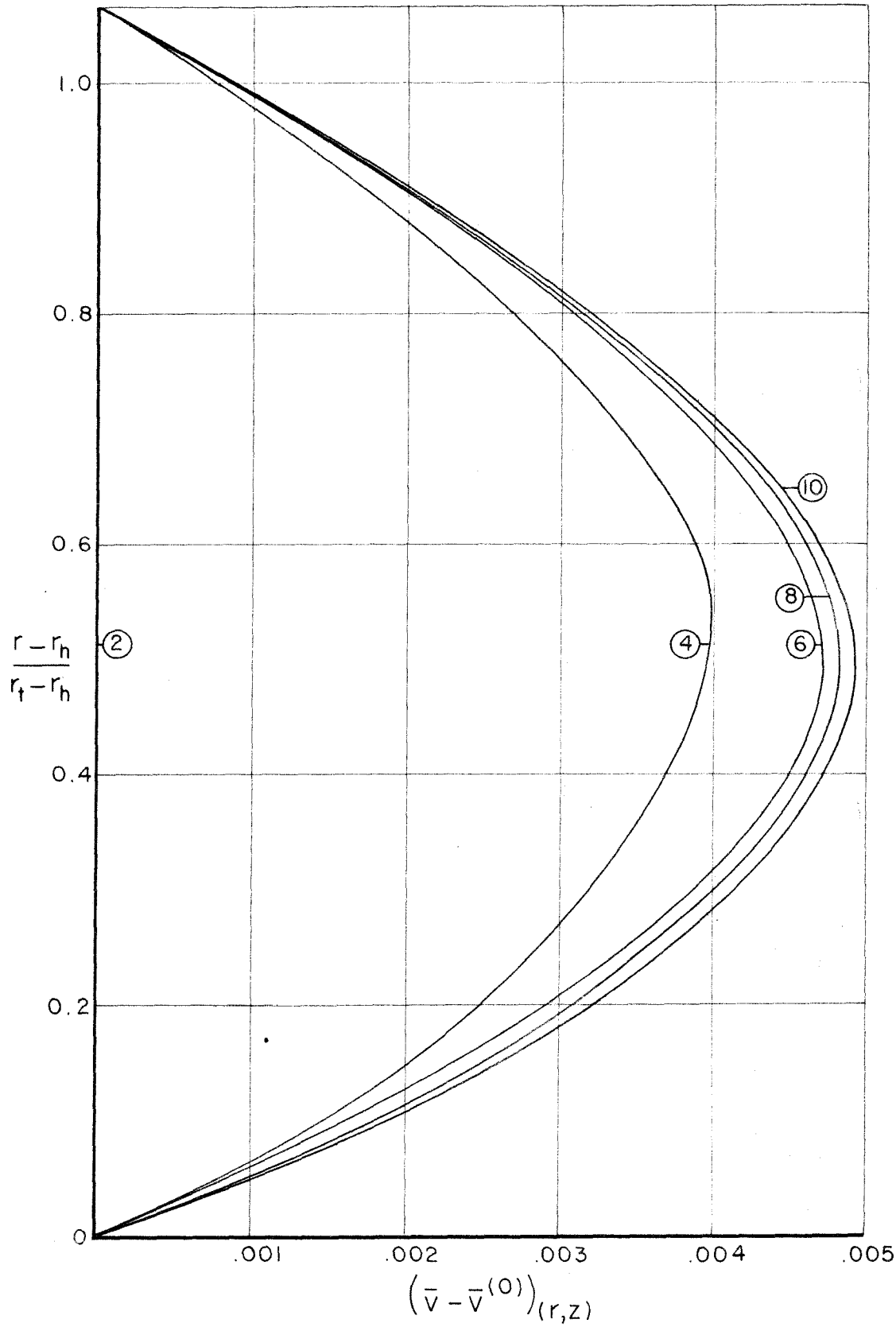

Fig. 25. Actuator Disc and Parallel Walls. Tangential Velocity.
$m^2 = 0.025$

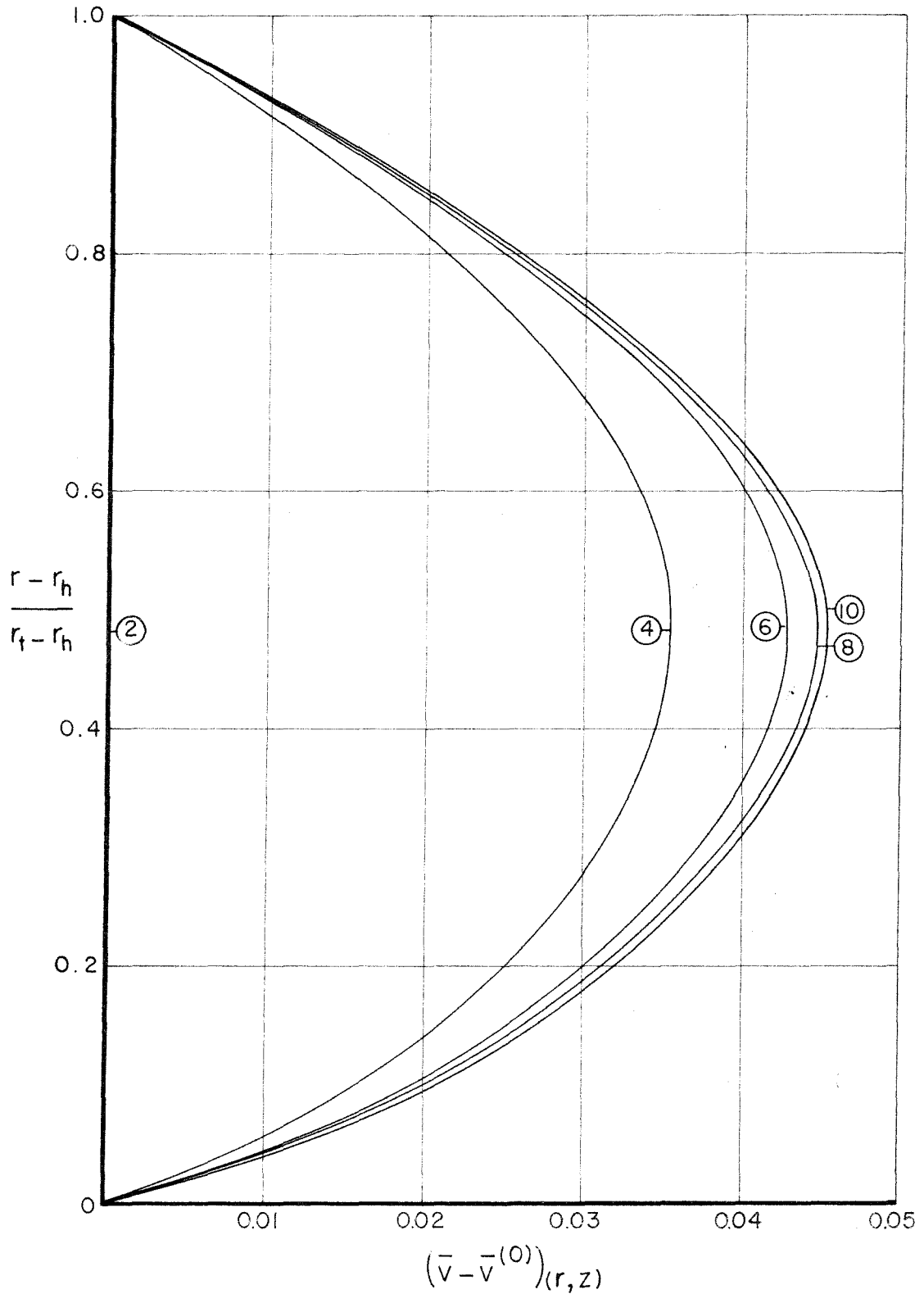

Fig. 26. Actuator Disc and Parallel Walls. Tangential Velocity $m^2 = 0.1$

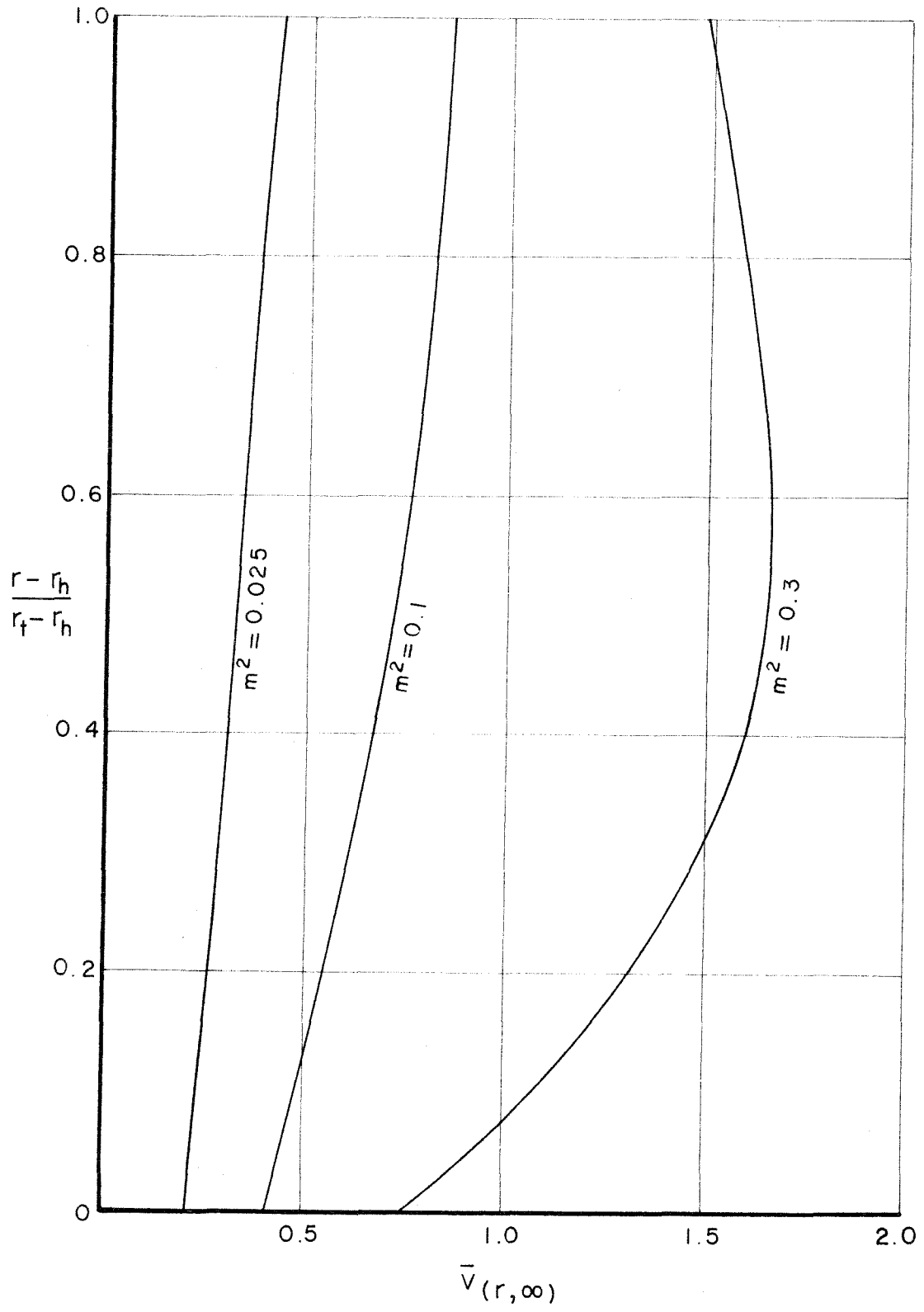

Figure 27. Outlet Tangential Velocity. Actuator Disc and Parallel Walls.

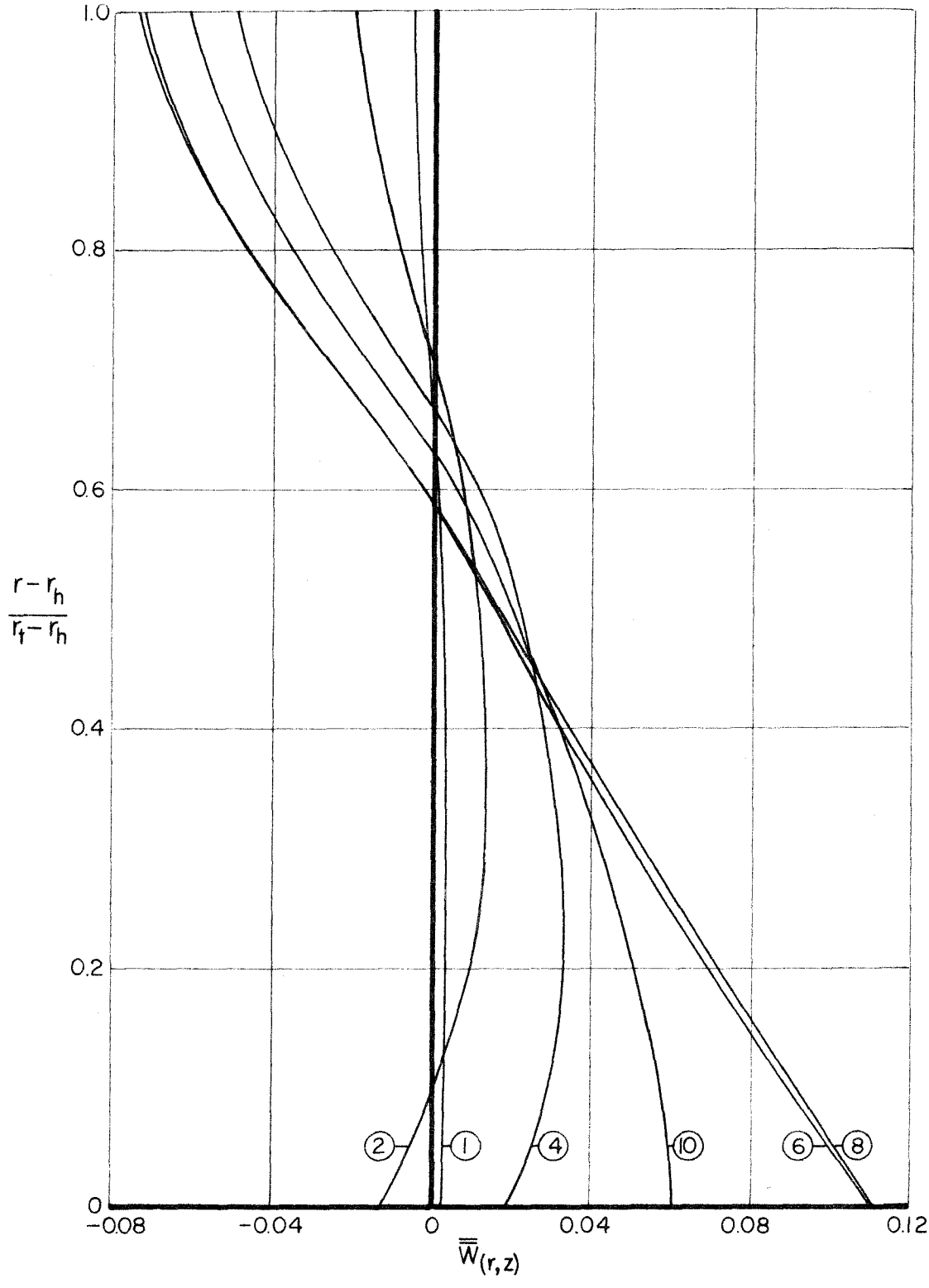

Fig. 28. Axial Velocity Perturbation. Actuator Disc at Entry to Simple Sinusoidal Step. $m^2 = 0.025$

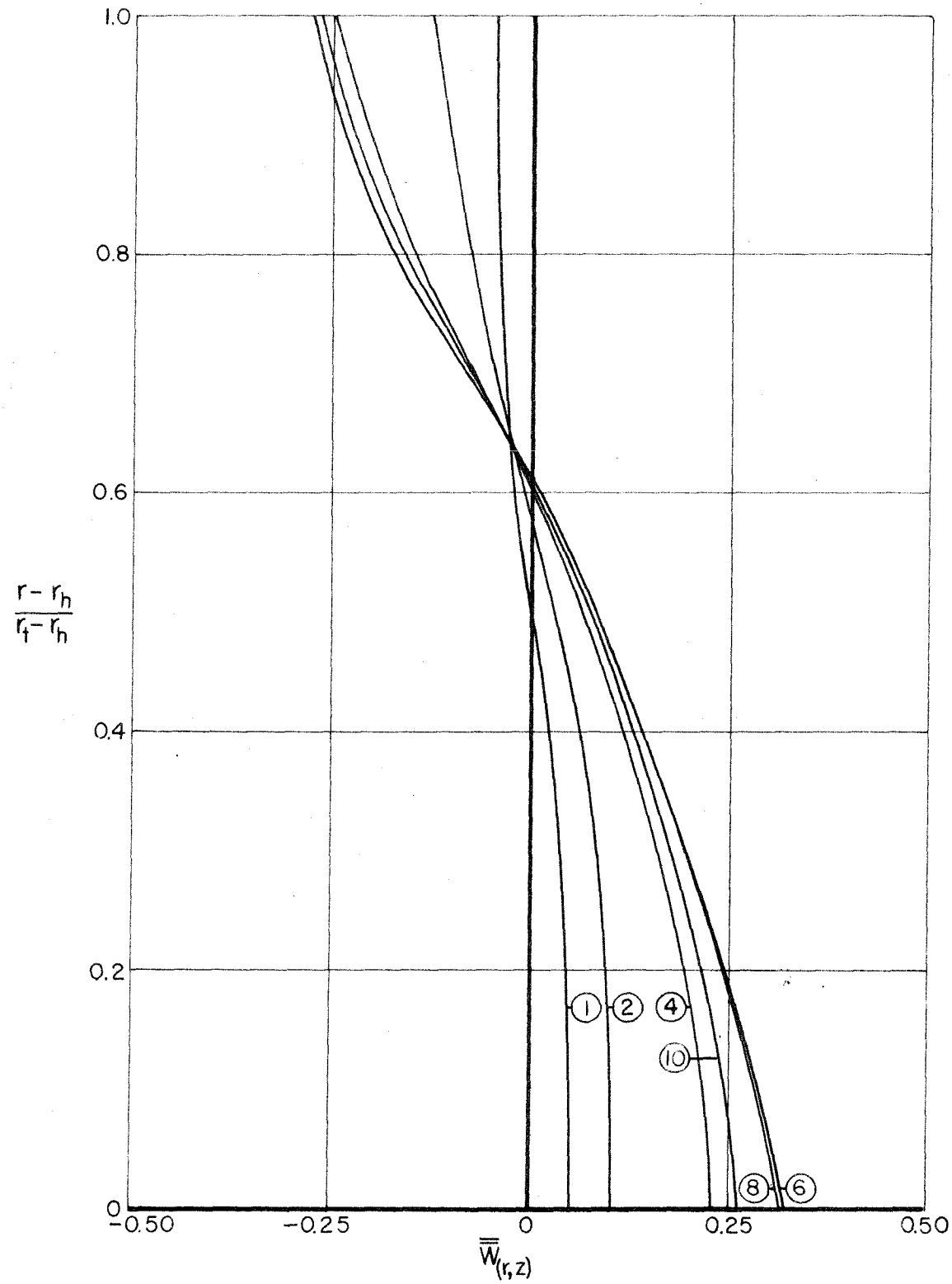

Figure 29. Axial Velocity Perturbation. Actuator Disc at Entry to Simple Sinusoidal Step. $m^2 = 0.1$

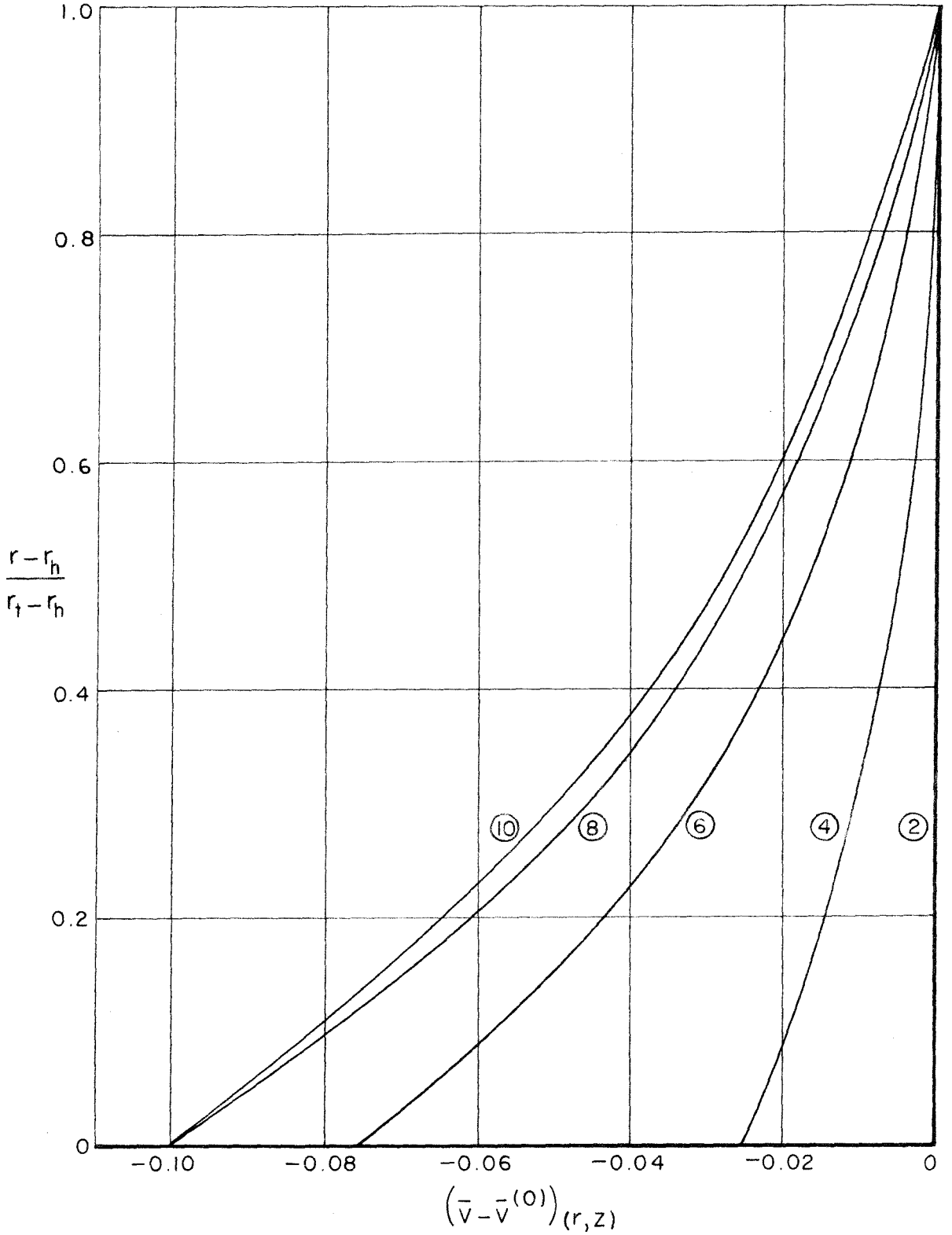

Figure 30. Tangential Velocity Perturbation. Actuator Disc at Entry to Simple Sinusoidal Step. $m^2 = 0.025$

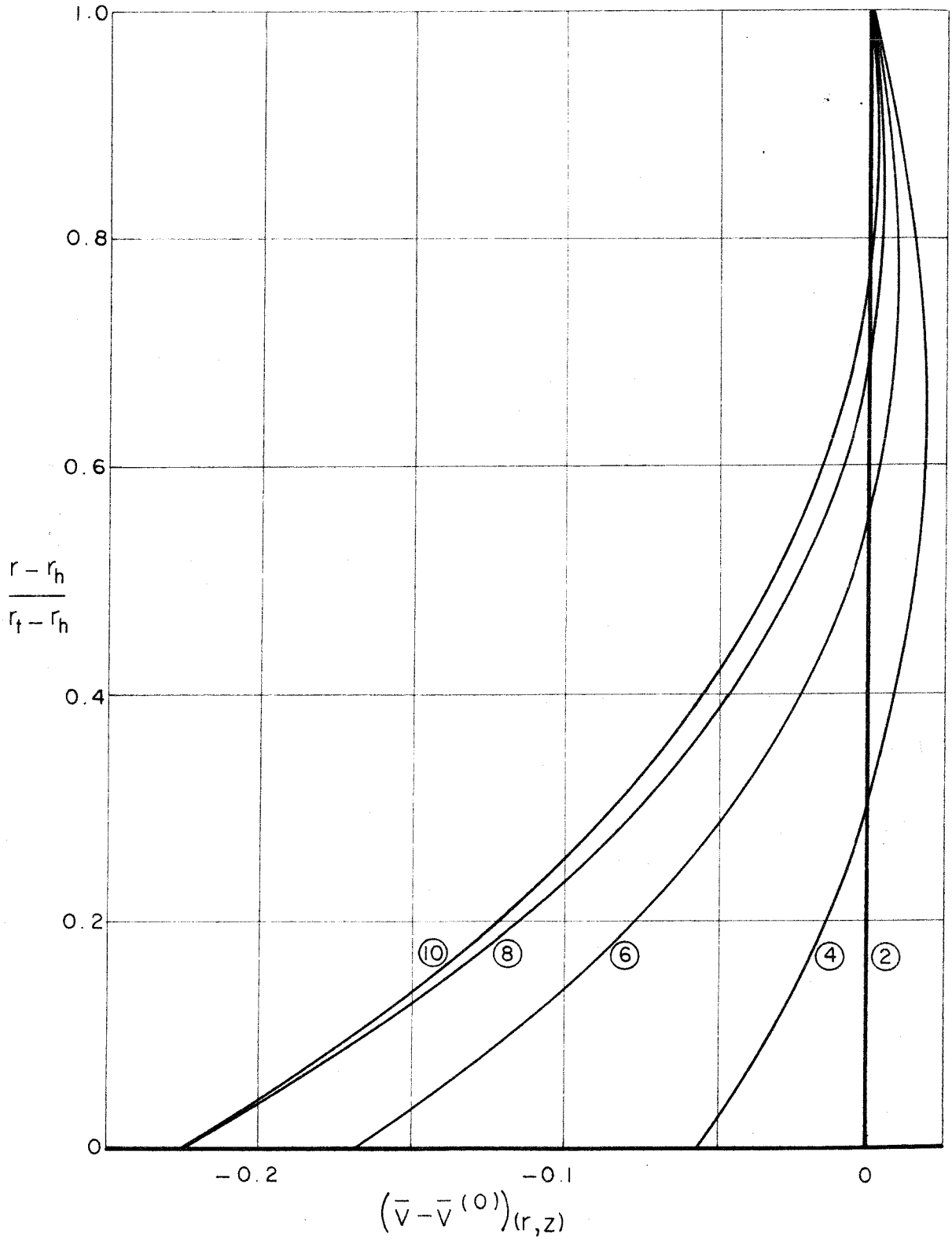

Figure 31. Tangential Velocity Perturbation. Actuator Disc at Entry to Simple Sinusoidal Step. $m^2 = 0.1$

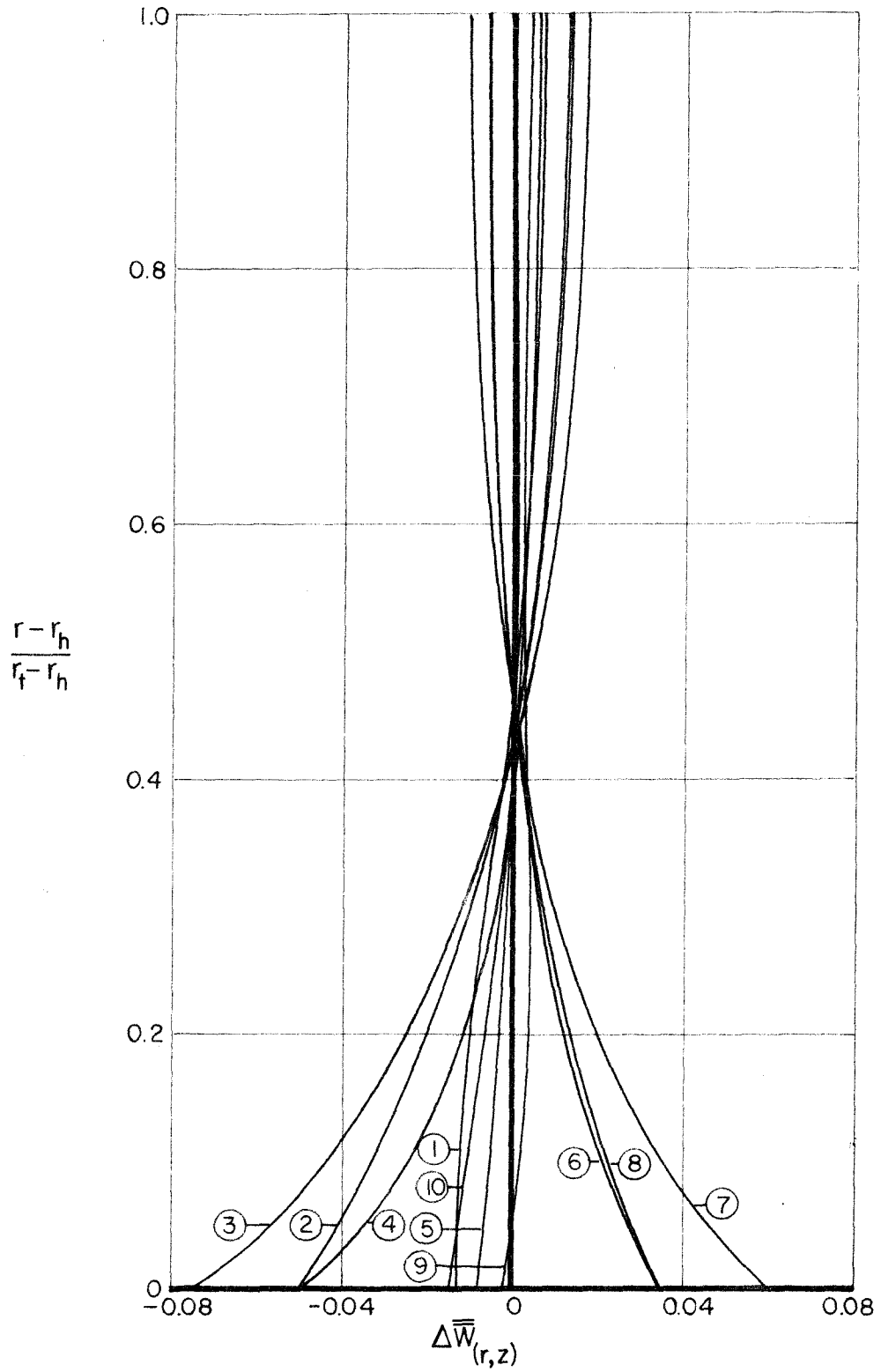

Fig. 32. Effect of Wall Only on Axial Velocity. Actuator Disc at Entry to Simple Sinusoidal Step. $m^2 = 0.025$

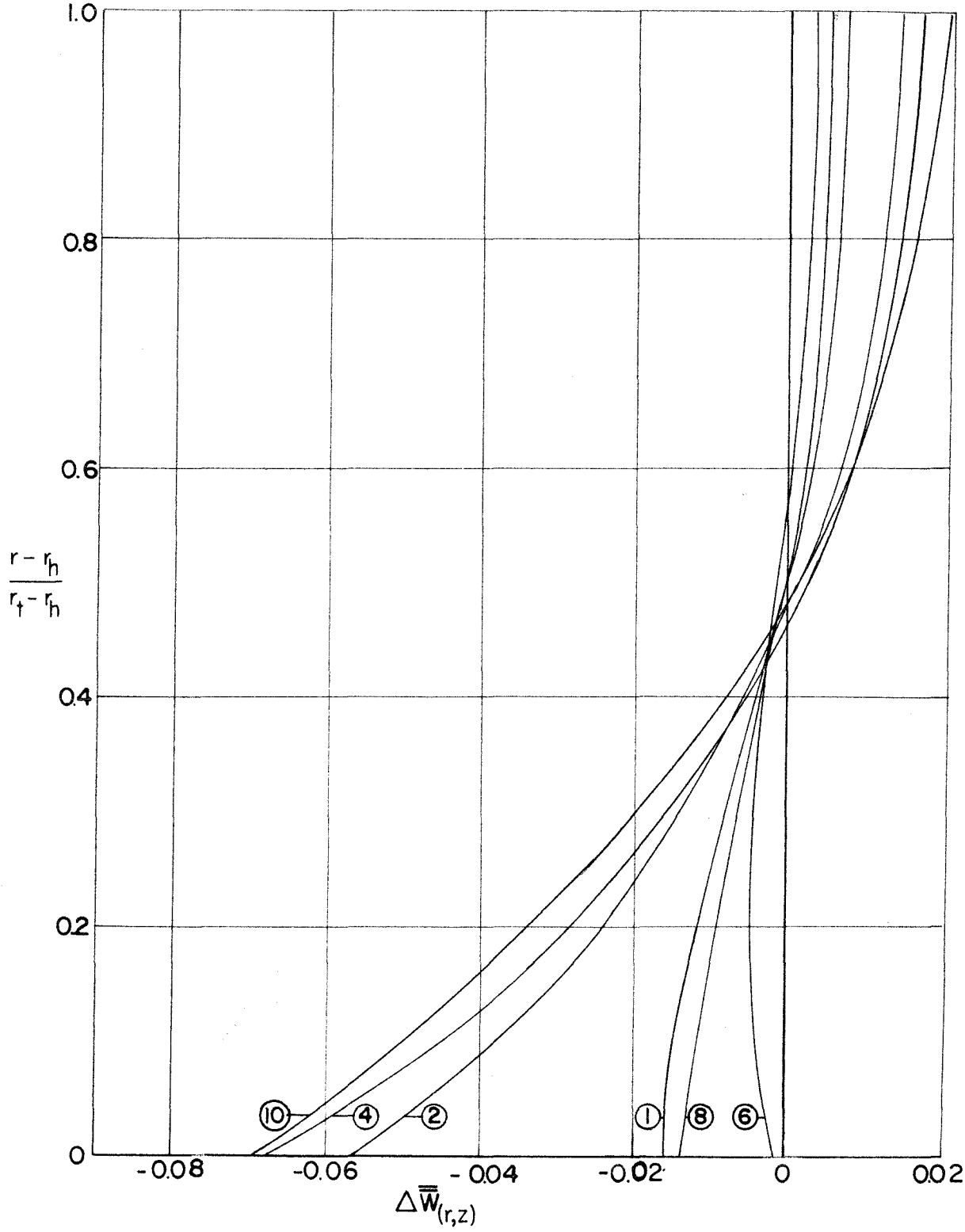

Figure 33. Effect of Wall Only on Axial Velocity. Actuator Disc at Entry to Simple Sinusoidal Step. $m^2 = 0.1$

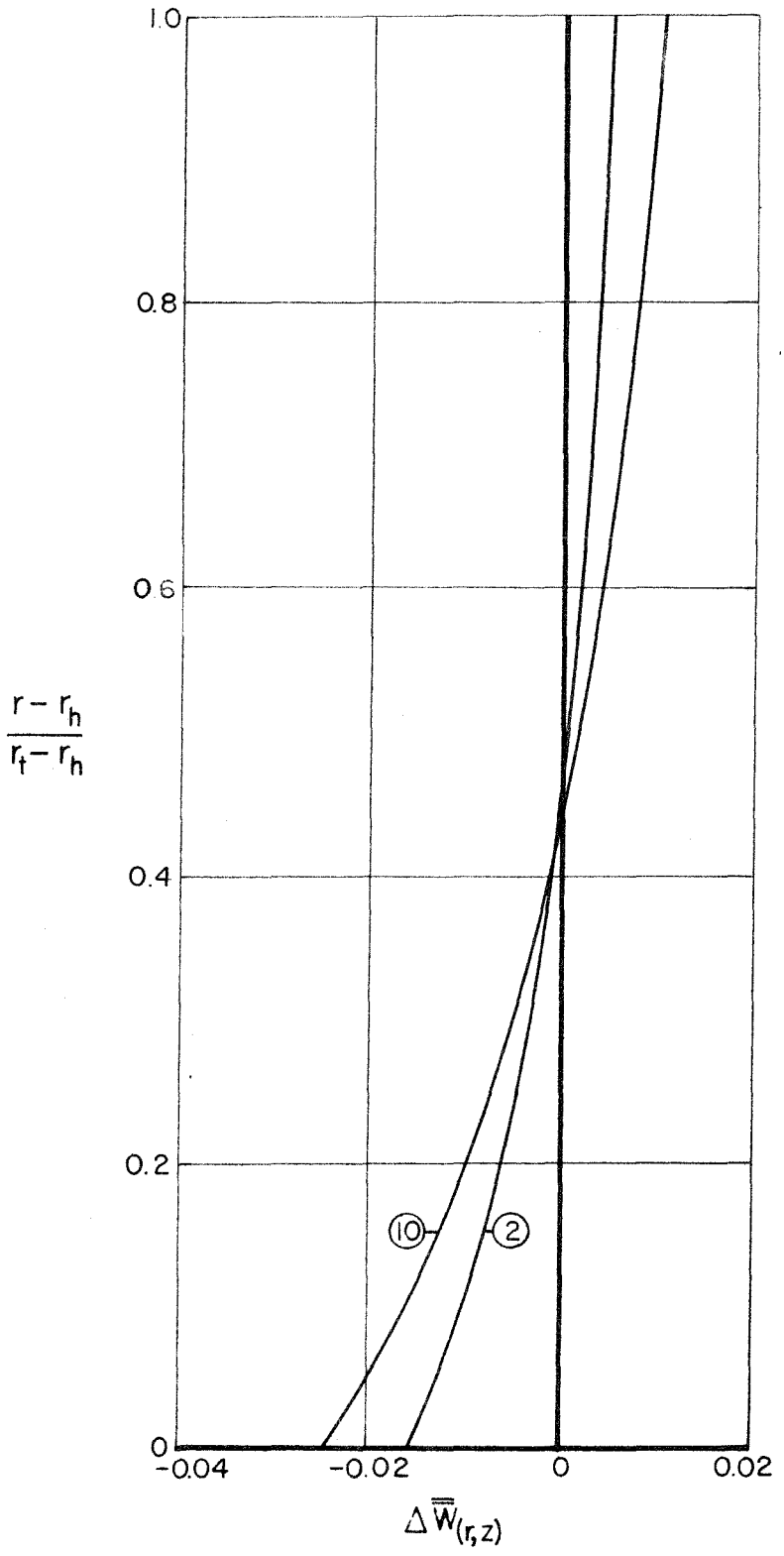

Figure 34. Correction to Axial Velocity Profiles. Obtained from Modified Boundary Conditions.

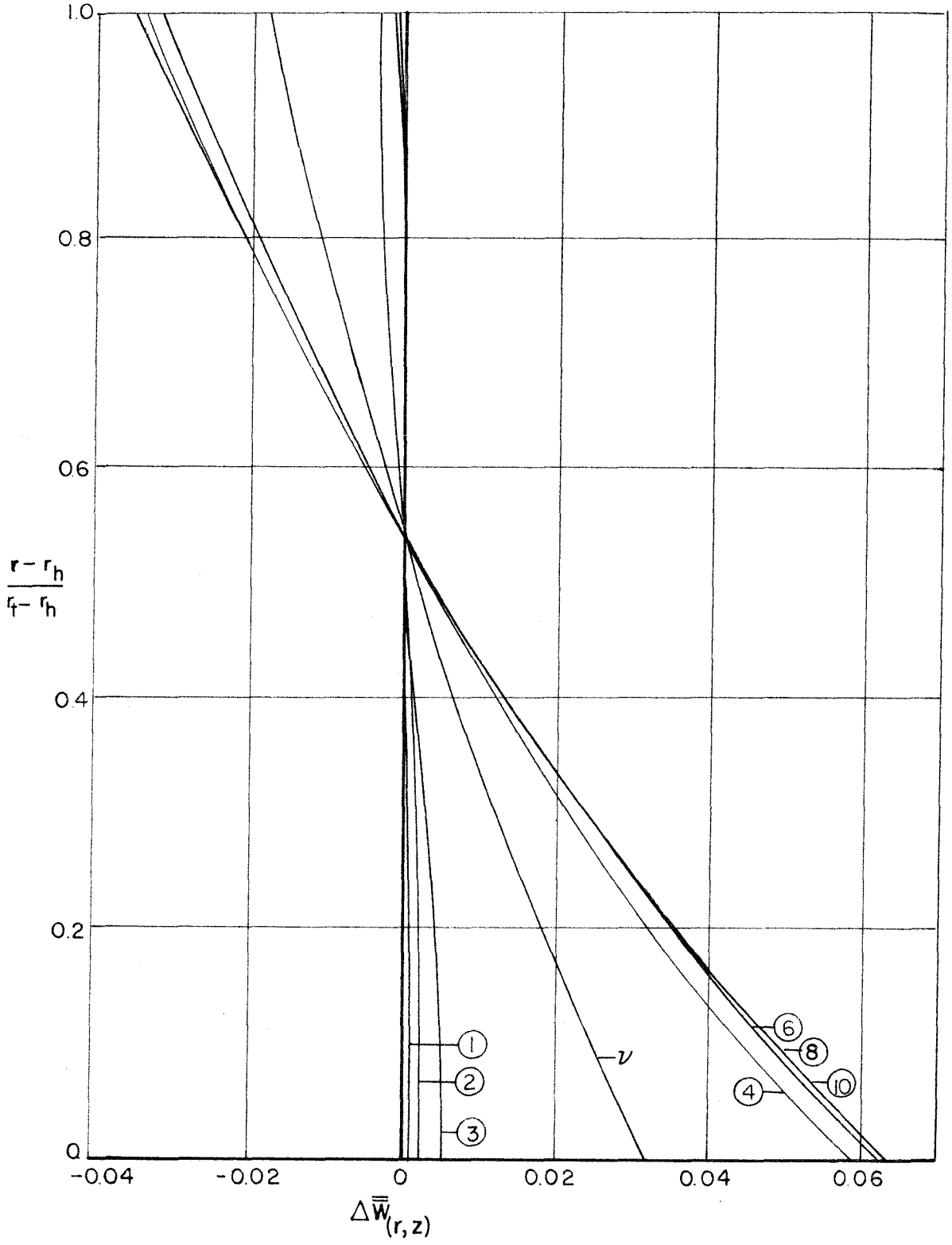

Figure 35. Effect of Adding Rotor Row to Flow With Actuator Disc.
$m^2 = 0.025$ $C = 0.1 W^{(o)}_{r_h}$

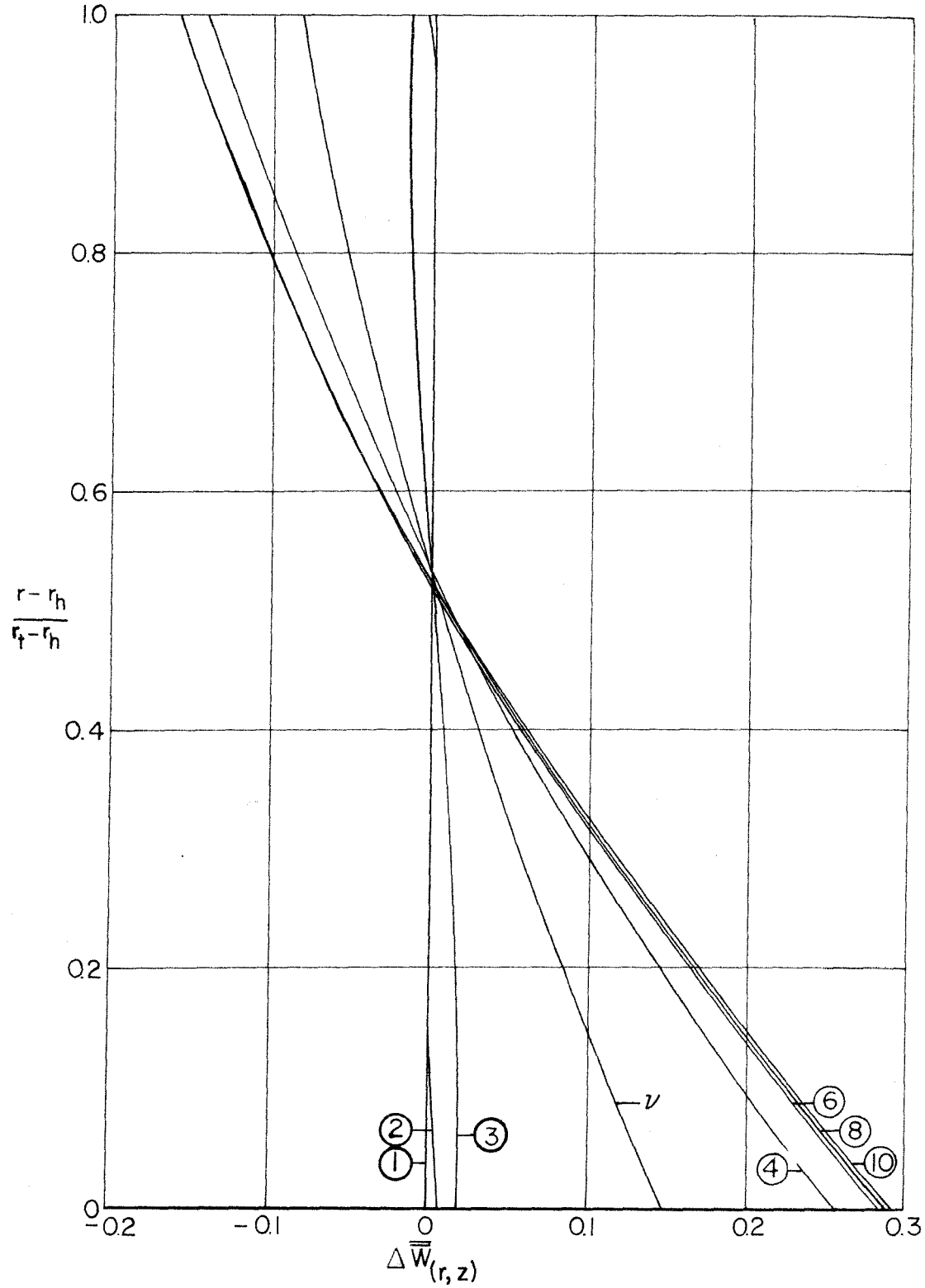

Figure 36. Effect of Adding Rotor Row to Flow With Actuator Disc.
$m^2 = 0.1$ $C = 0.2W^{(o)}_{r_h}$

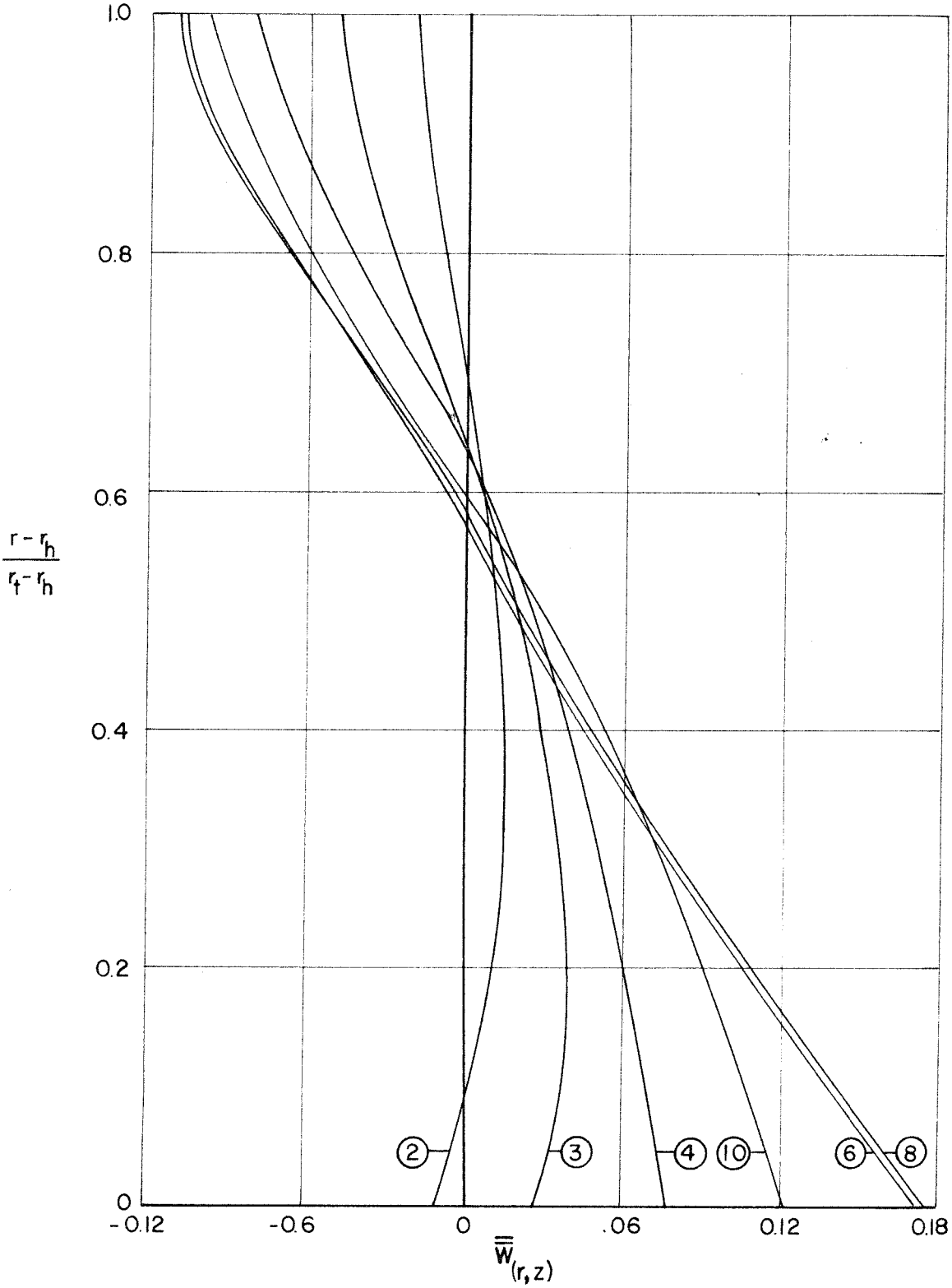

Fig. 37. Axial Velocity Perturbation. Actuator Disc at Entry to Simple Sinusoidal Step Followed by Lightly Loaded Rotor.

$m^2 = 0.025$ $C = 0.1 W^{(o)}_{r_h}$

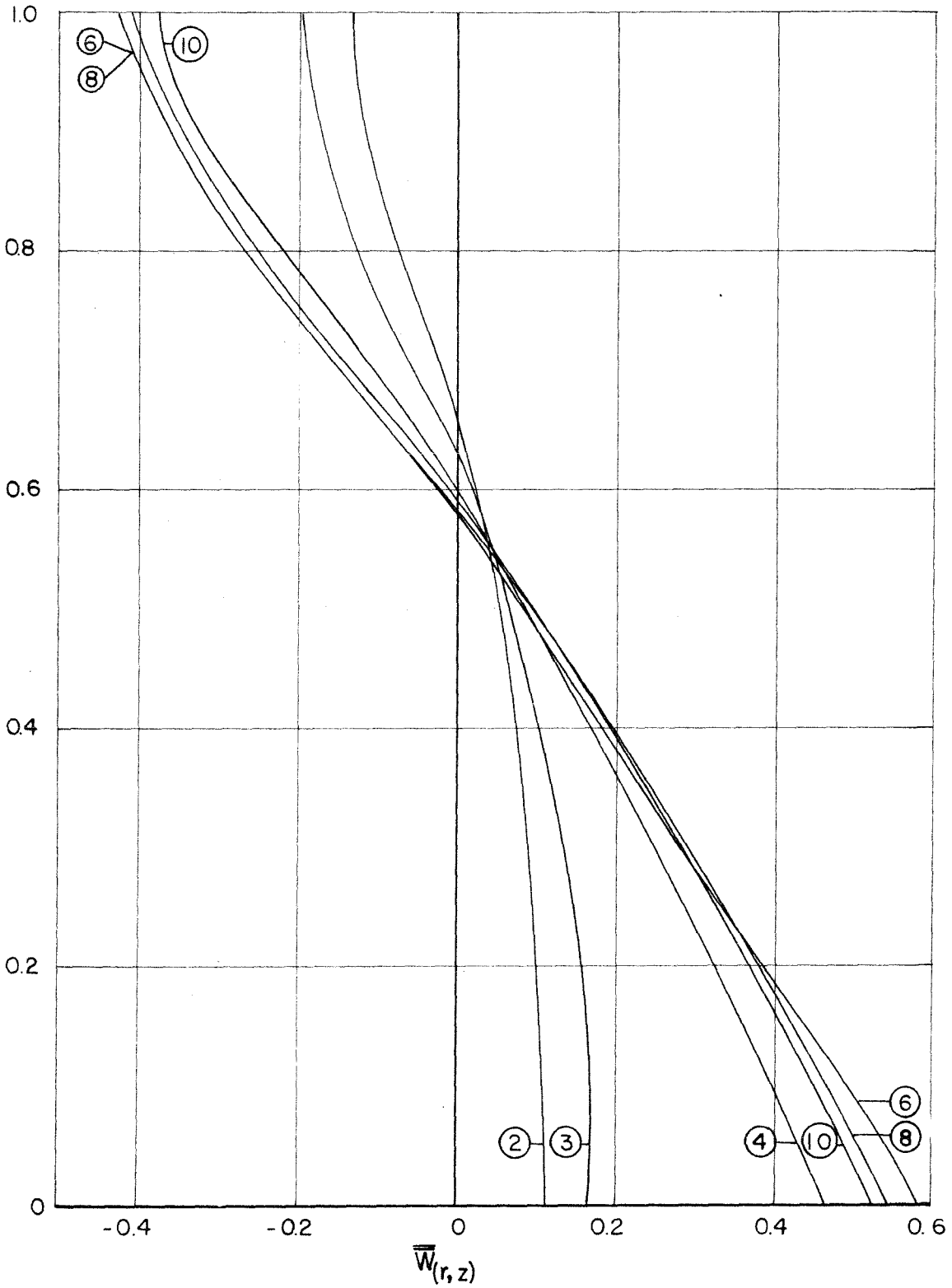

Fig. 38. Axial Velocity Perturbation. Actuator Disc at Entry to Simple Sinusoidal Step Followed by Lightly Loaded Rotor.

$m^2 = 0.1$ $C = 0.2W\overline{r}_h^{(\bullet)}$

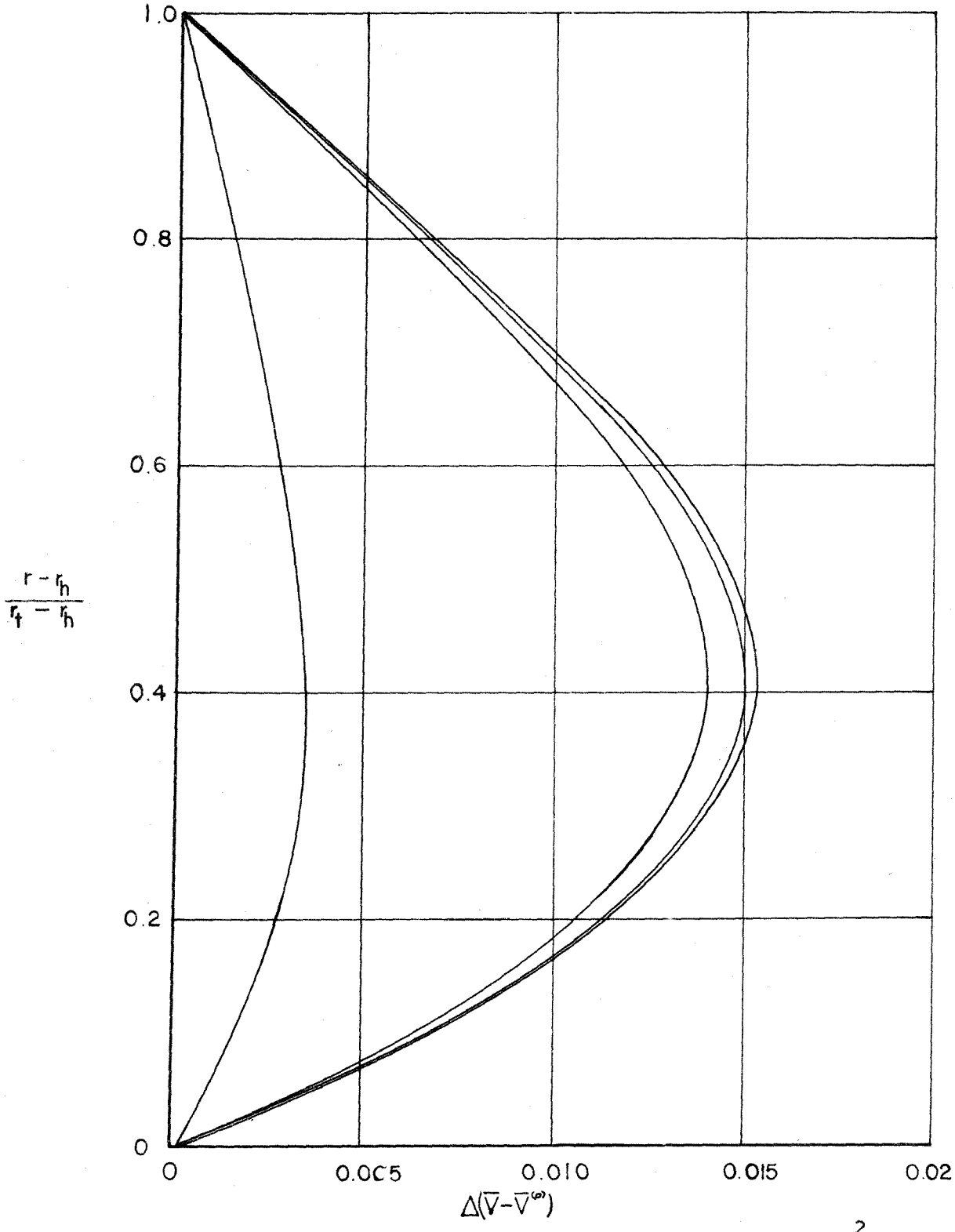

Figure 39. Effect of Rotor Row on Tangential Velocity. $m^2 = 0.1$; $C = 0.2W^{(o)}_{r_h}$